LARGE SCALE CpG ISLAND METHYLATION PROFILING OF SMALL B CELL LYMPHOMA

A Dissertation presented to the Faculty of the Graduate School at the University of Missouri-Columbia

---

In Partial Fulfillment
of the Requirements for the Degree

Doctor of Philosophy

---

by

FARAHNAZ B. RAHMATPANAH

Dr. Charles W. Caldwell, Dissertation Supervisor

MAY 2008

The undersigned, appointed by the dean of the Graduate School,
have examined the dissertation entitled

LARGE SCALE CpG ISLAND METHYALTION PROFILING OF
SMALL B CELL LYMPHOMA

Presented by Farahnaz B. Rahmatpanah,

A candidate for the degree of
Doctor of Philosophy,

and hereby certify that, in their opinion, it is worthy of acceptance.

_____

Charles W. Caldwell, MD. PhD

_____

Michael Lewis, PhD

_____

Carolyn Henry, DVM

_____

Douglas Anthony, MD. PhD

_____

Edward H. Adelstein, MD. DVM

DEDICATION

I would like to dedicate this dissertation to my husband Moz , my sons Parsa and Arwin whom I love so much for their inspiration, encouragement, and understanding throughout my educational career. I appreciate the joy and love they deliver on a regular basis. Without them, life has no meaning to me. I also dedicate this work to my family, especially my mother who I loved very much. I lost her in a battle against a very aggressive type of cancer, while I was working on my dissertation.

ACKNOWLEDGMENTS

I would like to extend my sincere appreciation to my mentor and advisor Dr. Charles Caldwell for his valuable guidance, assistance, and understanding during my doctoral work. My time in his cancer research lab has greatly elevated my capability and has made me a veteran in this new expanding field of cancer research. Many times he has presented me with many different opportunities that benefited me immensely.

I am grateful to the members of my dissertation committee, Dr. Carolyn Henry, Dr. Michael Lewis, Dr. Edward Adelstein and Dr. Douglas Anthony. All have given their time and expertise to enhance my work. I thank them for their contribution, encouragement, and support. I am also grateful to Dr. Kristen Taylor for her friendship, and sharing her expertise in the areas of genetics and epigenetics, that supported and enhanced my work. I also acknowledge Dr. Huidong Shi, and other colleagues who assisted and supported my research.

The last group of people that deserve equal amount of acknowledgement is my family. Little did I know that my family, who knew little to nothing about cancer research, could have had the most effect on my career. Everyday they would wait countless hours for me to finish my work. On the weekends, work would be the first priority, and they would be content with that. For many months my children did not have a mother, but they knew that sacrificing a few hours here and there, would pay off in the end. I know in my heart that all members of my family are behind me, and are more than happy with my accomplishment, which seems to be getting closer and closer than ever before. This is an exciting time for my family.

I thank everyone who has aided me in the past and present and I hope those people are still with me in the future, still offering their ever so precious guidance and aid. I am grateful to Dr. Neil Kay, Dr. Tait Shnafelt. (Department of Internal Medicine, Mayo Clinic), and Dr. James E. Wooldrige (Department of Internal Medicine and Holden Comprehensive Cancer Center, University of Iowa) for providing clinical samples for chapter two of this dissertation. I thank Susan Souchek, Laura Jacobus, Melinda Andreski, and Kathy Olsen for assistance with tissue banking. I also thank Dr. Nancy Hadfield and Dr. Janice Henson (English professors at Central Methodist University) for editorial assistance of this dissertation.

TABLE OF CONTENTS

LIST OF ILLUSTRATIONS

Figure **Page**

LIST OF TABLES

LIST OF ABBREVATIONS

5-Aza	5' AZA-2' deoxycytidine
aadUPT	Aminoallyl dUTP
ACTB	β-actin
ADAM12	ADAM metallopeptidase domain 12
APC2	Adenomatosis polyposis coli 2
APCL	Adenomatosis polyposis coli 2
AR	Androgen receptor
ARF4	ADP-ribosylation factor 4
AXIN2	Axin 2 (conductin, axin)
BCL2	B-cell CLL/lymphoma 2
BCL9	B-cell CLL/lymphoma 9
BCR	B-cell receptor
BLAST	Basic Local Alignment Search Tool
*BstU*1	Methylation sensitive restriction enzyme
CCND1	Cyclin D1
CCND2	Cyclin D2
CCND3	Cyclin D3
CD38	Cluster of differentiation 38
CDH1	E-cadherin
cDNA	Complementary deoxyribonucleic Acid
CGI	CpG island

COBRA	Combined Bisulftie Restriction Analysis
CREB1	CAMP responsive element binding protein 1
Ct	Cycle threshold value
CTBP2	C-terminal binding protein 2
DAPK	Death Associated Protein Kinase
DMH	Differential methylation hybridization
DKK1	Dickkopf homolog 1 (Xenopus laevis)
DLBLC	Diffuse Large B cell lymphoma
DLC-1	Deleted in liver cancer 1
DLEU7	Deleted in lymphocytic leukemia, 7
DMRT2	Doublesex and mab-3 related transcription factor 2
dNTP	Deoxyribonucleotide triphosphate
Dsh	Disheveled proteins
DUOX2	Dual oxidase 2
DVL2	Dishevelled, dsh homolog 2 (Drosophila)
*FBXW1*1	F-box and WD repeat domain containing 11
FBXW2	F-box and WD repeat domain containing 2
FBXW4	F-box and WD repeat domain containing 4
FL	Follicular Lymphoma
FOSL1	FOS-like antigen 1
FOXN1	Forkhead box N1
FZD	Frizzled homolog
FZD1	Frizzled homolog 1 (Drosophila)

FZD10	Frizzled homolog 10 (Drosophila)
FZD2	Frizzled homolog 2 (Drosophila)
FZD3	Frizzled homolog 3 (Drosophila)
FZD5	Frizzled homolog 5 (Drosophila)
FZD7	Frizzled homolog 7 (Drosophila)
FZD8	Frizzled homolog 8 (Drosophila)
GAPDH	Glyceraldehyde-3-phosphate dehydrogenase
GRM7	Glutamate receptor 7
GSK3β	Glycogen synthase kinase-3 β
HIF1	Hypoxia-inducible factor 1 alpha
HOXC10	Homobox C10
HP	Benign Follicular Hyperplasia
*Hpa*II	Methylation sensitive restriction enzyme
HPRT1	Hypoxanthine phosphoribosyltransferase 1
HSC	Hematopoietic stem cells
IgV	Immunoglobulin variable gene
IgVH	Immunoglobulin heavy-chain variable region
KCNK2	Potassium channel, subfamily K, member 2
LEF/TCF	Lymphocyte enhancing factor/T cell transcriptional factor
LHX2	LIM homeobox 2
LN	Normal lymph node
LRP1B	low density lipoprotein-related protein 1B (deleted in tumors)
LRP5	Low density lipoprotein receptor-related protein 5

LRP6	Low density lipoprotein receptor-related protein 6
M	Methylated
MCA	Methylated CpG island Associated
MCL	Mantel cell lymphoma
mRNA	Messenger RNA
*Mse*1	Methylation insensitive restriction enzyme
MSP	Methylation-specific PCR
NHL	Non-Hodgkin's Lymphoma
NKX6.1	NK6 homeobox 1
NL1	Normal female lymphocyte
NL2	Normal male lymphocyte
NLK	Nemo-like kinase
NRP2	neuropilin 2
P value	Probability value
PBL	Peripheral blood lymphocytes
PCDHGB7	Porotocadherin gamma subfamily B, 7
PCP	planar cell polarity
PCR	Polymerase chain reaction
POU3F3	POU class 3 homeobox 3
PPC	Positive PCR Control
PPP2CA	Protein phosphatase 2 (formerly 2A), catalytic subunit, alpha isoform
PPP2R1B	Protein phosphatase 2 (formerly 2A), regulatory subunit A, beta isoform
PPP2R3B	Protein phosphatase 2 (formerly 2A), regulatory subunit B, beta

PRKCE	protein kinase C, epsilon
PTPRO	Protein tyrosine phosphatase, receptor type, O
QPCR	Quantitative Real-time polymerase chain reaction
RAMP	receptor (G protein-coupled) activity modifying protein
RLGS	Restriction land mark genomic scanning
RLN2	Relaxin 2
RNA	Ribonucleic acid
RPL13A	Ribosomal protein L13a
RTC	Reverse transcriptional control
RT-PCR	Real time polymerase chain reaction
SAS	Statistical analysis software
SBCL	Small B cell lymphoma
SFRP2	secreted frizzled-related protein 2
SFRP4	Secreted frizzled-related protein 4
SOX	SRY (sex determining region Y)
SOX10	SRY (sex determining region Y)-box 10
SOX17	SRY (sex determining region Y)-box 17
SOX21	SRY (sex determining region Y)-box 21
SOX3	SRY (sex determining region Y)-box 3
SOX7	SRY (sex determining region Y)-box 7
SOX9	SRY (sex determining region Y)-box 9
SP1	transcriptional factor SP1
SssI	CpG methyl transferase

TCF7	Transcription factor 7 (T-cell specific, HMG-box)
TCL1	T-cell leukemia/lymphoma 1
TERT	Telomerase reverse transcriptase
TLE2	Transducin-like enhancer of split 2 (E (sp1) homolog, Drosophila)
TLE4	Transducin-like enhancer of split 4 (E (sp1) homolog, Drosophila)
TSA	Trichastin A Trichostatin A
TWIST2	Twist homolog 2 (Drosophila)
U	Unmethylated
VEGF	Vascular endothelial growth factor
WIP-1	WAS/WASL interacting protein family, member 3
WNT1	Wingless-type MMTV integration site family, member 1
WNT10A	Wingless-type MMTV integration site family, member 10A
WNT11	Wingless-type MMTV integration site family, member 11
WNT16	Wingless-type MMTV integration site family, member 16
WNT3	Wingless-type MMTV integration site family, member 3
WNT3A	Wingless-type MMTV integration site family, member 3A
WNT4	Wingless-type MMTV integration site family, member 4
WNT5A	Wingless-type MMTV integration site family, member 5A
WNT6	Wingless-type MMTV integration site family, member 6
WNT7A	Wingless-type MMTV integration site family, member 7A
WNT7B	Wingless-type MMTV integration site family, member 7B
WNT8	Wingless-type MMTV integration site family, member 8
WNT9A	Wingless-type MMTV integration site family, member 9A

ABSTRACT

Epigenetic events play a significant role in cellular differentiation and biologic activity through silencing of gene expression and also appear to be a factor in the progression of cancer. In the normal mammalian genome, methylation happens at cytosines 5' to guanosines and these CpG dinucleotides have been depleted from the mammalian genome over the course of evolution. Approximately 70% of the CpG dinucleotides in the mammalian genome are methylated at certain regions of the genome, while the 5' ends of genes, harbor the CpG rich domain (CpG islands), remain unmethylated in normal cells. However, in cancer cells the normally unmethylated CpG islands possess dense methylation, which results in loss of gene function. Aberrant DNA methylation of the DNA repair and tumor suppressor genes may promote cell growth and survival and subsequently can drive tumor formation in a range of tissues including breast, colon, skin and blood. In the past decade major advances in our understanding of how abnormal DNA methylation contributes to cancer have provided new platforms to identify biomarkers for early detection, prediction, and prognosis as well as drug development programs to identify new epigenetic modifying drugs. In this work we utilized a CpG island microarray (9K) for the genome wide characterization of DNA methylation in Mantel Cell Lymphoma (MCL), Chronic Lymphocytic Leukemia (CLL), and Follicular Lymphoma (FL) that comprise the Small B cell Lymphomas (SBCL).

From initial microarray analysis we identified 256 CpG island with differential methylation in MCL, CLL and FL. The hierarchical clustering analysis uncovered three different groups of SBCLs; the first group included all MCL cases and a subset of the B-CLL; the second group contained mainly FL and the third group included the FL, benign

follicular hyperplasia and another subset of the B-CLL. From a quantitative stand point, there appears to be more CpG islands hypermethylated in FL patients than in MCL and a subset of B-CLL samples. This differential methylation of SBCLs might be (at least in a part) related to their cellular origin during B –cell oncogenesis. It is tempting to speculate that follicular lymphoma patients with higher levels of methylation might respond better to treatment with demethylating agents such as 5 '-Aza deoxycytidine than MCL and a subset of CLL with low levels of methylation. In addition, further analysis of the DNA methylation profiles suggests that the patters in B-CLL may not be homogenous.

We hypothesized that variation in DNA methylation may relate to CD38 expression levels in CLL patients. One of the biomarkers that predicts prognosis in patients with CLL is the CD38 expression levels. It is known that the biological characteristics of CD38 positive ($CD38^{high}$) and negative ($CD38^{low}$) leukemic cells differs, and our study provides additional insights into a possible role of DNA methylation as a contributing factor for these differing characteristics. We utilized a CpG island microarray (12K) to investigate the relationship between the DNA methylation and the CD38 expression levels in CLL patients. Multiple genes (*PCDGHB7*, *APC2*, *ADAM12* and *LHX2*) were methylated across all CLL patients regardless of the CD38 expression levels, and therefore may affect the general biological behavior of all CLL in a similar manner. In addition, we identified genes that were preferentially methylated based on the CD38 expression levels. Methylation was present in the deleted lymphocytic leukemia, 7 (*DLEU7*) in all $CD38^{low}$ cases. Conversely, homeobox protein C10 (*HOXC10*) and secreted frizzled related protein 2 (*SFRP2*) were methylated mainly in the $CD38^{high}$ cases.

SFRP2 and *APC2* are negative regulators of the WNT signaling pathway. The WNT signaling pathway plays an important role in embryonic development and has been implicated in promoting many types of cancer including CLL. To investigate the expression levels of WNT signaling genes and the possible effects of epigenetic silencing of negative regulators of this pathway in CLL patient samples, we combined three powerful techniques, 1) Methylated CpG Associated (MCA) to detect changes in DNA methylation genome wide, 2) CpG island microarray with 244,000 probes to identify methylated genes associated with specific signaling, and 3) The PCR array to profile the expression of genes involve in WNT signaling. These findings demonstrate that the epigenetic regulation of WNT antagonists is another mechanism that activates WNT signaling in CLL tumorigenesis. Treatment of CLL cell lines with inhibitors of DNA methylation and histone deacetylase reactivated WNT signaling genes (*APC2*, *Groucho/TLEs*, and *SFRP2*), that were silenced through DNA methylation.

WNT signaling also plays important roles in providing proliferative signals for the immature progenitors of B cells and provides the signal for self renewal of hematopoietic stem cells (HSC). This study raised many questions, for example, does γ-Catenin have a similar role as the β-Catenin in the canonical WNT signaling pathway. A previous study has shown that in Acute Myeloid Leukemia (AML) increased expression of γ -Catenin is associated with increased WNT signaling. In this respect, exploring the mRNA expression and the protein levels of γ –Catenin in primary and CLL cell lines are of great interest.

Another question concerns the interaction between the WNT signaling pathway and the NOTCH pathway; recent data has shown that activation of WNT signaling in

hematopoietic stem cells leads to enhanced levels of Notch1 and HoxB4. It has been confirmed that NOTCH signaling is required for WNT mediated maintenance of undifferentiated HSCs. Therefore, it is important to study the role of the NOTCH pathway in CLL tumorigenesis.

In this study we report elevated expression levels of histone acetylase *p300, CJUN* and *FOSL1* in CLL B cells compared to normal B cells by at least by 10 fold. These genes are associated with very interesting biological functions whose abnormal expression has not been previously reported in CLL. It is important to perform immunofloresence or Western blot analysis in the future to investigate the protein levels of these genes in the nucleus and the cytoplasm of the leukemic cells.

Therapeutic intervention at many levels that manipulate the WNT signaling pathway in CLL is very important. The expression of WNT target genes and the positive regulators of WNT signaling along with the epigenetic silencing of genes (*APC2*, *Groucho/TLEs* and *SOX17*) encoding WNT pathway inhibitors could represent attractive targets for the therapeutic interventions.

Chapter 1

Differential DNA methylation patterns of small B-cell lymphoma subclasses with different clinical behavior.

Abstract

Non-Hodgkin's Lymphoma (NHL) is a group of malignancies of the immune system with variable clinical behaviors and diverse molecular features. Despite the progress made in classification of NHLs based on classical methods, molecular classifications are a work in progress. Toward this goal, we used an array–based technique called differential methylation hybridization (DMH) to study small B-cell lymphoma (SBCL) subtypes. A total of 43 genomic DMH experiments were performed. Several statistical methods were used to analyze these results and generate a set of differentially methylated genes for further validation. Methylation of *LHX2, POU3F3, HOXC10, NRP2, PRKCE, RAMP, MLLT2, NKX6.1, LPR1B,* and *ARF4* was validated in cell lines and patient samples and demonstrated subtype- related preferential methylation patterns. For *LHX2* and *LRP1B,* bisulfite sequencing, real time RT-PCR, and induction of gene expression following treatment with the demethylating agent, 5'-aza -2'-deoxycytidine (5-Aza), was confirmed. This new epigenetic information is helping to define molecular portraits of distinct sub-types of SBCL that are not recognized by current classification systems and is providing valuable potential insights into the biology of these tumors.

Introduction

Every year approximately 54,000 new cases of non-Hodgkin's Lymphoma (NHL) are diagnosed in the U.S. B-cell chronic lymphocytic leukemia/small lymphocytic lymphoma (B-CLL/SLL), mantle cell lymphoma (MCL) and follicular lymphoma (FL) referred to as small B- cell lymphoma (SBCL), comprises nearly one third of all NHL cases. [1] Current classification systems are based on clinical staging, chromosomal abnormalities [2], and cell surface antigens and offer important diagnostic information. However, there is still considerable overlap of biology, clinical behavior and genetic and epigenetic alterations among the SBCL subtypes. DNA methylation within the CpG island (CGI) in promoter (and other) regions plays an important role in cancers by potentially silencing a broad spectrum of genes. [3] Aberrant patterns of CGI methylation are not random, but are tumor type-specific, and they can influence the gene expression profile. [4] DNA hypermethylation of some genes such as *p57(KIP2), p15(INK4B)*, [5;6] *DAPK*,[7] SHP-1[8] and *p73* [9] are frequent occurrences in lymphoid malignancies.

The SBCL subtypes are B cell malignancies that correspond to different stages of normal B- cell differentiation and differ in clinical behavior. While B-CLL/SLL and FL are generally indolent, MCL is more rapidly progressive. B-CLL/SLL is not one disease but is comprised of at least two biological subtypes representing pre-germinal center and post germinal center B- cells. [10] MCL is a pre-germinal center derived malignancy, and FLs are of germinal center derivation. Expression microarray studies have provided information to assess clinical aggressiveness and guide the choice of treatment in FL .[11] Alizadeh *et a*l [12] used a lymphochip to monitor gene expression signatures of diffuse large B cell lymphoma (DLBCL) subgroups derived from distinct stages of B cell

differentiation. In addition, tumor classification can also be achieved by microarray based DNA methylation profiling.[13] Few published reports have focused on the identification of genes whose methylation profiles differ between currently recognized SBCLs. Rush *et al* using Restriction Landmark Genomic Scanning (RLGS), studied global CpG island methylation in 10 CLL patient samples.[14] The Secreted Frizzled Related Protein gene family (*SFRP*), a negative regulator of the Wnt signaling pathway, was found to be frequently methylated in CLL patients.[15] In this study we used a high throughput approach to classify SBCL subtypes (43 patient samples). Hierarchical clustering [16] of the DNA methylation data was used to group each subtype on the basis of similarities in their DNA methylation patterns. Our data revealed that there was diversity in DNA methylation among the different SBCL subtypes, and some genes were preferentially methylated in a subtype related manner. The main purpose of this study was to move closer to the determination of epigenetic signatures of SBCLs based on DNA gene promoter methylation profiling.

Materials and methods

Patient samples

Tissue and blood samples were obtained from patients following diagnostic evaluation in compliance with the local Institutional Review Board. DNA was isolated from a total of 43 patient samples, and control DNA was isolated from peripheral blood collected from 7 healthy male and 7 healthy female volunteers with a mean age of <30 years; these samples pooled separately as NL1 (female) and NL2 (male). QIAamp DNA Blood Minikit (Qiagen, Valencia, CA) was used to purify genomic DNA. Samples from 15 patients with FL, 12 with MCL, and 16 with B-CLL/SLL were used in this study. All cases of B-CLL/SLL had peripheral blood and bone marrow involvement and therefore, were technically categorized as having chronic lymphocytic leukemia but are referred to as B-CLL/SLL in this paper. All specimens contained > 80% neoplastic cells as determined by flow cytometry (data not shown). Complete flow cytometry reports were available for 12 of the 16 B-CLL/SLL patients used in this study; 6 patient samples were $CD38^+$ and 6 were $CD38^-$ (data not shown). Cells from 3 patients with benign follicular hyperplasia (HP) were also obtained. Total RNA was extracted from 4 samples of normal peripheral blood lymphocytes (PB), 2 normal lymph nodes (LN), 8 FL, 10 CLL, and 8 MCL patient samples, using the RNeasy kit (Qiagen, Valencia, CA).

Cell culture and drug treatments

Human NHL lines RL, Daudi, DB, Raji, Granta 519 and Mec-1 were maintained in RPMI 1640 media. The germinal center related cell line RL is derived from a male patient with FL and the t(14,18) translocation [17], and Daudi and Raji cells are also of germinal center derivation. The postgerminal center cell line DB was derived from a DLBCL patient and has undergone isotype switching. All four of these cell lines express surface

CD10, thus suggesting a germinal center relationship [18]. Granta 519 is an MCL cell line over-expressing cyclin D1 [19], and Mec-1 is a transformed B-CLL/SLL cell line [20]. For gene reactivation experiments, cells were cultured in the presence of vehicle (PBS) or 1.0μM 5-aza-2'-deoxycytidine (5 -Aza) with medium changed every 24 h. After 4 days, cells were either harvested or further treated with TSA (1.0μM) for 12 h and then harvested. Some cells were also treated with TSA alone for 12 h before harvest. Genomic DNA and total RNA were isolated using Qiagen kits (Qiagen, Valencia CA).Genomic DNA was used for methylation analysis and total RNA was used for gene expression analysis.

Preparation of CGI microarray

The schematic for CpG island preparation is depicted in figure1.1. This library was a generous donation from Dr. Cross[21]. Briefly, the *Mse*1 fragments containing CpG islands were purified from the genomic DNA of a normal male individual. The restriction enzyme *Mse*1 is a frequent cutter that cuts the genomic DNA into small fragments (100-1kb average); *Mse*1 cut site (TTAA) happens rarely within the CpG island, therefore, the *Mse*1 leaves intact CpG islands and small fragments from the genome. The *Mse*1 digested DNA was passed through the MeCP2 column. The methyl binding protein (MeCP2) was attached to a solid support column with a fractionation matrix that could separate methylated DNA fragments with high affinity. The column retained highly methylated DNA in the bulk of the genome. The next step involved removals of *Mse*1 fragments that are not highly methylated and bind weakly with the column. These fragments contained the promoter regions and the first exon of many transcriptional factors. The bacterial methyl transferases *SssI* was used to methylate non methylated CpGs in the fractions that

did not bind to the column. In the next step the in vitro methylated DNA, which had high binding affinity for the MeCP2 column, were passed through the MeCP2 column and they were retained in the column. Finally, fragments that were highly enriched for CpG islands were collected and organized in a 96 well plate format. However, it is important to mention that not all the promoter CGIs are flanked by *Mse1* restriction site. Therefore, these CGI fragments were not present in this version of the CGI library that we utilized in this study.

The CGI clones were organized in 96 well culture plates. We made two more copies of each of these plates in glycerol stocks and stored them in different freezers to protect against possible contaminations and clone mix up. The bacterial cells were grown overnight in a 50 ul LB broth at 37^{o}C. Then the CGI library was amplified using a small portion of clones from 96 well culture plates that moved to PCR plates. The primers *HGMP1* (5'CGG CCG CCT GCA GGT CTG ACC TAA 3') and *HGMP2* (5' AAC GCG TTG GGA GCT CTC CCT TAA 3') were used to perform colony PCR. The efficiency of PCR amplification was examined using a 96 well format gel electrophoresis. The unpurified PCR products were printed on a poly-lysine coated slide that we prepared in our laboratory according to the protocol described at the web site DeRist (www.microarrays.org.accessedJuly 2000). We used an Affymetrix/GMS 417 arrayer which permits the printing of unpurified PCR products because of its ring and pin system. In chapters 2 and 3 we have used newer arrays, including 12K and 244K to enhance our experimental designs over the 5 year course of these studies.

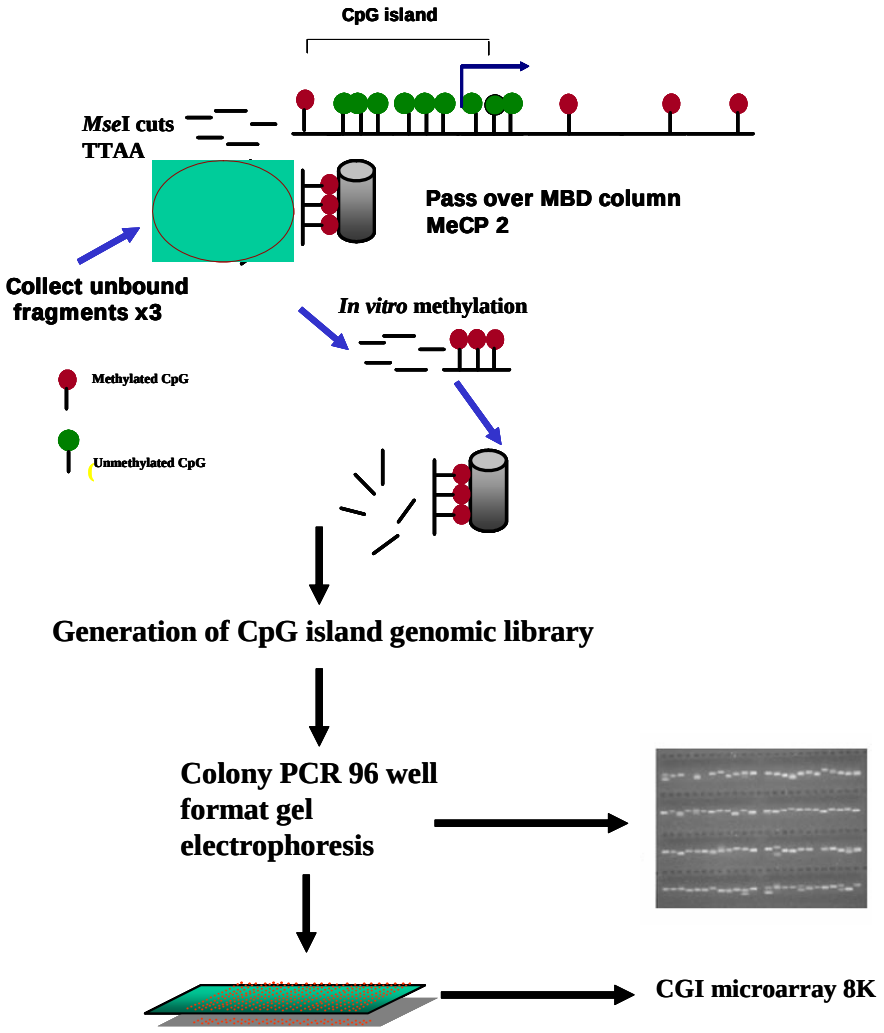

Figure 1.1: Schematic flowchart for CpG island microarray. This CGI microarray was prepared from a healthy male genomic DNA. The CGI fragments containing *Mse*1 restricted cut sites were subjected to in vitro methylation using bacterial *Sss*I. Methylated CpGs were retained and enriched by MeCP2 fractionation column. Individual clones were organized in the 96 well plates, and then the clones were amplified and prepared for printing on the poly lysine coated slides.

Amplicon preparation

Genomic DNA was isolated from samples taken from 43 SBCL patients, 3 patients with hyperplasia, and peripheral blood taken from normal individuals. The quantity and the quality of DNA was assessed using spectrophotometer and agarose gel to ensure the successful preparation of amplicons. The amplicon preparation is illustrated in Figure 1.2. Briefly, 2µg of genomic DNA was restricted with the restriction enzyme *Mse*1 (the same restriction enzyme that utilized to generate the CGI library). The *Mse*1 restricted fragments were ligated to the H12 (5'TAA TCC CTC GGA 3') and H24 (5'AGG CAA CTG TGC TAT CCG AGG GAT 3') linkers. These linkers were ligated to the DNA fragments in patient samples and the normal amplicons that were restricted by the *Mse*1 cutter. After the ligation of linker H12/H24, fragments were digested with the methylation sensitive restriction enzymes *BstU*1 and *Hpa*II and amplified for 20 cycles with H24 as a primer. This method is called Differential Methylation Hybridization assay (DMH) which is based on the use of methylation sensitive restriction enzymes that discriminate between the methylation profile of tumor samples and the profile of the normal controls.

The DNA was purified and amplified using a H24 primer; 20 cycles of amplification was performed. Amino-allyl labeling (aadUTP) and fluorescence dye coupling were performed. Labeled amplicons were purified with Micron YM-30 columns (Millipore, Bedford, MA), and equal amounts of Cy3 and Cy5 and 20µg of human *Cot*1 DNA were combined for hybridization on a 9K microarray chip. Prior to the hybridization, the printed DNA was cross linked to the slide using UV light. The hybridization was carried out using a hybridization chamber in a 60^{o} C water bath for 15 hours. It is important to point out that tumor samples were combined with the normal

DNA in a gender matched manner. In females one copy of the X chromosome is largely inactivated by DNA methylation; therefore women are expected to exhibit methylation of one allele of certain genes, such as the androgen receptor (AR) gene; whereas this occurs only in malignancy in males.

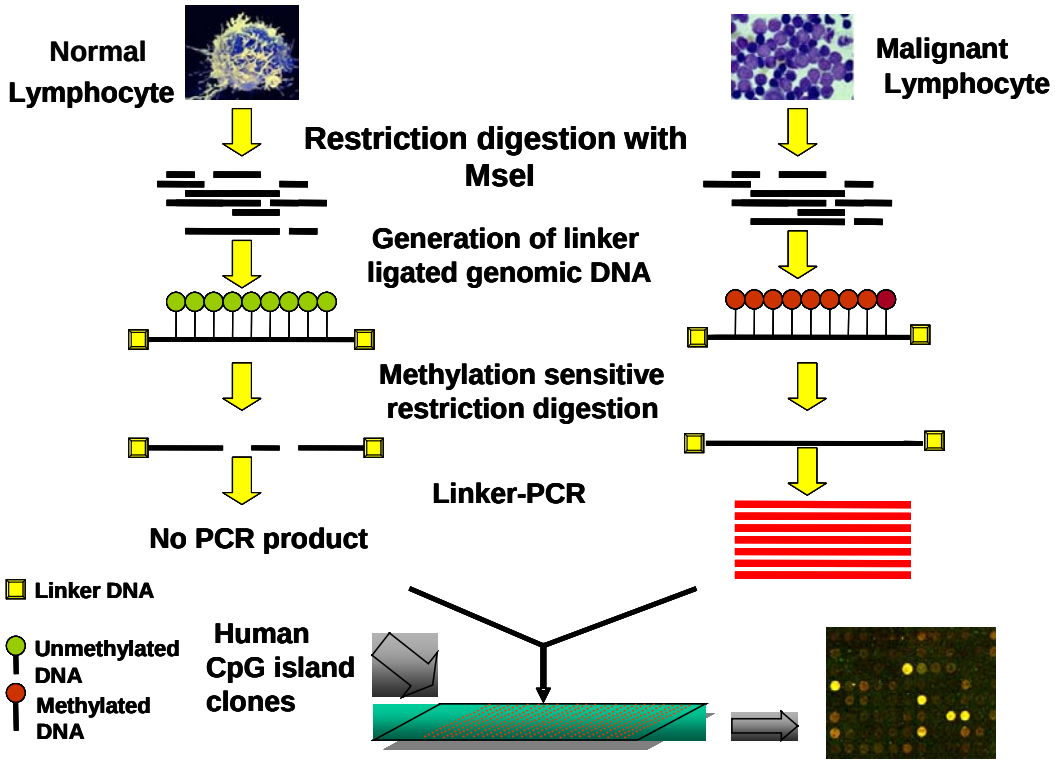

Figure1. 2: Schematic flow chart of DMH. First, genomic DNA was isolated from the normal peripheral blood, the hyperplasia samples, and the SBCL patient samples. Then, the genomic DNA was cut with the frequent cutter *Mse*1 that cuts the genomic DNA to small fragments and preserves fragments within the CpG islands. The CpG rich fragments were ligated to the universal linkers. Enrichment of the methylated DNA was obtained by cutting the DNA further with the methylation sensitive restriction enzymes, *Bstu1 and Hpa*II. Therefore, the methylated DNA in tumor cells were protected from the cleavage and were amplified, whereas the same unmethylated DNA in normal cells were cleaved with the methylation sensitive restriction enzymes and were not e amplified. The differential methylation between the tumor and the normal cells provided a pool of DNA that was enriched for the methylated DNA but not the unmethylated DNA. Florescence amplicons representing the pools of methylated SBCL DNA (Cy5) relative to normal DNA (Cy3) were combined in a gender matched manner and cohybridized to a 9KCGI microarray.

Microarray data analysis

Each spot on the slide appears as a colored dot comprised of differing amounts of red (Cy5) and green (Cy3). The intensity levels of red and green in each spot signify the amount of methylation found in the cancer (red) and normal (green) cells. Both red and green intensities were background-corrected and global normalization applied, with the assumption that the methylation level of both cancer and normal cells is similar in most loci (red/green ≈1). After array normalization, an across-array analysis was performed for each spot. These filtered loci were then subjected to further statistical testing to determine which loci were differentially methylated across subtypes of NHL. The Kruskal-Wallis test, because of its ability to compare more than two data distributions and its nonparametric nature was performed on the group of samples at each locus. The *p*-value threshold was calculated using the Benjamini and Hochberg method. [22] The loci corresponding to the *p*-values $p_{(1)} \leq p_{(2)} \leq \ldots \leq p_{(J)}$ were classified as differentially methylated. Hierarchical clustering algorithms were used to separate SBCLs based on similarities in DNA methylation patterns. Nucleotide sequencing results came from the Der laboratory (Toronto, Canada) http://derlab.med.utoronto.ca/CpGIslandsMain.php. Sequence identification information was obtained by the BLAST method.

Methylation confirmation by methylation specific PCR (MSP)

The DNA methylation status of selected candidate genes from specific regions of the microarray clusters was confirmed using MSP. Each set of primers was first optimized on cell line DNA and then confirmed on patient DNA. The following 10 selected genes were examined: *MLLT2, LHX2, LRP1B, HOXC10, NKX6.1, ARF4, NRP2, RAMP, NRP2*, and *POUF3.* The primer sequences used to confirm selected genes are listed in Table 1.1.

Briefly, this assay is based on modification of DNA by sodium bisulfite, converting all unmethylated, but not methylated, cytosine to uracil. The bisulfite treated DNA is amplified with primers specific for methylated versus unmethylated DNA. One of the advantages of this technique over other methods used for detecting methylation is the sensitivity. MSP is sensitive to 0.1% methylated allele of a given CpG island locus, and can be performed on very small amounts of DNA. Primers were designed using MethPrimer (www.urogene.org/methprimer/index.html). Products (5-9 µl) were directly loaded on a 2.5-3% agarose gel stained with SYBR Green (Cambrex Bio Science Rockland, ME), visualized under UV light, and quantified using Kodak gel documentation system.

Gene Name	CPG ISLAND	Antisense PCR Primer	Length	Annealing Temp
HOXC10	YES	Antisense: 5'- TTAAAGTTATGGTTTGTTGG -3' Sense: 5'- AAAACCACTAAAACTCCAAA -3'	186	60
ARF4	YES	Antisense: 5'- TGGAAGTAAGGTTTATTATTTTGA -3' Sense: 5'- AAAATTAACCAATTTCACTAACATA -3'	210	52
LHX2	YES	Antisense: 5'- TAGTTTATTTTGTTGGGGTAAATGG -3' Sense: 5'- TCAAATAATTCAACTTCCACTCAAA -3'	199	52
LRP1B	YES	Antisense: 5'- AAGTTTGTGTTGGAGATTGTTTG -3' Sense: 5'- CCAATAACATTTATAAATACCACCATT	105	57
MLLT2	YES	Antisense: 5'-GAGAGTAGGTAGTTTTGTAATATTGG-3' Sense: 5'- AAAATCTTCCATCCATAAACACC -3'	124	58
NKX6-1	YES	Antisense: 5'- TTTTAGAGTGGTTGTTTGTAGTTGA -3' Sense: AATCTCATATATTTTCTCTTTCCATC -3'	117	60
RAMP	YES	Antisense: 5'- GAATTTTGTTAGTTTTGAGTAGTGG -3' Sense: 5'- TCTCAACTAAAACTTTTCCTCCAAC -3'	123	60
POU3F3	YES	Antisense: 5'-TGTATATATATATATATGAGGAAGTGG-3' Sense: 5'- AAAATACCAATCAACAAAACCATACA -3'	187	60
NRP2	YES	Antisense: 5'- TTTTAGAGATTAGTGTTGTAGTTGA -3' Sense: 5'- AAAACCAAAACTAAAACCTCCAC -3'	168	60
PRKCE	YES	Antisense: 5'-TTGGTAAGTTTGTAGTGATAAAGTTGT-3' Sense: 5'- AAACCTCAAAAACCACTAAAACAAA -3'	138	60

Table 1.1: Primers used for MSP and PCR conditions. Primer sequences and the PCR conditions are summarized in this table. The primers were designed using MethPrimer software www.urogene.org/methprimer/index.html. These primers are specific to the CGI region of every examined gene.

Bisulfite genomic sequencing analysis

Genomic DNA was treated with sodium bisulfite. Primer sequences and PCR conditions are listed in Table1.2. Amplified PCR products for the *LHX2* and *LRP1B* genes were sub-cloned using the TOPO-TA cloning system (Invitrogen, Carlsbad CA). Plasmid DNA of 6- 8 insert positive clones was isolated using the Montage Plasmid Miniprep^{96} kit (Millipore Corporation, Billerica, MA) and sequenced using ABI 3730 sequencing systems (Applied Biosystems, Foster City, CA). The primer sequences and the PCR conditions are summarized in Table 1.2.

Gene Name	Sense PCR Primer	Length	Annealing Temp
LHX2	5'GGTTGAATAGTAAAAAGTAGAAATAAATTT-3'	130	57
	5'ACTCCAAAACACCTAATAACTAAAA-3'		
LRP1B	5'-TAGGGTTAGTTTTTTGGTAAT-3'	206	51
	5'TAAAAAATTTCCAATAACATTTATAAATAC-3'		

Table 1.2: Primers and PCR conditions: The designed primers were used to perform bisulfite genomic DNA sequencing. Primers were designed using Methprimer software.

Real time RT –PCR

Two μg RNA were reverse transcribed in the presence of SuperScript II reverse transcriptase (Invitrogen, Carlabad, CA). The generated cDNA was used for SYBR green based RT-PCR amplifications with appropriate reagents in the ABsolute^{TM} QPCR SYBR mix (AB genes, Rochester, NY) as recommended by the manufacture. Real time RT-PCR was carried out in an I- Cycler (BioRad, Hercules, CA). Quantitative expression of four genes (*LRP1B*, *LHX2, ARF4* and *POU3F3*) was measured in three SBCL cell lines (RL, Mec-1 and Granta519) before and after treatment with the demethylating agent 5-Aza. Relative expression of *LHX2* and *LRP1B* was further studied in subsets of patient samples. It is important to note that these samples are not all from the same patients that we studied in microarray and MSP analysis due to sample limitations. Each experiment was repeated 3 times, and the median was calculated. For quantification, the ratio of target gene to reference gene (*HRPT1*) for each gene was calculated as $\tilde{2}^{\Delta\Delta Ct}$, where Ct is the cycle threshold. I-Cycler conditions were as follows: 45 cycles with 15s at 95^{o} C, 30s at 60^{0}C (for *ARF4, LRP1B*), 64^{0}C (for *POU3F3*), and 68^{0}C for *LHX2*, 30 s at 72^{0}C. Melt curve analysis was always performed after each run. The primer sequences are summarized in Table 1.3.

Gene Name	Sense RT Primer	Antisense RT Primer	Length
LHX2	5'-CCAAGGACTTGAAGCAGCTC-3'	5'-GTAAGAGGTTGCGCCTGAAC-3	105
ARF4	5'-TGCACAAGTGGCTTGAACAT-3'	5'-GGCCATCAGTGAAATGACAG-3	82
POU3F3	5'-AGTTCGCCAAGCAGTTCAAG-3'	5'-ACACGTTGCCGTAGAGTGTG-3'	120
LRP1B	5'-CATGATCACAACGATGGAGGT-3'	5'-CTTGAAAGCACTGGGTCCTC-3'	96
HPRT1	5'-GGTCCTTTTCACCAGCAAGCT-3'	5'-TGACACTGGCAAAACAATGCA-3'	93

Table 1.3: Primers and PCR conditions used to perform quantitative real time RT-PCR. Primers were developed for SYBR green assay using Primer3 software.

Statistical analysis

To assess the extent to which the MSP results were confirmed by bisulfite sequencing, the kappa statistic (a type of intra-class correlation) was computed for *LHX2* and *LRP1B.* Kappa equals one when there is perfect agreement, negative one when there is perfect disagreement, and zero when there is chance agreement. [23] For this data, the estimated value of kappa is 0.545 [95% CI: (0.196, 0.894]), which is significantly different from zero (exact p=0.021, ASE=0.178). Thus, the agreement between MSP and bisulfite sequencing is 54% greater than what would be expected by chance. Overall, the proportion of agreement is 79% (19/24). Considering bisulfite sequencing as the gold standard, the sensitivity of MSP is 87%, while the specificity is 67%. It has been noted that MSP is more sensitive than specific. In addition, for comparisons of gene promoter

methylation between classes of NHLs, the chi-square statistic was employed. All the analyses were implemented in SAS (Statistical Analysis Software).

Results

Segregation of SBCL subtypes by hierarchical clustering

Genomic DNA methylation microarrays were used to characterize these SBCLs. A total of 15 *de novo* patient samples from those with FL, 16 B-CLL/SLL, 12 MCL and 3 samples of nonmalignant hyperplasia (HP) were all probed for the presence of methylated DNA, mainly in the promoter and 1st exon regions of genes and initially analyzed by hierarchical clustering as shown in (Figure 1.3). The upper dendrogram illustrates the relationships of patient samples to each other on the basis of DNA methylation patterns; those most alike cluster under a single branch of the dendrogram. In all, 256 CGI loci were selected based on statistical testing described.

For each CGI locus of interest, the related gene was identified by searching the associated database of CGI sequences found at the Der laboratory web site. Moving from left to right represents a "drilling down" into the microarray data to ultimately discover named genes that are differentially methylated candidates. For example, the branch indicated by the purple horizontal bar includes all the MCL samples, but no others. This separation appears to involve mainly clusters of gene loci from within regions A and D of the overall hierarchical cluster, as well as the paucity of methylated loci from within regions B and C where considerable methylation is indicated for FL and a subset of B-CLL/SLL samples. Thus, the observed patterns in MCL patients were distinct from FL and a subset of B-CLL/SLL patients, but associated with another subset of B-CLL/SLL indicated by the green horizontal bar.

Further analysis of the profiles separated the B-CLL/SLL patients into 2 distinct groups. Seven of 16 (44%) B-CLL/SLL samples (indicated by the green horizontal bar) clustered adjacent to MCL (an aggressive pre-germinal center subtype of NHL). [24] Flow

cytometry revealed that 2/7 (28%) of these were CD38+, 3/7 (43%) were CD38- (flow cytometry results were not available for the remaining 2 samples).Conversely, 9/16 (56%) B-CLL/SLL samples clustered with FL (indicated by the red horizontal bar). Of these, 4/9 (43%) were CD38+, 3/9 (33 %) were CD38- . Flow cytometry results were not available for the remaining 2 samples. While there is no clear association of methylation with CD38 expression, this observation still suggests that DNA methylation patterns in B-CLL/SLL may not be homogeneous and perhaps methylation patterns relate to unrecognized subsets of B-CLL/SLL. Those B-CLL/SLL samples that clustered near MCL (purple horizontal bar) were characterized in the overall cluster as having few loci illustrated as methylated in regions A, B, and C, but there was a small block within region D that was conspicuously indicated as hypermethylated, similar to block D in MCL cases.

Cells from FL are similar in their biological characteristics to cells found in the germinal centers of lymph nodes. From a quantitative standpoint, there appears to be more CGI loci hypermethylated in FL patients than in MCL patients and in a subset of B-CLL/SLL samples (Figure 1.3). Therefore, to further examine relationships between classes, this data was re-clustered in a pair-wise manner (Figure 1.4). Sequence characterization and chromosomal location of differentially methylated CGI loci are shown in Appendix 1. Most of these loci are located in the promoter or the first exon regions of known genes with a known function, but in some cases these loci are found in introns.

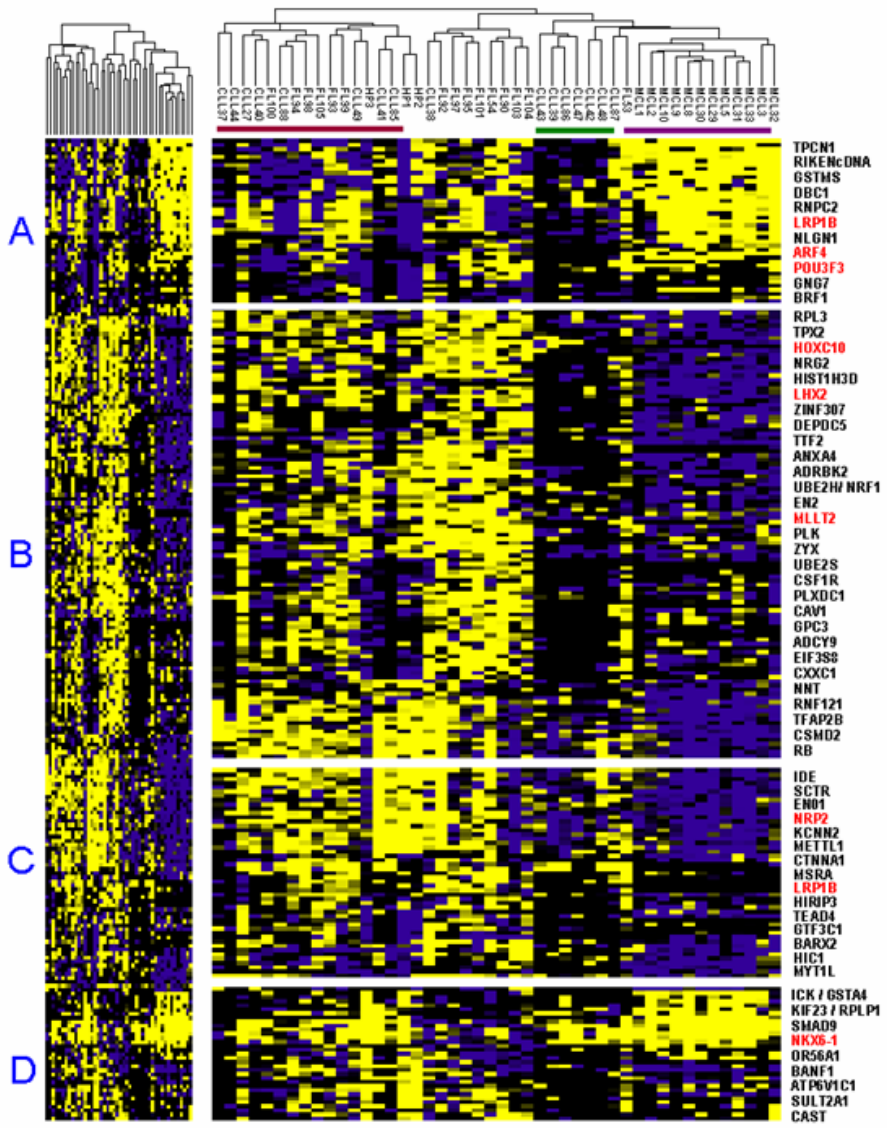

Figure 1.3: Hierarchical clustering analysis of DNA methylation data. The dendrogram on the top lists the patient samples from the small B-cell lymphoma subtypes (MCL, B-CLL, FL) and benign follicular hyperplasia (HP). This illustrates a measure of the relatedness of DNA methylation across all loci for each sample. Each column represents one sample and each row represents a single CGI clone on the microarray chip. The florescence ratios of Cy3/Cy5 are measures of DNA methylation and are depicted as a color intensity (-2.25 to + 2.25). In a log 2 base scale, yellow indicates CpG loci that share higher level of methylation, blue indicates lower level of methylation and black indicates no change. Regions A-D in the left panel illustrates patterns from the overall array. Interesting sub regions for each of these are expanded in the middle panel, and the labels on the right identify named genes that are candidates for further study.

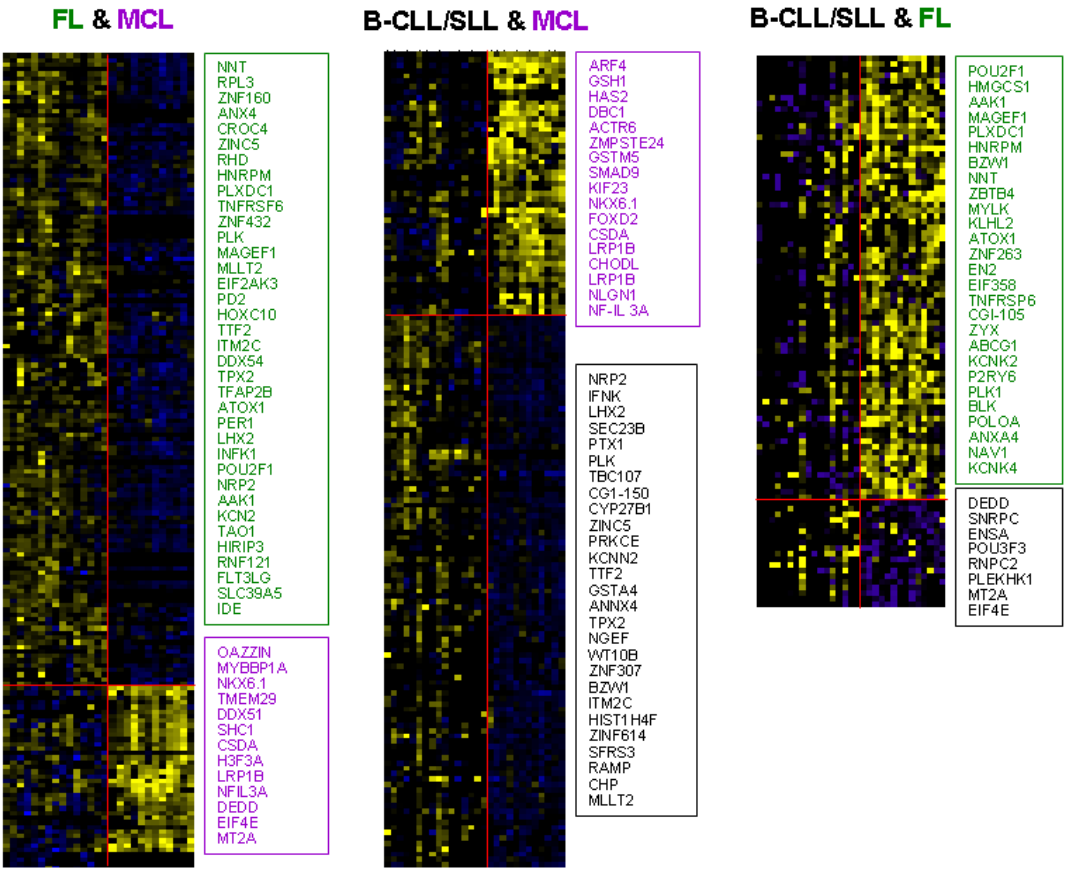

Figure 1.4: Pair wise hierarchical clustering analysis of FL and MCL, B-CLL/SLL and MCL, B-CLL with FL. Regions of each pairing that show preferential methylation of named genes are shown to the right of each set. The florescence ratios of Cy3/Cy5 are measures of DNA methylation and are depicted as a color intensity (-2.25 to +2.25) in log2 base scale.

Confirmation of microarray findings

Microarrays are excellent discovery tools but additional confirmation of selected results is prudent. In order to independently confirm the DNA methylation status of 10 known genes (*NKX6.1, LRP1B, MLLT2, LHX2, ARF4, HOXC10, RAMP, NRP2, POU3F3*, and *PRKCE*) selected to represent each region of the hierarchical clusters, MSP primers were produced, and the conditions optimized using a series of NHL cell lines and then confirmed in SBCL patient. Sequence characterization and chromosomal location of differentially methylated CGI loci are shown in Table1.4

Clone Location	Gene Name	Accession #	CpG Island Location	Amplicon Location	Assay
chr9 : 123858628-123858970	*LHX2*	AF124735	chr9: 123852801-123860507	Chr9 : 123858851-123858949	MSP
chr3 : 57557703-57558663	*ARF4*	BC016325	chr3: 57558061-57558651	Chr3 - 57558364-57558563	MSP
chr2 : 142721862-142722346	*LRP1B*	AF176832	chr2: 142721457-142722285	Chr2 : 142722049-142722154	MSP
chr2 : 45782052-45782913	*PRKCE*	NM_005400	chr2: 45788830-45791336	Chr2 : 45782662-45782800	MSP
chr4 : 85773754-85774366	*NKX6-1*	NM_006168	chr4: 85774839-85777978	Chr4 : 85774136-85774253	MSP
chr12 : 52675489-52676226	*HOXC10*	BC001293	chr12: 52675381-52675787	Chr12 : 52675687-52675873	MSP
chr2 : 104927795-104928343	*POU3F3*	NM_006236	chr2: 104927370-104932006	Chr2 : 104927960-10492983	MSP
chr2 : 206376414-206376687	NRP2	BC009222	chr2: 206375106-206376822	Chr2 : 206376438-206376606	MSP
chr1 : 208596523-208597879	RAMP	BC033297	chr1: 208597233-208597759	Chr1 : 208597643-208597766	MSP
chr4 : 85773754-85774366	NKX6-1	NM_006168	chr4:85771177-85772053 & chr4:85774839-85777978	chr4:85773783-85773994	COBRA

Table 1.4: Independently validated novel epigenetic markers in SBCL.

Eight of these 10 genes were methylated in both cell lines and in *de novo* NHL tumors. The *MLLT2* and *RAMP* genes were examined but were not methylated in any patient samples by MSP, despite the methylation shown in the RL cell line (Figure 1.5). Thus, these genes were not included in any further analyses. Hypermethylation of only one gene, LIM homeobox protein 2 (*LHX2*), was present in all NHL cell lines and a high proportion of patient samples, but the remaining genes were differentially methylated in the various cell lines, which was an observation that would be expected given the relationships of the cell lines to the various stages of differentiation. Interestingly, the remaining genes were predominantly methylated in the germinal center derived cell lines but less so in Granta 519 and Mec-1 cell lines derived from MCL and B-CLL/SLL respectively.

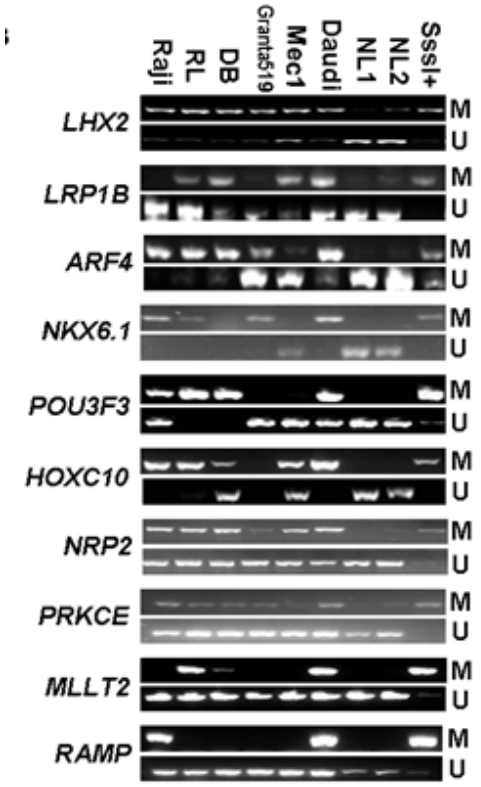

Figure 1.5: MSP validation of a subset of candidate genes from microarray studies using NHL cell lines. One microgram of genomic DNA was bisulfite treated, and then PCR was performed for 35 cycles with primers specific for methylated (M) or unmethylated (U) templates, and the products were analyzed on 3% agarose gel. Normal female (NL1) and normal male (NL2) peripheral blood lymphocyte DNA was used as negative controls, and in vitro methylated DNA using *SssI* methyl transferase was the positive control.

Analysis of CGI methylation patterns in *de novo* SBCL samples

Consistency was found between promoter methylation of the selected genes in NHL cell lines and primary NHLs with the exception of *MLLT2* and *RAMP*. The 8 genes confirmed as described above were examined in 42 NHL patient samples using MSP (Figure1.5).For each of the genes confirmed in patient samples there was a higher incidence of DNA methylation in germinal center-related FLs than in pregerminal center-related NHLs (MCL and B-CLL/SLL) (Figure1.6). For instance, methylation of *POU3F3* was observed in 3/16 (19%) B-CLL/SLL cases, 5/12 (41.6%) MCL cases, and 13/15 (87%) FL cases ($p \leq 0.01$). Due to the nature of the disease, patient samples were not purely tumor DNA (> 80% neoplastic cells); therefore the unmethylated allele that amplified in each patient sample represents either normal tissue found within the tumor or the heterogeneity of methylation within the tumor sample itself. It is important to point out that MSP is more sensitive when identifying one locus at a time. However, the technique we used to generate a hierarchical clustering algorithm (DMH) is for large scale interrogation of highly methylated CGI loci. Therefore, the frequencies of methylation shown in MSP do not always strictly correlate with DMH results.

The percentage of patient samples methylated in each gene promoter and the statistical significance of these observations using the chi-square test, are presented in Table1.5. For instance, in the comparison of B-CLL/SLL with MCL, of the 8 gene promoters examined, only *ARF4* ($p \leq 0.001$) and *HOXC10* ($p \leq 0.05$) revealed differences at $p < 0.05$. For the comparison of FL to B-CLL/SLL, 5 gene promoters were significantly different at $P \leq 0.05$*: LRP1B, ARF4, NKX6-1, POU3F3,* and *NRP2*, but when FL and MCL are compared only 3 gene promoters, *LRP1B, POU3F3*, and *NRP2,* were

statistically different. In the case of *POU3F3*, while all 3 classes revealed DNA methylation, they were all highly different in proportion. Therefore, we were able to confirm that promoter DNA methylation (with the exception of *LHX2*, 3rd intron), as discovered in the microarray experiments, was present in 8 of the 10 genes tested in *de novo* SBCL samples, while all 10 were methylated in NHL cell lines. Gel images, the genomic DNA regions and the chromosomal locations of these genes are depicted in Figures 1.7-1.14.

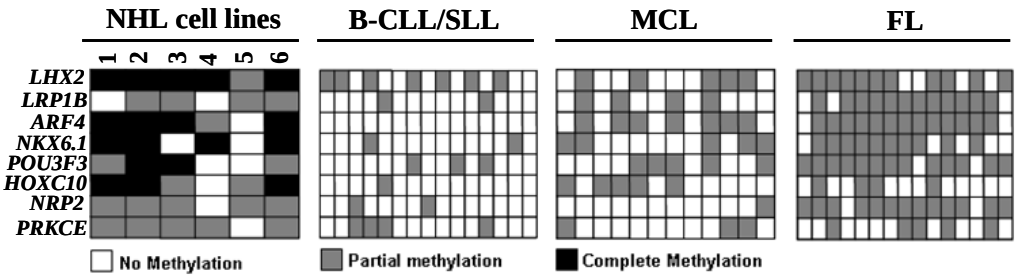

Figure 1.6: Determination of DNA methylation of eight genes from microarray findings in SBCL subsets (MCL, B-CLL/SLL and FL). The left panel shows patterns in the NHL cell lines including Raji(1), RL(2), DB(3), Granta519(4), Mec1 (5), and Daudi(6); the *de novo* tumor groups are indicated at the top of each additional panel, with the gene names listed to the left. The methylation status of a given gene in a particular patient is indicated by a filled square.

N=42	B-CLL/SLL		MCL		FLI		B-CLL/SLL / MCL	B-CLL/SLL /FL	FL/MCL
Genes	M	%	M	%	M	%	P-Value results are all ≤ the number shown		
LHX2	7/15	46.6	5/12	41.6	11/15	73	1.0	0.2	0.1
LRP1B	2/15	13.3	4/12	33.3	13/15	86.6	1.0	0.001	0.01
ARF4	0/15	0	7/12	58.3	13/15	86.6	0.001	0.001	0.1
NKX6-1	2/15	13.3	5/12	41.6	10/15	66.6	0.1	0.01	0.2
POU3F3	3/15	20	5/12	41.6	13/15	86.6	1.0	0.001	0.025
HOX10	1/15	6.6	5/12	41.6	4/15	26.6	0.05	0.2	1.0
NRP2	2/15	15.3	1/12	8.3	13/15	86.6	1.0	0.001	0.001
PRKCE	4/15	26.6	3/12	25	5/15	33.3	1.0	1.0	1.0

Table 1.5: Statistical evaluation of comparative DNA methylation (N=42). For each gene validated in patient samples, the proportion of samples from each class of NHL that were methylated and the pair wise chi square analysis are shown.

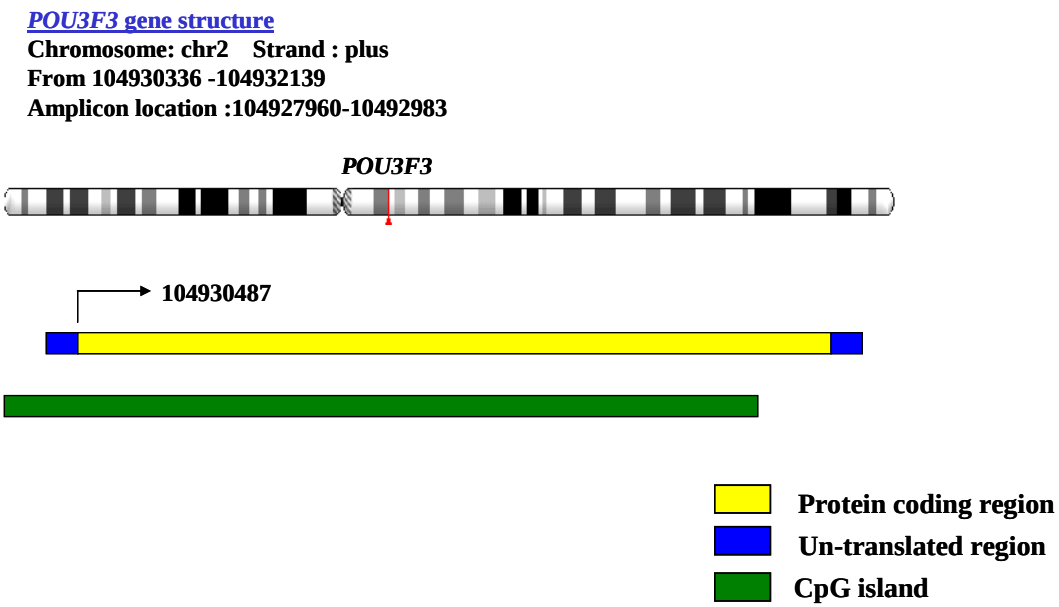

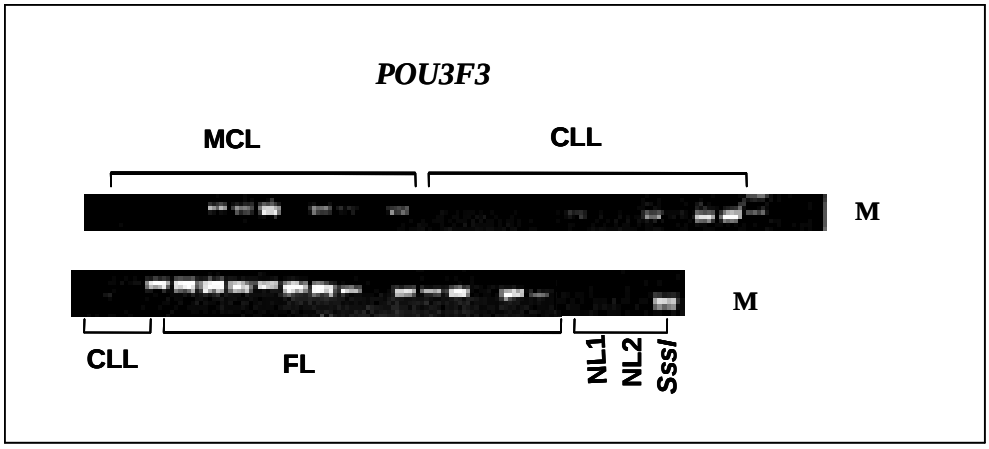

Figure 1.7: Methylation Specific PCR analysis of *POU3F3*. To study the DNA methylation status of *POU3F3* which is located on chromosome 2, Methylation specific PCR (MSP) was performed on 12 MCL, 15 CLL, and 15 FL. 1µg of DNA initially was used to do bisulfite conversion. Primers representing methylated and unmethylated allele were designed. The PCR products from these primers were separated on 2% agarose gel. The presence or absence of band in the methylated lane signifies the methylation status of interrogated CGI locus. The position of amplicon in respect to the *POU3F3* gene structure is indicated. This information was obtained from http://dbtss.hgc.jp/.

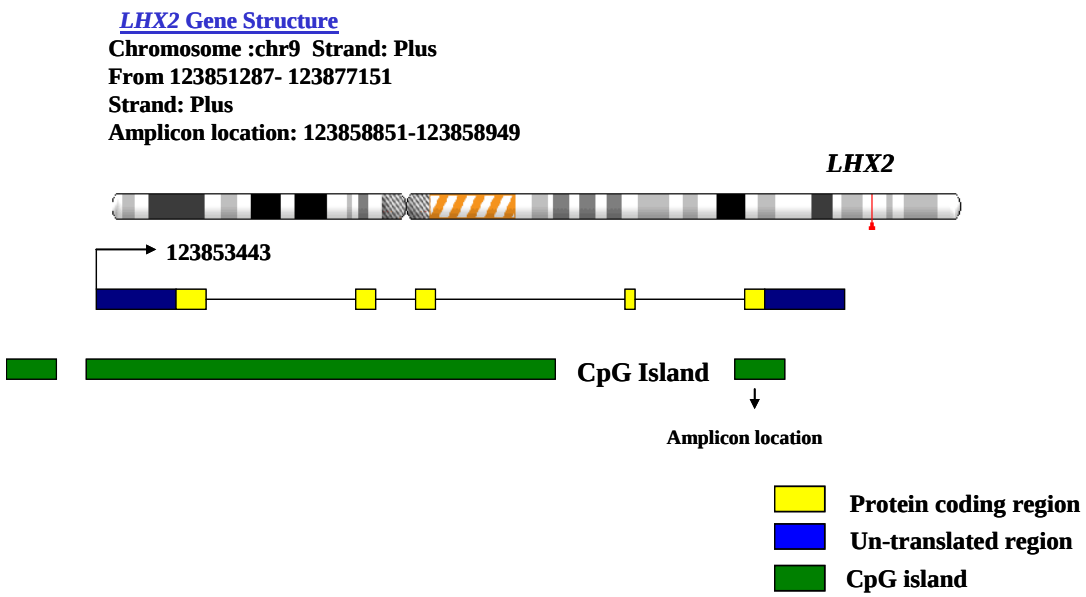

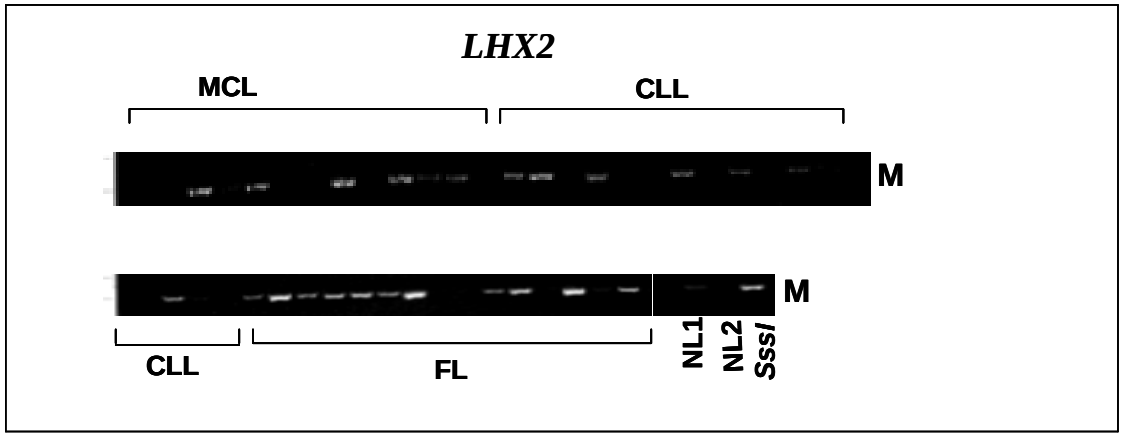

Figure 1.8: MSP analysis of *LHX2*. Methylation specific PCR (MSP) was performed to study the DNA methylation status of a clone that is located in the third intron of *LHX2* gene.

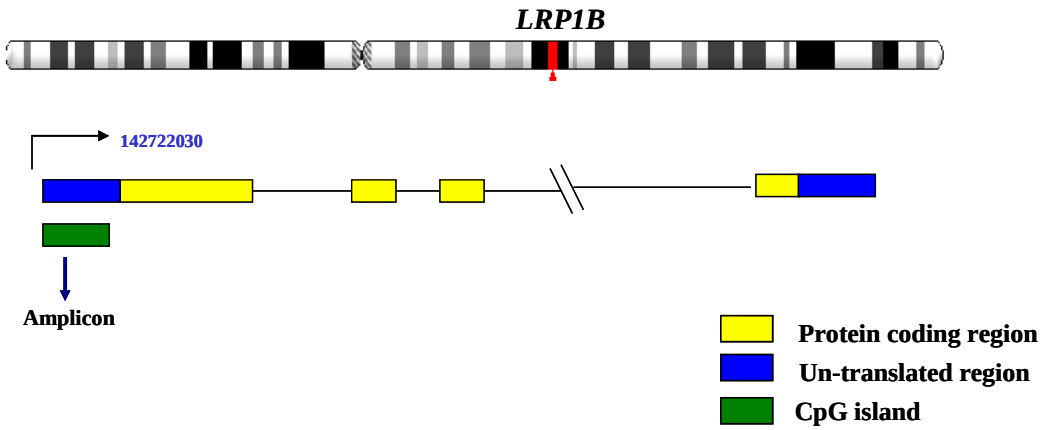

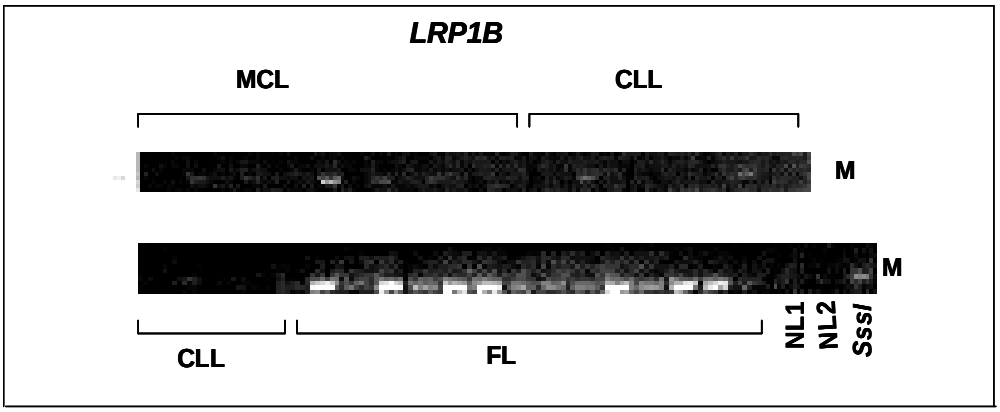

Figure 1.9: MSP analysis of *LRP1B*. Methylation Specific PCR analysis of a CGI clone located in the promoter region of the *LRP1B* gene in SBCLs, normal female peripheral blood lymphocyte (NL1), male normal peripheral blood lymphocytes (NL2) and in vitro methylated DNA using *SssI* was investigated.

***NRP2* gene structure**

Chromosome: Chr2 Strand: Plus
From 206360438-206499991
Amplicon location : chr2: 206376438-206376606

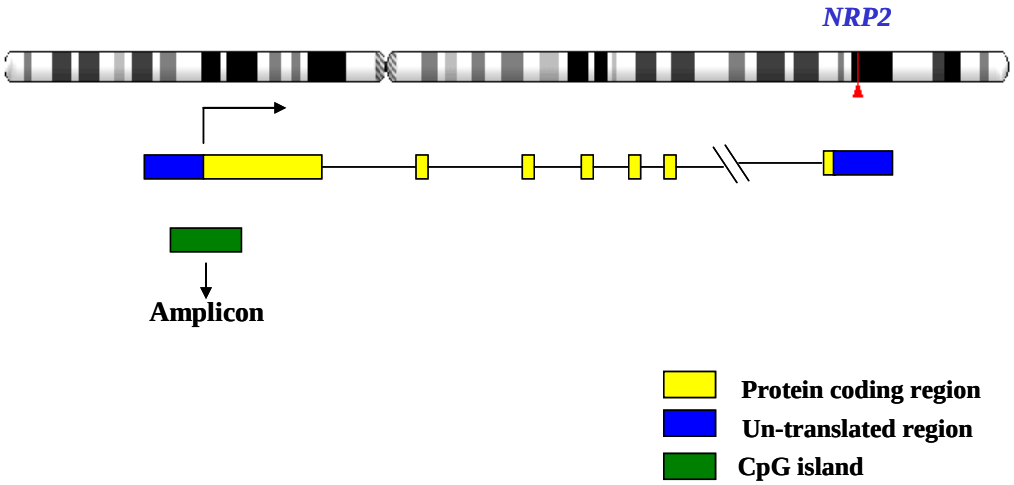

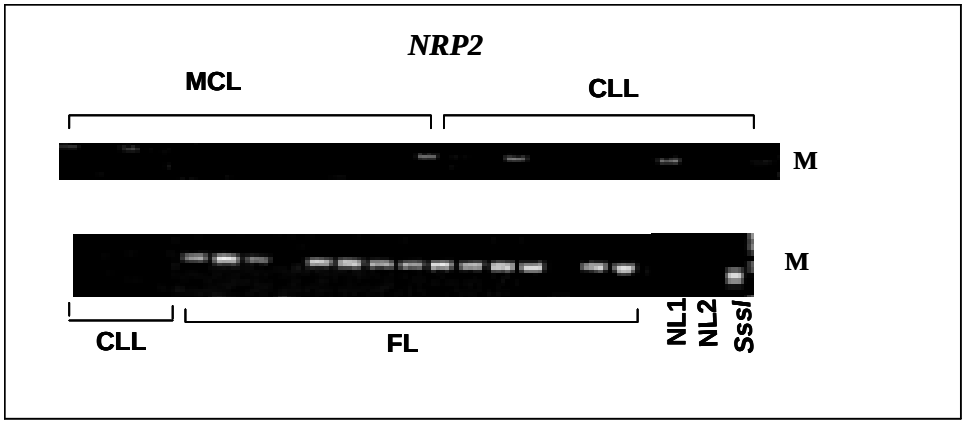

Figure 1.10: MSP analysis of *NRP2*. Methylation Specific PCR (MSP) was performed to study the DNA methylation status of CpG clones located in the promoter region of the *NRP2* gene in SBCL patient samples ,the normal control and the positive control.

***ARF4* gene structure**

Chromosome :Chr3 Strand :Minus
From: 57529505-57561004
Amplicon location :Chr3 57558364-57558563

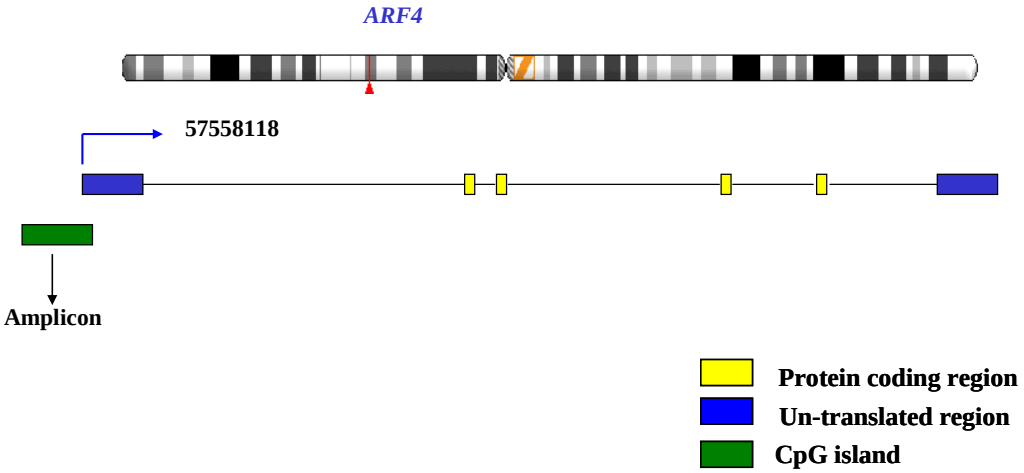

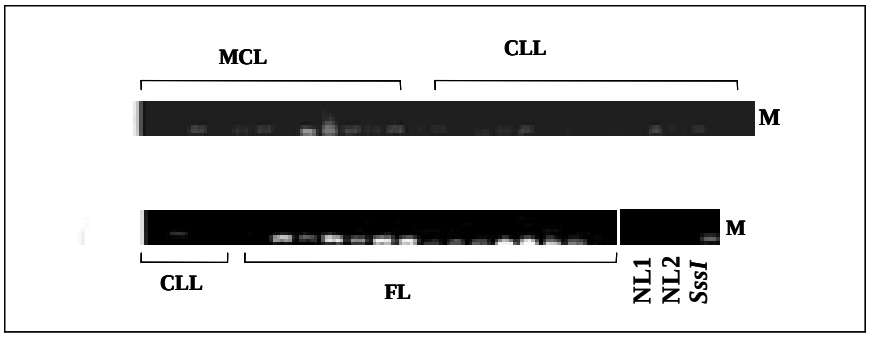

Figure 1.11: MSP analysis of *ARF4*. Schematic map showing the *ARF4* gene structure. The CpG island is indicated as a thick horizontal green bar, directly beneath this is the region investigated by MSP analysis. The translational start site is marked by a left arrow. The methylated DNA is indicated.

***NKX6.1* Gene Structure**
Chromosome: Chr4 Strand: Minus
From 85771119-85777061
Amplicon location : Chr4: 85773783-85773994

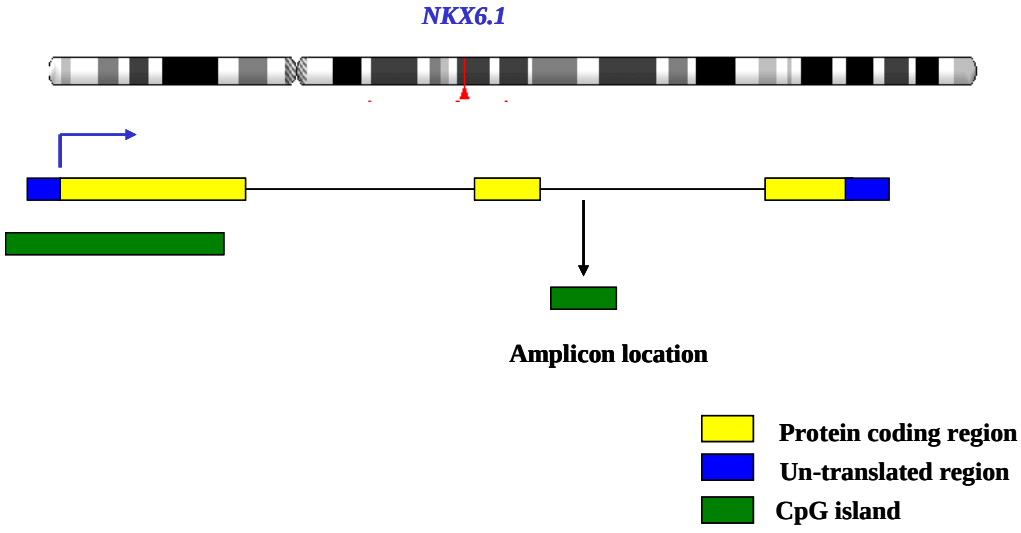

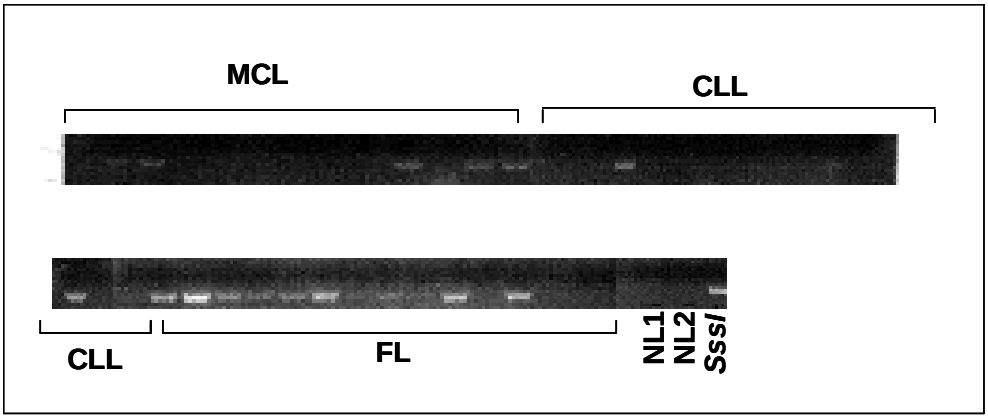

Figure 1.12: MSP analysis of *NKX6.1*: Representative results of methylation specific PCR analysis of the *NKX6.1* in SBCLs are shown. The CpG clone (amplicon) includes parts of the second intron.

HOXC10 gene structure
Chromosome: Chr12 Strand: Plus
From 52664594-52670848
Amplicon location, chr12 52675687-52675873

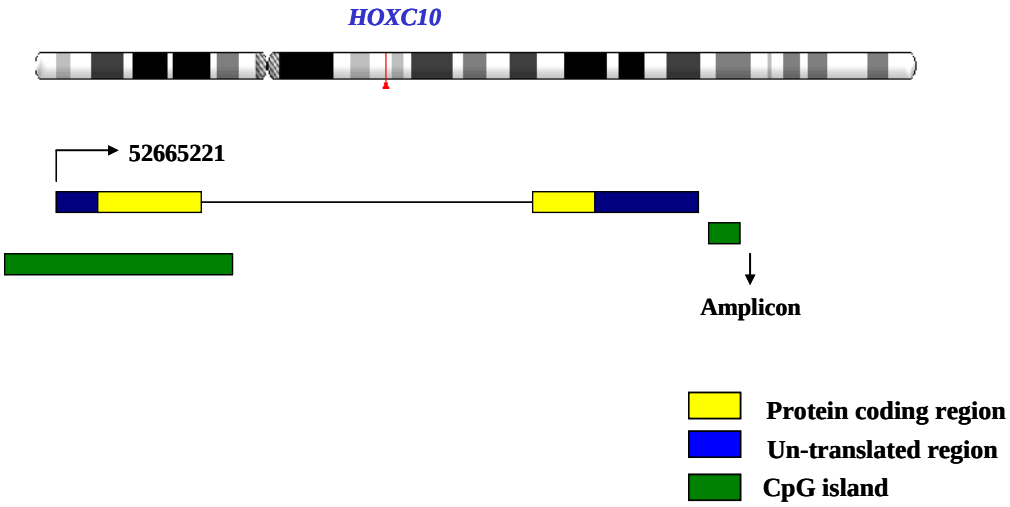

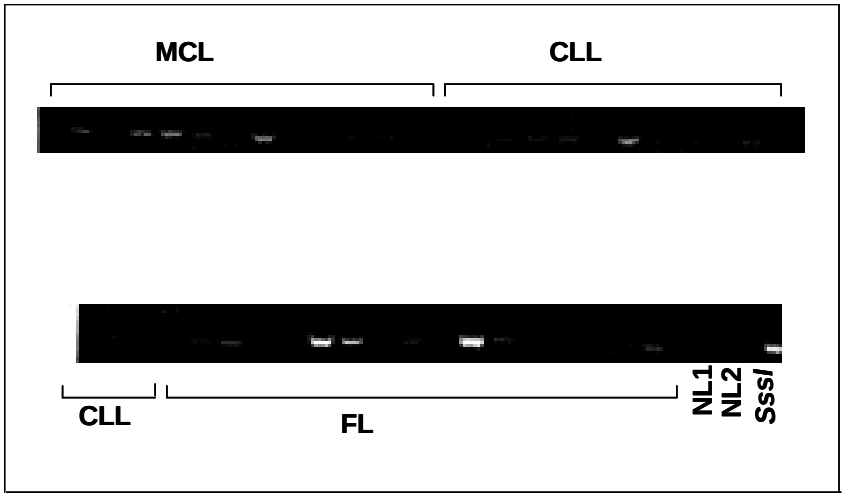

Figure 1.13: MSP analysis of *HOXC10*. Schematic map showing the structure of the *HOXC10* gene. The position of CGI clone (amplicon) is illustrated. The primer sets used for amplification are designated as methylated (M).

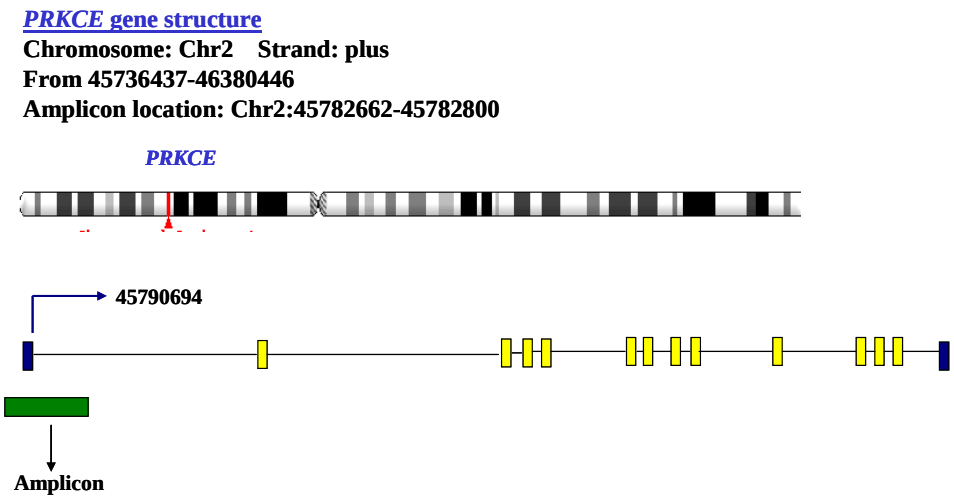

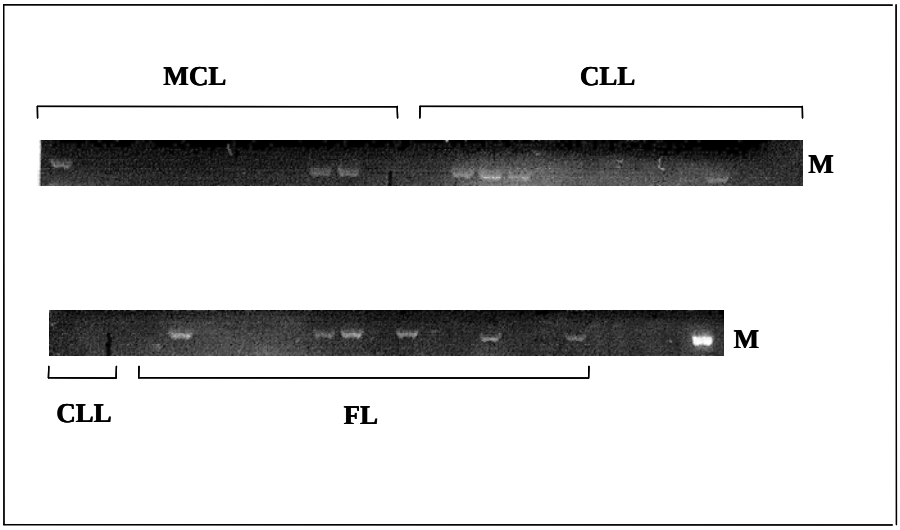

Figure 1.14: MSP analysis of *PRKCE*. Methylation Specific PCR analysis of CGI clone located in the promoter region of the *PRKCE* gene in SBCLs is shown. Normal peripheral blood lymphocyte and *in vitro* methylated DNA serve as negative and positive controls respectively.

Bisulfite Genomic Sequencing of *LRP1B* and *LHX2*

To further evaluate the quality of the array data, we used bisulfite sequencing to assess the methylation status of each CpG dinucleotides within the 2 CGI loci that were found to be differentially methylated (Figure 1.15 A). Consistent with microarray and MSP analysis, two out of three MCL patient samples showed high levels of DNA methylation in the CpG island of *LRP1B*, whereas all three B-CLL/SLL patient samples had no, or very low, levels of methylation (Figure 1.15 B). Conversely, *LRP1B* tended to be extensively methylated in three FL patient samples. Bisulfite sequencing on *in vitro* methylated DNA (*SssI* treated DNA) showed dense methylation in CG sites; whereas normal blood showed no methylation in that region. Moreover, bisulfite sequencing of *LRP1B* in NHL cell lines was in complete agreement with MSP results.

We also studied the DNA methylation patterns of *LHX2*, a known biomarker in early B cell differentiation [25]. The NHL cell lines displayed a near complete methylation of the *LHX2* amplified fragment. In primary tumors, *LHX2* showed a heterogeneous pattern of DNA methylation in CpG dinucleotides sites (Figure1.15 B). It is important to mention that the lower frequency of methylation in primary tumor compared to corresponding cell lines could be the result of contamination of the primary tumor (80% tumor cells) with normal lymphoid tissues and the unavailability of corresponding normal samples, causing underestimation.

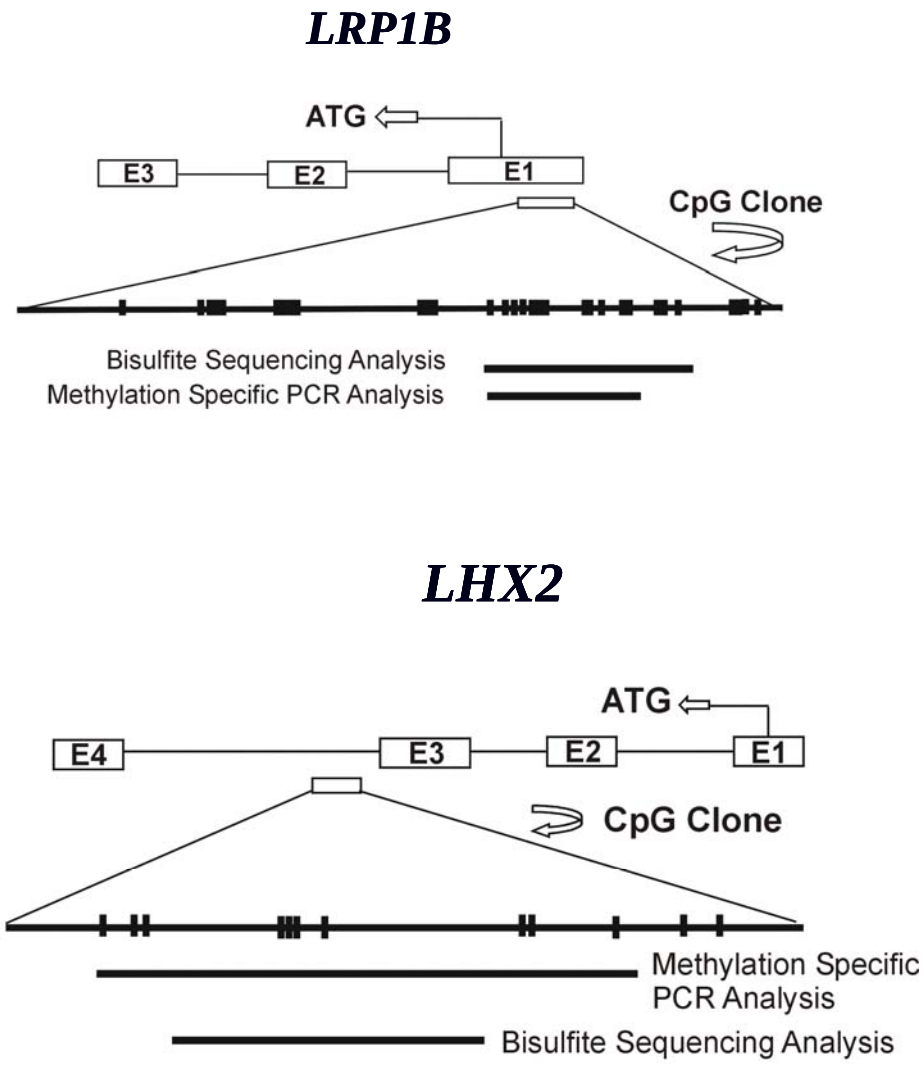

Figure 1.15 A: Schematic map of *LRP1B* and *LHX2* in the genome. Schematic maps showing the CpG island segments, including the CpG clone for the *LRP1B* and *LHX2*. The CpG loci is indicated by the thick horizontal bar, directly beneath this are the regions investigated by MSP and bisulfite sequencing analysis. CpG sites are shown as vertical thick lines on the expand axis; exon1is indicated by an open box labeled E1. Location of the CGI clone is shown as an open box, and the translational start site is marked by a left arrow. For *LRP1B,* the CpG clone includes the parts of exon1 that occur prior to the translational start site and for *LHX2* the clone is located in the third intron.

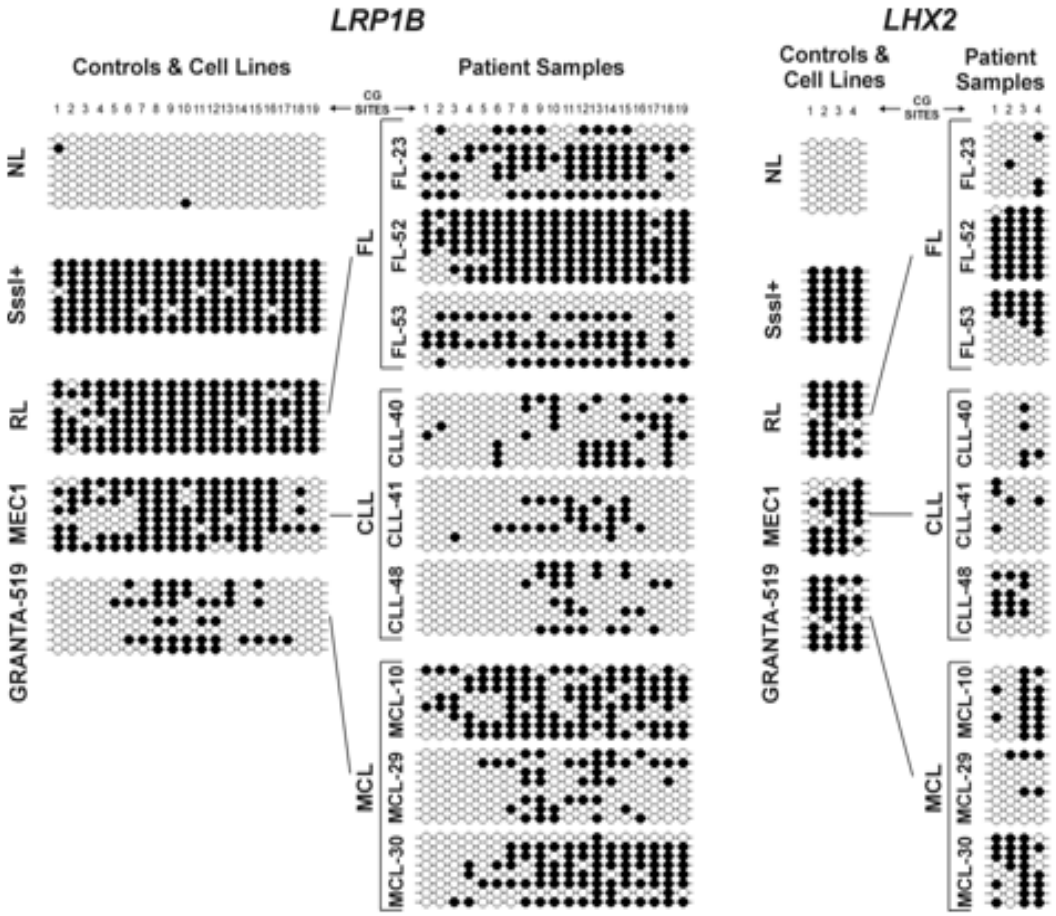

Figure 1.15 B: Bisulfite sequencing of *LRP1B* and *LHX2* in NHL cell lines and SBCL. The left and right panels represent *LRP1B* and *LHX2* respectively. Sequencing for both genes was performed on 9 SBCL patient samples (three patients from each subset) and three NHL cell lines. In addition, normal peripheral blood lymphocyte and *in vitro* methylated DNA (*SssI* treated DNA) served as negative and positive controls, respectively. Each row represents the sequence of individual clones; closed circles indicate methylated CpG sites and open circles indicate unmethylated CpG sites.

To assess the extent to which the MSP results were confirmed by bisulfite sequencing, the kappa statistic (a type of intra-class correlation) was computed for *LHX2* and *LRP1B*. Kappa equals one when there is perfect agreement, negative one when there is perfect disagreement, and zero when there is chance agreement. [23] For this data, the estimated value of kappa is 0.545 [95% CI: (0.196, 0.894]), which is significantly different from zero (exact p=0.021, ASE=0.178). Thus, the agreement between MSP and bisulfite sequencing is 54% greater than what would be expected by chance. Overall, the proportion of agreement is 79% (19/24). Considering bisulfite sequencing as the gold standard, the sensitivity of MSP is 87%, while the specificity is 67%. It has been noted that MSP is more sensitive than it is specific.

Epigenetic reactivation of methylated genes

To determine whether the differential methylation was associated with gene silencing and to explore the effect of demethylation on restoring the expression of *LRP1B*, *LHX2, POU3F3* and *ARF4* in NHL cell lines, we conducted a quantitative real time RT-PCR, with each experiment repeated three times and the median was calculated. Results illustrated in (Figure 1.16A) show that all of these genes were either expressed at low level or they were undetectable in the cell lines before treatment. Induction of these genes occurred after treatment with 1μm 5-Aza, with exception of *LHX2* in the Granta 519 cell line.

LRP1B and *LHX2* mRNA expression in primary SBCL samples

We next assessed levels of *LRP1B* and *LHX2* mRNA in primary SBCL tumor cells and non-malignant lymphoid cells. Results shown in Figure 1.16B indicate that *LRP1B* is detectable at low levels (at least 100 fold) in FL, B-CLL/SLL, and MCL compared to the normal peripheral blood lymphocytes. Within the SBCL group, *LRP1B* was highest in MCL patients when compared to FL and B-CLL/SLL, in spite of showing a high frequency of methylation by bisulfite sequencing. It should be noted that the actual patient samples used for expression analysis and bisulfite sequencing were not all the same due to sample limitations. We also tested *LHX2* expression, and found low levels of mRNA in all 3 types of SBCL, as well as in normal lymph node samples, compared to normal peripheral blood lymphocytes. Study conducted by XU *et a*l revealed that the precursor B-cells express high levels of *LHX2* expression, whereas more mature B-cells have lower levels. The higher levels in normal peripheral blood lymphocyte are likely a reflection of the presence of mainly T-cells, where there does not appear to be a differentiation-related expression pattern.

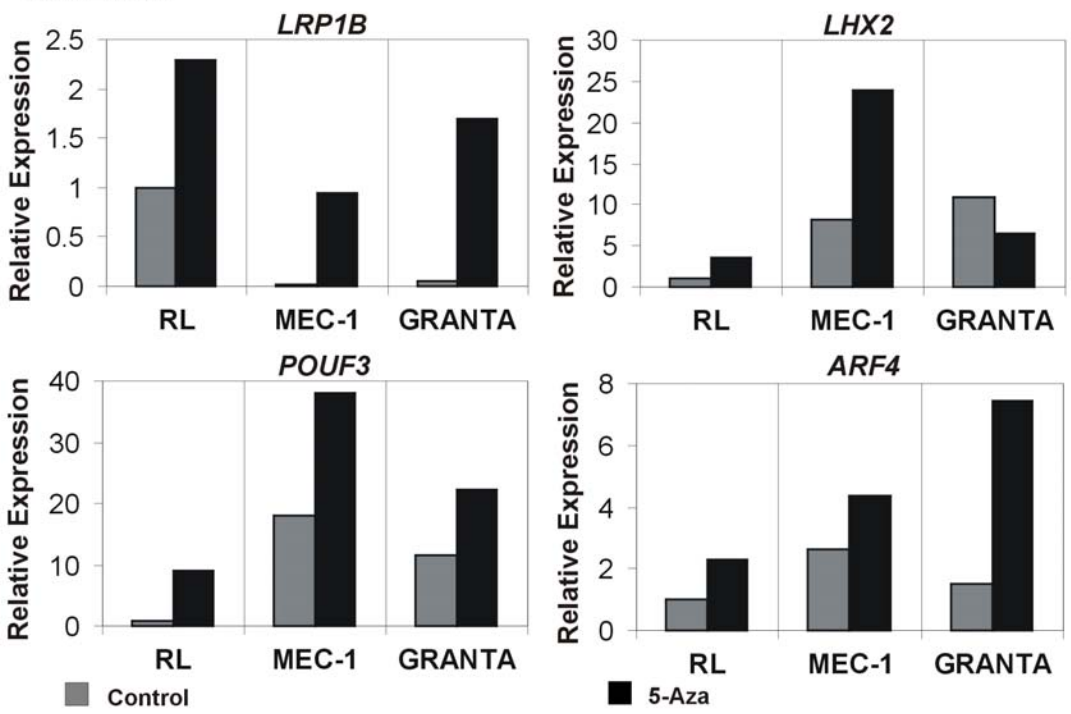

Figure 1.16 A: Expression analysis of *LRP1B*, *LHX2*, *POU3F3* and *ARF4* in three CLL cell lines. Expression levels of these genes quantified using real time RT-PCR in untreated RL, Mec1, and Granta 519, cell lines following treatment with demethylating agent 5'Aza at 1μM concentration. *HPRT 1*(house keeping gene*)* was used as an internal control. The relative expression was determined using $2^{\Delta\Delta Ct}$, where Ct is the cycle threshold.

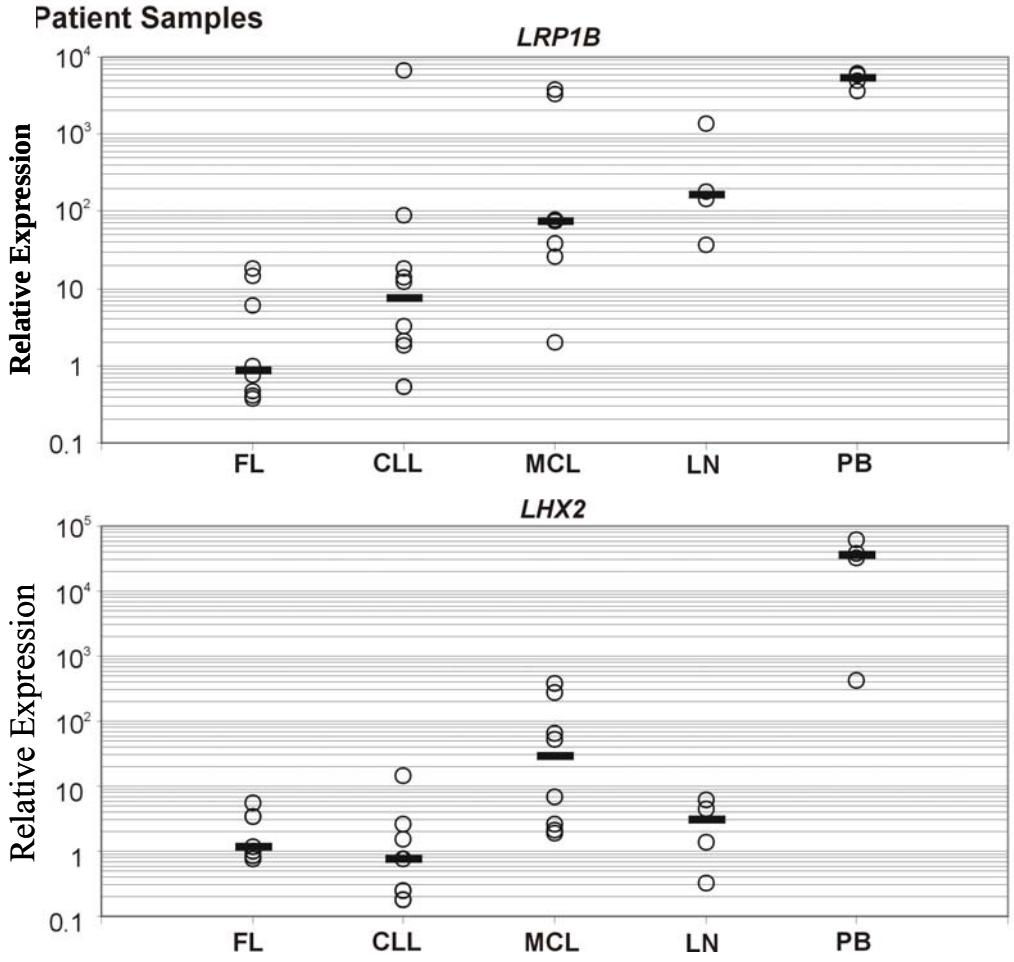

Figure 1.16 B: Expression of *LRP1B* and *LHX2* transcripts in SBCL patient, lymph node and normal peripheral blood lymphocyte samples.
Each circle represents a unique sample, and the solid horizontal bar indicates the median.

Discussion

It is now becoming clear that despite the enormous contribution of the Human Genome Project to developing a sequence of human DNA, it is just the beginning in terms of understanding the human cancer genome. An entire area of non-sequence-related alterations known as epigenetics is now accepted as having profound effects on human cells; thus there is a need to further dissect the cancer epigenome. Some of these epigenetic alterations include the methylation and/or acetylation status of histones, hypomethylation of genomic DNA, and hypermethylation of gene promoter DNA, as well as others yet to be described. [26;27] The epigenome is becoming even more important because there have been a great deal of recent pharmaceutical development that can potentially reverse epigenetic alterations.[28;29]. It is toward the goal of characterizing the human lymphoma epigenome that this study of 3 classes of NHL was undertaken.

The SBCLs exhibit a spectrum of clinical behaviors and the cell of origin of each subtype is thought to be related to a putative stage of normal B-cell differentiation. The mutational status of the variable region of immunoglobulin heavy chain (V_H) genes is a useful marker for identifying different developmental stages of NHLs and relates to processes that occur in the germinal center reaction. MCL is understood as arising in cells at the pre-germinal center stage where V_H genes have not yet become mutated. [30] In FL, somatic hypermutation of V_H genes characteristic of the germinal center reaction suggests that this class of NHL derives from a germinal center stage of differentiation. Approximately half of B-CLL/SLL cases are CD38+ with unmutated V_H genes (poor prognosis), and the remaining half are CD38- with mutated V_H genes (better prognosis). Thus, B-CLL/SLL may represent two separate stages of differentiation: pre-germinal

center and post-germinal center, respectively. The SBCL subtypes studied represent a spectrum of pre-germinal center, germinal-center, and post germinal-center stages of B-cell differentiation and provide a good model to study epigenetic alterations as they might relate to the various compartments of secondary lymphoid tissue cell differentiation.

High-throughput technologies have clearly advanced our understanding of the gene expression repertoire of human tumors. However, such studies do not address the underlying reason(s) for changes in gene expression. The CGI microarray was utilized to investigate part of the NHL epigenome of SBCL subtypes based on interrogation of promoter DNA methylation a process that plays a role in human cancers by frequently silencing not only tumor suppressor genes, but also genes that are critical to the normal functions of cells. A study conducted in our laboratory using a Methylation Specific Oligonucleotide microarray on SBCLs (The actual patient samples used in this study were completely different from those that we included in our current study) identified a different set of genes that are of biological interest and represent candidate diagnostic and prognostic markers.[31]

Our statistical analysis of data from the CGI microarray identified approximately 256 named, variably methylated genes within SBCL subtypes and recognized genes that are important to many intracellular processes. Additional CGI loci were also differentially methylated, but at this time some are hypothetical genes and some have not yet been investigated for identity. The *LHX2* gene belongs to a superfamily of homeobox-containing genes conserved during evolution which functions as transcriptional regulatory proteins in control of lymphoid and neural cell differentiation. The *LHX2* gene found to be methylated by our array data, MSP and bisulfite sequencing across all the

NHL cell lines and subsets of SBCL patient samples. In B-cell differentiation, *LHX2* was found to be expressed in early stages of B cell differentiation but not in plasmacytoma cell lines. Low levels of *LHX2* expression were detected in FL, CLL and MCL patient samples, which are also more mature B-cells. The POU family proteins (POU3F3) act as transcriptional factors and regulate tissue-specific gene expression at different stages of development in the nervous system [32] ; and POU3F3 is preferentially methylated in FL patients, as was non-kinase neuropilin 2 (*NRP2*). The *NRP2* gene encodes a member of the neuropilin family of receptors that binds to *SEMA3C* (sema domain, Ig domain, short basic domain, secreted, semaphoring 3C) protein and also interacts with vascular endothelial growth factor (VEGF) [33], which is an important mediator of angiogenesis. Additionally, ADP ribosylation factor 4 (*ARF4*), which plays a role in vesicular trafficking and is an activator of phospholipase D, was methylated in 7/12 (58.3%) of MCL and 13/15 (87%) FL cases ($p \leq 0.001$). Phospholipase D is an enzyme involved in the CD38 signaling pathway which regulates lymphocyte activation and differentiation. [34] The *LRP1B* gene is frequently deleted in various tumor types, but this study shows a higher frequency of gene promoter methylation in germinal center SBCLs compared to the other subtypes ($p \leq 0.001$). CGI promoter hypermethylation of this gene has also been detected in esophageal squamous cell carcinomas. [35]

This study demonstrates the value of the high-throughput CGI microarray [36] in cancer research. In a recent study [37] comparing this 9K library to another containing 12,192 (12K) clones, only 753 were found to be common between the 2 libraries, thus suggesting that the present study examined ~50% of potential MseI- restricted CGI sequences in the human genome. Nevertheless, this does not diminish the value of finding

many new epigenetically altered genes that segregate with subclasses of NHL. Additional more targeted studies using the 12K CGI library are currently in process and should further advance our attempts to begin addressing the human lymphoma epigenome. This study also illustrates a very interesting biological finding: there is preferential methylation of multiple gene promoters in germinal-center tumors such as FL compared to pre-germinal center tumors (MCL and some B-CLL/SLL) and post-germinal center tumors (subset of B-CLL/SLL). The reasons for this are not entirely clear but may be related to the ongoing somatic hypermutations and the process of DNA strand breaks and repair (both effective and ineffective) that accompany germinal-center biology, and which may be possibly carried over into germinal-center NHLs. The findings of this study provide a basis for further investigations of gene promoter DNA methylation in NHLs and begin to provide insights into the functional epigenomic signatures of human lymphomas as a prelude to characterizing and understanding the cancer epigenome.

Reference List

1. Jaffe ES. Anaplastic large cell lymphoma: the shifting sands of diagnostic hematopathology. Mod.Pathol. 2001;14:219-228.

2. Dohner H, Stilgenbauer S, Benner A et al. Genomic aberrations and survival in chronic lymphocytic leukemia. N.Engl.J.Med. 2000;343:1910-1916.

3. Egger G, Liang G, Aparicio A, Jones PA. Epigenetics in human disease and prospects for epigenetic therapy. Nature 2004;429:457-463.

4. Costello JF, Fruhwald MC, Smiraglia DJ et al. Aberrant CpG-island methylation has non-random and tumour-type-specific patterns. Nat.Genet. 2000;24:132-138.

5. Li Y, Nagai H, Ohno T et al. Aberrant DNA methylation of p57(KIP2) gene in the promoter region in lymphoid malignancies of B-cell phenotype. Blood 2002;100:2572-2577.

6. Cameron EE, Baylin SB, Herman JG. p15(INK4B) CpG island methylation in primary acute leukemia is heterogeneous and suggests density as a critical factor for transcriptional silencing. Blood 1999;94:2445-2451.

7. Katzenellenbogen RA, Baylin SB, Herman JG. Hypermethylation of the DAP-kinase CpG island is a common alteration in B-cell malignancies. Blood 1999;93:4347-4353.

8. Koyama M, Oka T, Ouchida M et al. Activated proliferation of B-cell lymphomas/leukemias with the SHP1 gene silencing by aberrant CpG methylation. Lab Invest 2003;83:1849-1858.

9. Kawano S, Miller CW, Gombart AF et al. Loss of p73 gene expression in leukemias/lymphomas due to hypermethylation. Blood 1999;94:1113-1120.

10. Byrd JC, Stilgenbauer S, Flinn IW. Chronic lymphocytic leukemia. Hematology.(Am.Soc.Hematol.Educ.Program.) 2004163-183.

11. Glas AM, Kersten MJ, Delahaye LJ et al. Gene expression profiling in follicular lymphoma to assess clinical aggressiveness and to guide the choice of treatment. Blood 2005;105:301-307.

12. Alizadeh A, Eisen M, Davis RE et al. The lymphochip: a specialized cDNA microarray for the genomic-scale analysis of gene expression in normal and malignant lymphocytes. Cold Spring Harb.Symp.Quant.Biol. 1999;64:71-78.

13. Adorjan P, Distler J, Lipscher E et al. Tumour class prediction and discovery by microarray-based DNA methylation analysis. Nucleic Acids Res. 2002;30:e21.

14. Rush LJ, Raval A, Funchain P et al. Epigenetic profiling in chronic lymphocytic leukemia reveals novel methylation targets. Cancer Res. 2004;64:2424-2433.

15. Liu TH, Raval A, Chen SS et al. CpG island methylation and expression of the secreted frizzled-related protein gene family in chronic lymphocytic leukemia Cancer Res 2006;66:653-658.

16. Eisen MB, Spellman PT, Brown PO, Botstein D. Cluster analysis and display of genome-wide expression patterns. Proc.Natl.Acad.Sci.U.S.A 1998;95:14863-14868.

17. Beckwith M, Longo DL, O'Connell CD, Moratz CM, Urba WJ. Phorbol ester-induced, cell-cycle-specific, growth inhibition of human B-lymphoma cell lines. J.Natl.Cancer Inst. 1990;82:501-509.

18. Yang H, Chen CM, Yan P et al. The androgen receptor gene is preferentially hypermethylated in follicular non-Hodgkin's lymphomas. Clin.Cancer Res. 2003;9:4034-4042.

19. Amin HM, McDonnell TJ, Medeiros LJ et al. Characterization of 4 mantle cell lymphoma cell lines. Arch.Pathol.Lab Med. 2003;127:424-431.

20. Stacchini A, Aragno M, Vallario A et al. MEC1 and MEC2: two new cell lines derived from B-chronic lymphocytic leukaemia in prolymphocytoid transformation. Leuk.Res. 1999;23:127-136.

21. Cross SH, Charlton JA, Nan X, Bird AP. Purification of CpG islands using a methylated DNA binding column. Nat.Genet. 1994;6:236-244.

22. Hochberg Y, Benjamini Y. More powerful procedures for multiple significance testing. Stat.Med. 1990;9:811-818.

23. Alan Agresti. Categorical Data Analysis.: Wiley: New York ; 2002.

24. Jaffe ES, Harris NL, Stein H, Vardiman JE. World Health Organization Classification of Tumors. Pathology and Genetics of Tumours of Haematopoietic and Lymphoid Tissues. Lyon: IARC Press; 2001.

25. Xu Y, Baldassare M, Fisher P et al. LH-2: a LIM/homeodomain gene expressed in developing lymphocytes and neural cells. Proc.Natl.Acad.Sci.U.S.A 1993;90:227-231.

26. Jones PA, Baylin SB. The fundamental role of epigenetic events in cancer. Nat.Rev.Genet. 2002;3:415-428.

27. Laird PW. Cancer epigenetics. Hum.Mol.Genet 2005;14 Spec No 1:R65-R76.

28. Shaker S, Bernstein M, Momparler LF, Momparler RL. Preclinical evaluation of antineoplastic activity of inhibitors of DNA methylation (5-aza-2'-deoxycytidine) and histone deacetylation (trichostatin A, depsipeptide) in combination against myeloid leukemic cells. Leuk.Res 2003;27:437-444.

29. Laird PW. The power and the promise of DNA methylation markers. Nat.Rev.Cancer 2003;3:253-266.

30. Stevenson FK, Sahota SS, Ottensmeier CH et al. The occurrence and significance of V gene mutations in B cell-derived human malignancy. Adv.Cancer Res. 2001;83:81-116.

31. Guo J, Burger M, Nimmrich I et al. Differential DNA methylation of gene promoters in small B-cell lymphomas. Am.J.Clin.Pathol. 2005;124:430-439.

32. Schreiber J, Enderich J, Sock E et al. Redundancy of class III POU proteins in the oligodendrocyte lineage. J.Biol.Chem. 1997;272:32286-32293.

33. Chen H, Chedotal A, He Z, Goodman CS, Tessier-Lavigne M. Neuropilin-2, a novel member of the neuropilin family, is a high affinity receptor for the semaphorins Sema E and Sema IV but not Sema III. Neuron 1997;19:547-559.

34. Moreno-Garcia ME, Lopez-Bojorques LN, Zentella A et al. CD38 signaling regulates B lymphocyte activation via a phospholipase C (PLC)-gamma 2-independent, protein kinase C, phosphatidylcholine-PLC, and phospholipase D-dependent signaling cascade. J.Immunol. 2005;174:2687-2695.

35. Sonoda I, Imoto I, Inoue J et al. Frequent silencing of low density lipoprotein receptor-related protein 1B (LRP1B) expression by genetic and epigenetic mechanisms in esophageal squamous cell carcinoma. Cancer Res. 2004;64:3741-3747.

36. Yan PS, Chen CM, Shi H et al. Dissecting complex epigenetic alterations in breast cancer using CpG island microarrays. Cancer Res. 2001;61:8375-8380.

37. Heisler LE, Torti D, Boutros PC et al. CpG Island microarray probe sequences derived from a physical library are representative of CpG Islands annotated on the human genome. Nucleic Acids Res. 2005;33:2952-2961.

Chapter 2

DNA methylation in Chronic Lymphocytic Leukemia segregates with CD38 expression

Abstract

B-cell chronic lymphocytic leukemia (CLL) is a biologically heterogeneous disorder with a clinical course that ranges from indolent to rapidly progressive. The level of CD38 expression is related to B-cell receptor signaling in CLL B cells and is one biomarker that predicts prognosis in patients with CLL. A discovery-based study was initiated to determine if DNA methylation was related to leukemic B- cell CD38 expression (1%-92%). Following initial microarray discoveries, the data were analyzed as a two-class problem of CD38 expression as a discriminator of DNA methylation. Although many loci were either methylated or unmethylated across all CD38 levels, differential methylation was also present. Fifteen genes (*ADAM12*, *APC2*, *DLC-1*, *DLEU7*, *DMRT2*, *DUOX2*, *HOXC10*, *KCNK2*, *LHX2*, *LRP1B*, *NRP2*, *PCDHGB7*, *POU3F3*, *RLN2*, and *SFRP2*) identified from DNA methylation microarrays and prior studies, were selected for further validation by alternative methods. Genomic sequencing of *DLEU7* confirmed extensive cytosine methylation preferentially in patient samples with low CD38 expression ($\leq$ 10%) and the mutated immunoglobulin variable heavy-chain gene (IgV_H). We also investigated the relationship between methylation and expression of genes before and after treatment with epigenetic modifiers. This study demonstrates that CLL is characterized by nonrandom CpG island methylation patterns that segregate with CD38 expression. Such epigenetic modifications might therefore contribute to differing biological behaviors of the CD38 subsets and/or impact epigenetic therapies.

Introduction

Formerly, B chronic lymphocytic leukemia (CLL) was considered a single disease occurring mainly in the elderly, with a variable but generally indolent clinical course. It is now clear that CLL is a heterogeneous disease with at least 2 subtypes in terms of both biological make-up and prognosis (reviewed in [1]). Some patients survive for many years without any therapy, while others progress rapidly within months of diagnosis requiring early initiation of treatment. An enhanced understanding of how biological make-up impacts clinical prognosis is needed to identify new, clinically useful, biomarkers or to enhance the utility of existing biomarkers.

Over the past decade several biomarkers have been identified that appear to separate patients with CLL into low- and high-risk patient groups. Low-risk CLL is perhaps best characterized by immunoglobulin variable heavy-chain gene (IgV_H) mutation ($\geq$ 2% compared to germline) and low CD38 ($CD38^{low}$) and ZAP-70 expression, while high-risk CLL shows a reverse pattern (unmutated IgV_H-genes and high expression of CD38 ($CD38^{high}$) and ZAP70. The precise definition of $CD38^{low}$ and $CD38^{high}$ is debatable, with proposed thresholds ranging from 7% to 30%[2-4]. While it has been proposed that CD38 and ZAP-70 expression are surrogates for IgV_H mutational status, more recent studies suggest that each parameter is independently prognostic[5;6]. The CD38 protein is a multifunctional ectoenzyme that regulates calcium (Ca^{++}) homeostasis and can convert NAD+ to cyclic ADP-ribose and nicotinamide by an ADP-ribose cyclase reaction in a variety of cell types, including CLL [7-10]. CD38 is thought to be involved in co-signaling events with the B-cell receptor (BCR) in CLL [8-10]. Expression of CD38 is tightly regulated in normal B-cell ontogeny, with low expression

in resting B-cells and higher expression in stimulated B-cells [11]. Both CD38 and BCR signaling are known to be altered in, and segregated with, clinical subsets of CLL patients but the reasons for this are unclear. Therefore, based on our previous studies suggesting variation of genome methylation in small B-cell lymphomas, including CLL [12;13], we hypothesized epigenetic modifications may relate to CD38 expression.

We now present data from discovery-based DNA methylation studies of CLL patients with a range of CD38 expression and demonstrate both similarities and differences in the methylation status of specific genes in relationship to CD38 expression levels. It is known that the biological characteristics of CD38 positive and negative leukemic cells differ, and our studies were aimed at providing additional insights into a possible role of DNA methylation as a contributing factor for these differing characteristics.

Materials and Methods

Samples

Blood samples were obtained from patients following diagnostic evaluation at Ellis Fischel Cancer Center in Columbia, MO, the Holden Cancer Center in Iowa City, IA, and the Mayo Clinic in Rochester, MN, in compliance with the local Institutional Review Boards. Genomic DNA was isolated from the patient samples as described in chapter 1. The 38 patients had levels of CD38 expression on the CLL cells varying from 1% to 92%, as examined by flow cytometry [14]. All patient samples contained >60% (range 60 – 96) neoplastic cells as determined with CD19/CD5/CD23 expression by flow cytometry performed in each laboratory (data not shown). The percentage of CD38 expression was adjusted for CD19 expression and used as a variable in the clustering analyses.

Genomic DNA was purchased from Promega (Madison, WI, USA) and used as an unmethylated normal control. In addition, CD19+ non-malignant B-cells were also used as a normal control. CD19+ B cells were isolated from the peripheral blood of normal donors (n = 10) using the Dynal B-cell negative isolation kit (Invitrogen, Carlsbad, CA).

Cell Culture & Drug Treatment

Included in this study were three CLL cell lines with differing levels of CD38 expression; WAC3CD5[15] (4.7 % CD38), MEC1[16] (69.5% CD38) and MEC2[16] (96.6% CD38). These were maintained in a serum free RPMI 1640 media. MEC1 was initially obtained 3 years after diagnosis from the peripheral blood lymphocytes (PBL) of a 58 year-old Caucasian patient with CLL. A year later, a second cell line (MEC2) was obtained from the PBL of the same patient. Analysis of IgV_H showed that these cell lines

had not undergone somatic hypermutation, but they differ in expression of CD23 and FMC7 [16]. The WAC3CD5 line was induced by cytokines and infected with the Epstein-Barr virus [15]. Gene reactivation experiments were performed as described in chapter 1.

Real Time RT-PCR

Total RNA was extracted from the cell lines as described in chapter1. The cDNA was used for expression analysis of the following eight genes: *LHX2*, *NRP2*, *DLEU7*, *KCNK2*, *DLC-1*, *ADAM12*, *APC2*, and *SFRP2*, in CLL cell lines. For the analysis of *LHX2*, *NRP2*, and *KCNK2* generated cDNA was used for SYBR green-based reverse transcriptase (RT)-PCR amplifications with appropriate reagents in the Absolute QPCR SYBR mix (AB gene, Rochester, NY, USA). For expression studies of *DLEU7*, *ADAM12*, *SFRP2* and *APC2* cDNA was used for (RT)-PCR amplifications using, SuperArray RT^2 Real Time primers and SYBR green PCR master mix (Bioscience, MD, USA).Taqman primers and probes were utilized to study expression of *DLC-1* and *GAPDH* in B- CLL cancer cell lines. Real-time PCR was carried out in an I Cycler IQ (BioRad, Hercules, CA, USA). In order to examine the effects of epigenetic reversals of DNA methylation and/or inhibition of histone deacetylase, quantitative expression of these mRNAs was measured in three CLL cell lines before and after treatment with 5'-Aza, TSA, or both combined. The primer sequences and PCR conditions are summarized in Table 2.1.

CpG island (CGI) microarrays, amplicon prep & hybridization

Microarray slides containing ~12,000 CGI clones were obtained from the Microarray Centre, University Health Network, Toronto, Canada. The slides were

processed after hybridization using the Pronto Universal Microarray Reagents (Corning Life Science). DNA samples were prepared for hybridization as previously reported [17;18] . Procedures for amplicons preparation, labeling, hybridization and post-hybridization processing were essentially as previously reported [17;18], except that a different microarray was used. These protocols are reported in detail in chapter1 of this dissertation.

Methylation Confirmation

Fifteen genes were validated in the cell lines and patient samples using methylation specific PCR (MSP) or Combined Bisulfite Restriction Analysis (COBRA) as previously reported [17;18] Primers were designed using MethPrimer (www.urogene.org/methprimer/index.html).

Bisulfite genomic sequencing analysis

The genes *ADAM12* and *DLEU7* were further interrogated using bisulfite sequencing analysis [17;18]. Sodium bisulfite treatment of CLL cell lines and primary tumors was performed as described in chapter1. Primer sequences and PCR conditions are listed in Table 2.2.

Gene	RT PCR Primers	Length	Annealing temp(C)
LHX2	(F)- CCAAGGACTTGAAGCAGCTC (R)- GTAAGAGGTTGCGCCTGAAC	176	68
NRP2	(F)- CTCTGGAAAGGGGAATCCAT- (R)- GAAGGCTTTTTCGCCTTTCT	110	60
KCNK2	(F)- TAACAACTATTGGATTTGGTGACTAC (R)- GCCCTACAAGGATCCAGAAC	100	58
HPRT1	(F)- TGACACTGGCAAAACAATGCA- (R)- GGTCCTTTTCACCAGCAAGCT	90	58

Table 2.1: Primers tested for real time RT-PCR SYBR green analysis. The product sizes are approximate. The Taqman primer and probe was utilized for *DLC-1* and *GAPDH*. The RT^2 real time primers were utilized for *ADAM12*, *DLEU7*, *APC2*, and *SFRP2*.

Gene	Primers	Amplicon Location	Product Size, Tm		Restriction Enzyme
DLC-1	**(F)**GTTTTTAGTTAGGATATGGT	chr8:13,034,845-13,035,136	292	56	***BSTU1***
	(R)CTTCTTTCTACACATCAAACA				
KCNK2	**(F)**TTTAGTAAAGGGGTTTTGTTTTGAG	chr1:213,322,021-213,322,249	230	56	***Hpy99I***
	(R)AACCCTAACTTCTTCCAATCTACAC				
ADAM12	**(F)**GTGGATTTATTTTATAGGTTTGTTTTTT	chr10:128,066,859-128,067,044	186	56	***BSTU1***
	(R)CTAAACTCTTCTAACCTTTCATTTTTAAAA				
LHX2	**(F)-** GTTAGTTAAGTTTGTTAGGGTGGTG	chr9:125,834,465-125,834,702	238	63	***BSTU1***
	(R)- AAAAAATACTCTACCTACCTTCC				
DLEU7	**(F)-**TGGTTGATGGAGGTTATTAAGG	chr13:50,315,746-50,316,012	267	62	***BSTU1***
	(R)-TTCAAACAACTTTAAATCAAAACAC				
DMRT2	**(F)-**TTGGTGAAGGGTTAATGATTTTATT	chr9:1,038,332-1,038,597	266	56	***BSTU1***
	(R)-ATACCTAAAACTACTCCCAACAACC				
SFRP2**	**(F)-**TTTTTATTTTTTAGATTTGTATAAAAA	chr4:154,929,678-154,929,994	316	54	***BSTU1***
	(R)-AACCAAAACCCTAACACATC				
POU3F3	**(F)-**TTTATATTAGGGTTATTTTGGGGGT	chr2:104,838,934-104,839,170	236	56	***BSTU1***
	(R)-AATACACCAAACTCTAAACTCCACC				
PCDHGB7	**(F)**TGGGGTAGAATAAAGGTAGTAGTAAAGGAA	chr5:140,777,593-140,777,963	371	56	***BSTU1***
	(R)-ACAATCCCACACAAAACCTCTAAAC				
LRP1B	**(F)-**TAGGAAAGTTAAGGAAGTTAGGGGA	chr2:142,604,635-142,604,955	319	56	***Taq^{a}1***
	(R)-CACATCCTACTCCAAACAAAAAAA				
***APC2*(CGI3)**	**(F)-**GGGTAAGAATAGAGTAGGGTTGGAG	chr19:1,418,674-1,419,012	339	56	***BSTU1***
	(R)-TCAACAATAAAACTAAACTAAATCC				
HOXC10	**(F)-**TTTTTTTTGAAAATGATATGTTTT	chr12:52,665,299-52,665,647	349	56	***BSTU1***
	(R)-TACAACAAACATTCTCCTCCTTAAC				
DUOX2	(F)-TTTTAATCGGATTTAAGTGTCGG (M)	chr15:43,192,664-43,192,828	164	60	**MSP**
	(R)-AATATCAAACTCCTCTAACGACGAA (M)				
	(F)-TTTTAATTGGATTTAAGTGTTGG (U)		162	62	
	(R)-TATCAAACTCCTCTAACAACAAA (U)				
NRP2	(F)-TTTTAGAGATTAGCGTTGTAGTCGA (M)	chr2:206,259,130-206,259,300	169	60	**MSP**
	(R)-AAACCGAAACTAAAACCTCCG (M)				
	(F)-TTTTAGAGATTAGTGTTGTAGTTGA (U)		170	60	
	(R)-AAAACCAAAACTAAAACCTCCAC (U)				
RLN2	(F)-AGATTAGTGGTAGGTGAGAGTTTTC (M)	chr9:5,294,231-5,294,382	151	60	**MSP**
	(R)-CACGACTAAATAAAAACTAAACGAT (M)				
	(F)- TAGTGGTAGGTGAGAGTTTTTGT (U)		148	60	
	(R)-CCACAACTAAATAAAAACTAAACAAT (U)				
***APC2*(CGI2)**	**(F)-** TGTTTTTGTTGTTGTAAATTTTTTA	chr19:1,407,976-1,408,199	224	56	***BSTU1***
	(R) -**CAACCAATCCCAACAAATCTC**				

Table 2.2: primer sequences, amplicon locations, and PCR conditions. Primers were designed using MethPrimer software.

Statistical Analysis

For each of the 15 genes validated using COBRA and MSP, 2 x 2 contingency tables were formed with the rows indicating CD38 level (> 10% and ≤ 10%) and the columns indicating the methylation status (methylated/unmethylated). The number of samples in each table ranged from 29 to 36. For each table (one table per gene), we carried out Fisher's Exact Test to determine if the CD38 level was associated with methylation status. This test was chosen as an alternative to the Chi-square Test of Independence because, for many genes, the small expected cell counts would cause the Chi–square test to perform poorly, and Fisher's does not suffer this limitation. We also computed odds ratios (OR), log odds ratios, and confidence intervals for the log odds ratio. The strength of the association between the two variables (categorical CD38 expression and methylation) increases as the OR moves above a value of one.

12 K microarray design and library:

The 12 K chip contains 13,056 CGI clone organized into 48 blocks of 272 spots in 17 rows and 16 columns. There are 579 negative controls in this library, 192 of these spots are DNA from Arabidopsis. Included in this array are 260 blank spots. All the human clones in this library are sequenced using M13and T7 primers. The DNA sequence information was provided by the Der Laboratory (http://derlab.med.utoronto.ca/). We found 9011 CGI clones that had some sequence information using the two primers. 5853 of these clones have sequence length of 200 or longer, and out of these clones there are 1074 clones without *Bstu*1 (CGCG) and *Hpa*II (CCGG) cut sites in both M13 and T7 sequences. Therefore, those sequences without the

cut site in tumor (Cy5) and normal (Cy3) samples are expected to hybridize equally to the microarray chip. Thus the expected methylation ratio for those clones is 1. These clones are used as control for normalization. We also found that only 3988 of the CGI clones aligned with known genes. Out of these clones, only 3405 clones were found to have a sequence length of 200 or longer. The hybrid normalization technique that combines the Loess and global normalization were utilized to normalize the microarray data. The global normalization factor was calculated using negative control spots (Arabidopsis), blank spots, and spots from the non cut site clones. We also used statistical analysis (Wilcoxon) to determine the clones that were differentially methylated across the CLL patients with different CD38 expression levels. The *p* value of <0.05 was used to identify 100 differentially methylated CGI clones using the Wilcoxon measures. A clustering analysis was performed using patient samples and clones. The resulting clusters were visually analyzed using Mev TIGR software (http://www.tm4.org/).

In addition, we used Statistical Analysis Software (SAS) to determine the quality of the hybridization for the all 38 microarray experiments. Median values were collected for the two dye (Cy5 and Cy3) foreground and background intensities, and the GPR files from the scanner were loaded into SAS. The Log2 intensities of both dyes, LgF635/LgF532 were plotted to determine if there was anything unusual in the way the dyes hybridized to the slides (Figure 2.1) .When LgF635/Lg F532 were plotted, no specific patterns were seen in foreground intensities. However, when LgB635 was plotted versus LgB532, there was slight bias toward the Cy5 (Figure 2.2).This dye effect was removed after normalizing the data.

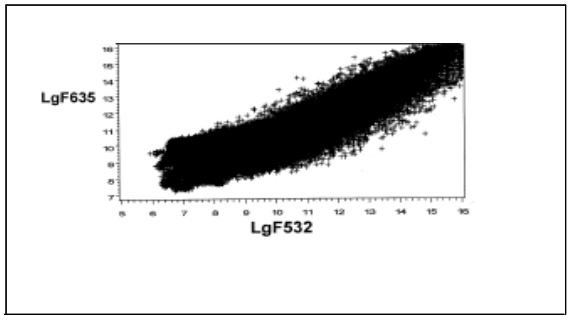

Figure 2.1: Pair wise comparison of Cy5/Cy3. The log2 of the foreground intensities for Cy5/Cy3 was plotted.

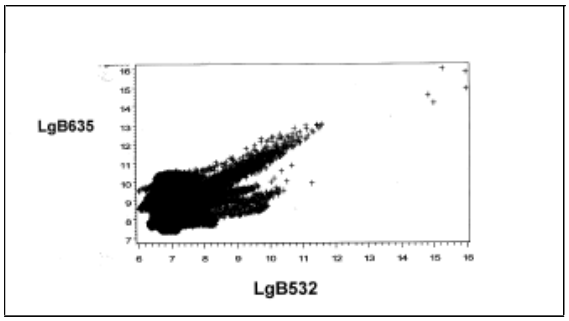

Figure 2.2: Pair wise comparison of Cy5/Cy3. The Log2 of the background intensities for Cy5/Cy3 was plotted. There is a slight bias toward the Cy5.

The distributions of data were compared for all arrays for Cy5 intensities, and the result revealed a need for normalization; for example, foreground intensity for Cy5 was different across the different slides (Figure 2.3).

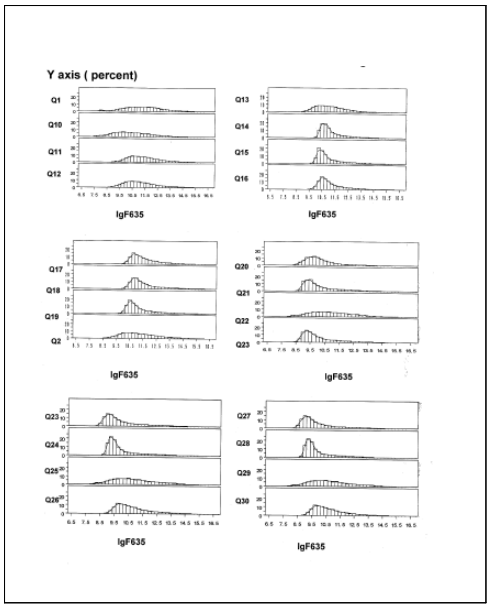

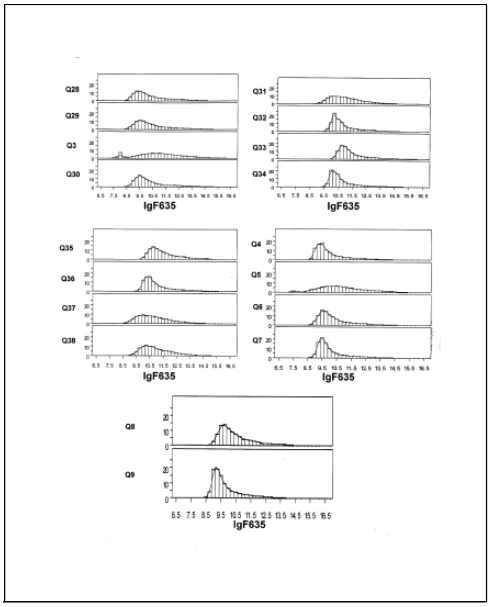

Figure 2.3: Distribution comparison of Cy5 intensity across different slides before normalizing data.

Results

Methylated Gene Discovery

Previous methylation microarray experiments by our group using a different set of ~9,000 clones with the DMH method resulted in hierarchical clustering that suggested at least two different groups of CLL patient samples based on DNA methylation [17]. The methylation profile of one group clustered closely with samples of mantle cell lymphoma (MCL), while the other group clustered more with follicular lymphoma (FL) samples. At that time, we did not have CD38 expression data for enough of the CLL samples to assess the correlation between methylation and CD38 expression to draw definitive conclusions , but the study suggested another set of experiments that are now reported using a ~12,000 feature microarray from the Microarray Centre (Toronto, Ontario, CA)[19].

For the current study a total of 38 primary CLL patient samples with a range of CD38 expression were studied using DMH [17;20]. Samples were initially assigned to the $CD38^{high}$ class if they expressed $\geq$20% CD38. Levels of CD38 expression ranging from 7% to 30% have been put forth to predict clinical behaviors [2-4], so we arbitrarily started our investigation at the mid-range. This resulted in 20 and 18 samples in the $CD38^{high}$ and CD 38^{low} classes respectively. To identify loci that were differentially (or universally) methylated between these two classes, we first filtered the data and considered only those loci that satisfied the following criteria: non-blank spots on the array, non-mitochondrial DNA sequences, non-control sequences, the locus contained a DNA sequence length >100 bp, and the sequence contained methylation-sensitive enzyme restriction sites for *Bstu1* and /or *Hpa*II. This filter reduced the loci under consideration to 5,853. The filtered loci were then subjected to statistical analysis using

the Wilcoxon- Mann-Whitney and t-test. Data from each locus was then ranked in increasing order based on *P*-values. The gene list was used to produce a hierarchical clustering (Figure 2.4, 2.5 and 2.6). The upper dendrogram (rotated 90^0 and enlarged on the right) illustrated the relationship of CD38 expression values of CLL samples to each other on the basis of their DNA methylation patterns. For each locus of interest, the related gene was identified by searching the associated database found at the Microarray Centre.

Visually, the separation of cases into >20%CD38 and ≤20% CD38 was not very clear. Therefore, it was appropriate to further assess the more definitive separation of CD38 expressing CLL clones. From the published literature, it has been suggested that clinical behavior best segregates with CD38 expression ranging from 7% to 30% [2-4]. For simplicity, we chose to re-examine the data from our clustering analysis with CD38 expression thresholds of 10, 20, and 30%. The difference between clustering at an expression level of 7% versus 10% would have changed the grouping for only 2 patients who were reported to have a CD38 expression of 9%. After initial evaluation of the 3 levels, the 10% threshold (Figure 2.4) demonstrated the best homogeneity of methylation in class separation. In contrast, the clusters at both 20% and 30% threshold levels produced quite heterogeneous clustering results (Figure 2.5 and 2.6).

The segregation at 10% resulted in a number of genes/loci with differential frequencies of methylation in $CD38^{high}$ (≥10%) and $CD38^{low}$ (≤10%) CLL samples, but also some that appeared methylated universally across the samples. Methylated genes in group A (Figure 2. 4) were almost exclusively (20/26 cases) associated with samples having $CD38^{high}$ expression. Group B genes were slightly more likely to be methylated in

CD38^{low} CLL samples (11/18 cases), but 7 CD38^{high} samples also clustered with the CD38^{low} CLL samples and are shown in blue (Figure 2. 4).

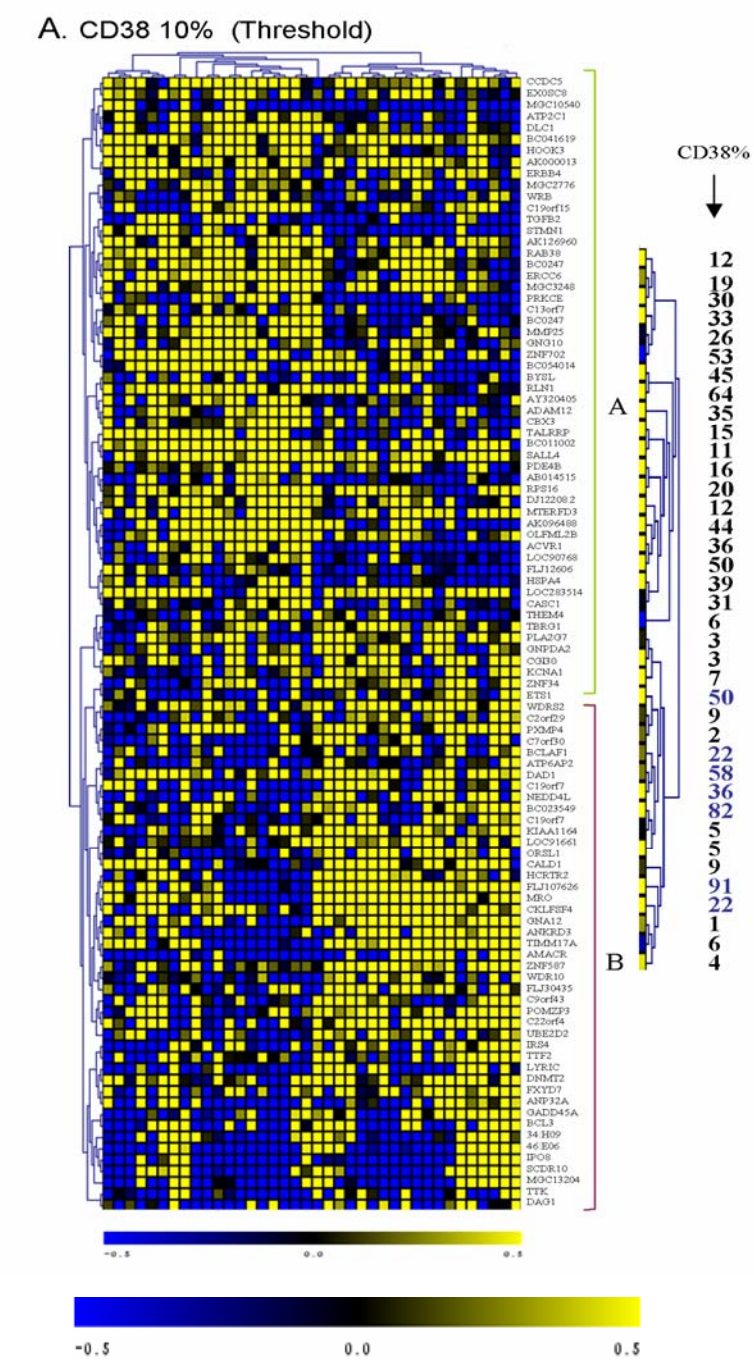

Figure 2.4: Hierarchal clustering analysis of DNA methylation based on 10% CD38 expression level. This illustrates a measure of relatedness of DNA methylation across all loci for each sample. Each column represents a patient sample and each row represents a clone/locus on microarray chip. The florescence ratios of cy3/cy5 are measures of DNA methylation and are depicted as a color intensity (-1 to +1) in log base 2; yellow indicates loci that share a higher level of DNA methylation, blue indicated lower level of methylation and black indicates no change. The dendrogram from the top of the cluster (rotated 90^{o} and enlarged on the right) represents the CD38 expression level of each sample. The numbers shown in blue color represent the patients with CD38 ^{high} that are clustered in the $\leq$10% group.

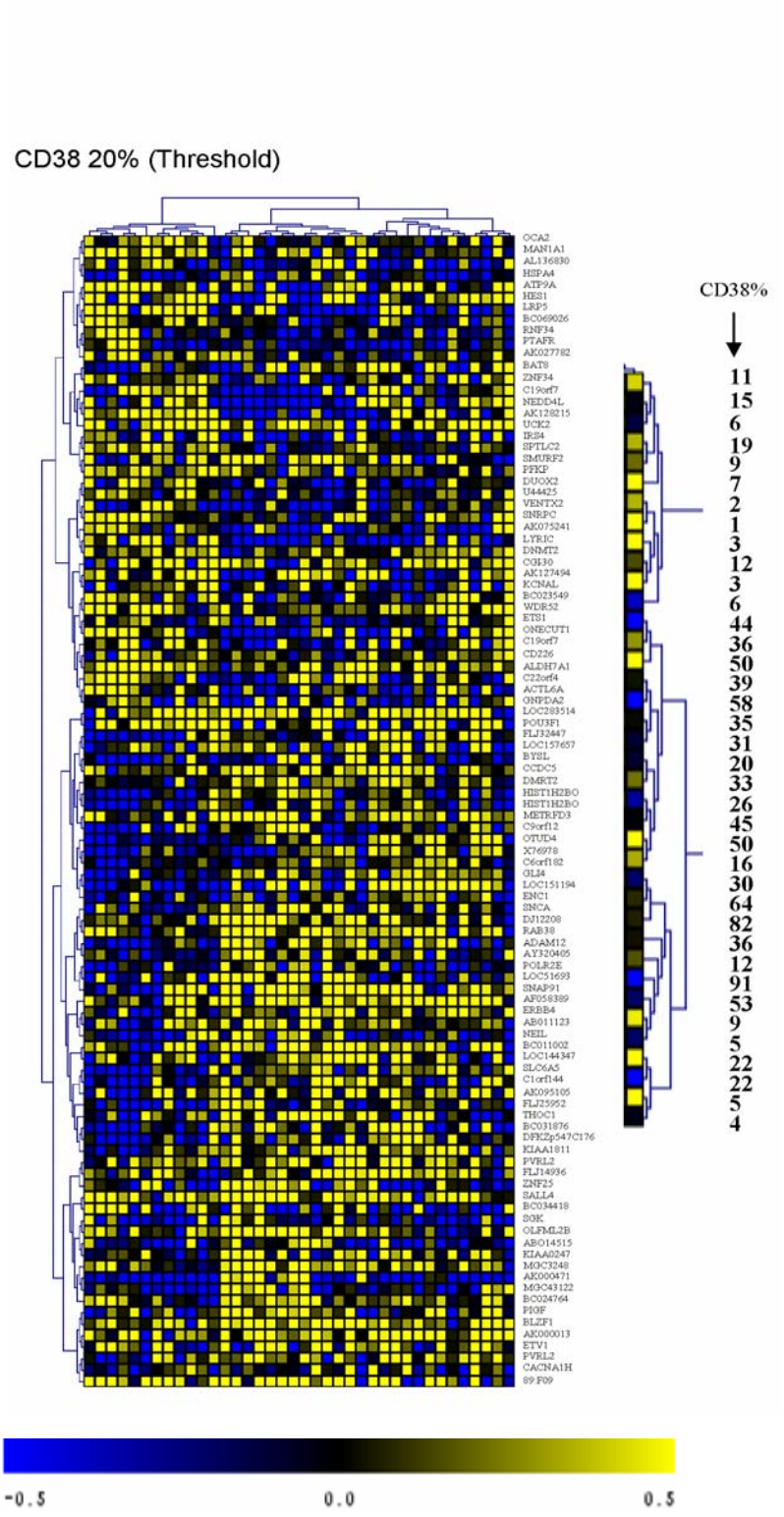

Figure 2.5: Hierarchical analysis of DNA methylation with thresholds of 20% CD38 expression. This figure illustrates a measure of the relatedness of DNA methylation across all loci for each sample. Each column represents a patient sample, and each row represents a clone/locus on a microarray chip.

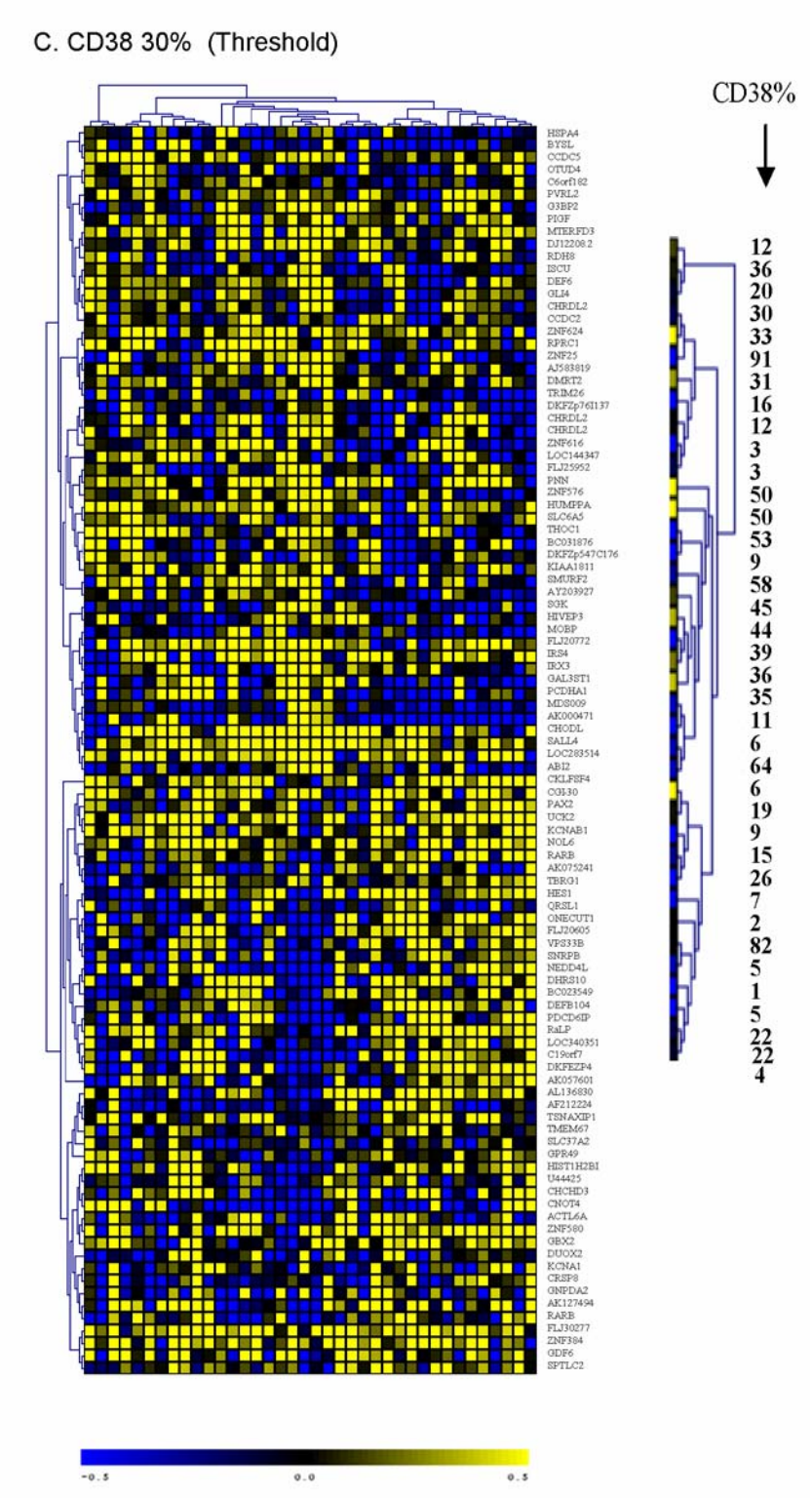

Figure 2.6: Hierarchical analysis of DNA methylation with thresholds of 30% CD38 expression. This figure illustrates a measure of the relatedness of DNA methylation across all loci for each sample. Each column represents a patient sample and each row represents a clone/locus on microarray chip.

Independent Confirmation of Methylation

While microarrays are useful discovery tools, it is remains important to independently validate representative observations to avoid false positive and false negative results. Therefore, we selected 15 regions/loci for further confirmation by COBRA and MSP to validate DNA methylation in three CLL cell lines with different CD38 expression levels (MEC1 69.5%, MEC2 96.6% and WAC3CD5 4.7%). These genes were selected based on the microarray results as described in chapter 1of this work, as well as previous work in our laboratory suggesting differential methylation in CLL subsets. The MSP assay was used to study methylation of *NRP2*, *DUOX2*, and *RLN2*, and the other validations were carried out using COBRA (Figure 2.7). [17]

Additionally, we recently reported on the performance of ultradeep bisulfite sequencing (454 technology) of 4 lymphoid malignancies, including CLL, for 25 gene regions [21]. Four genes, *ADAM12*, *DLC-1*, *LRP1B*, and *KCNK2*, were also included in that study which confirms the presence of DNA methylation in specific cytosine molecules of these genes in CLL. The results varied among the three CLL cell lines (Figure 2.7). Methylation was present in *APC2* (CGI2, CpG island located inside of the *APC2* gene), *HOXC10*, *NRP2*, *POU3F3*, *ADAM12*, *PCDHGB7*, *DLC-1*, *LHX2*, *LRP1B* in all 3 cell lines, while *DUOX2*, *APC2* (CGI3, CpG island located in the 3'region of the *APC2* gene), *RLN2*, and *KCNK2* were only methylated in WAC3CD5 and MEC1. Fewer genes (10/16) were methylated in MEC2, which expressed a higher level of CD38 (96.6 %) than in WAC3CD5 (14/15) or MEC1 (16/16) which have lower levels of CD38 (4.7 % and 69.5 %) respectively.

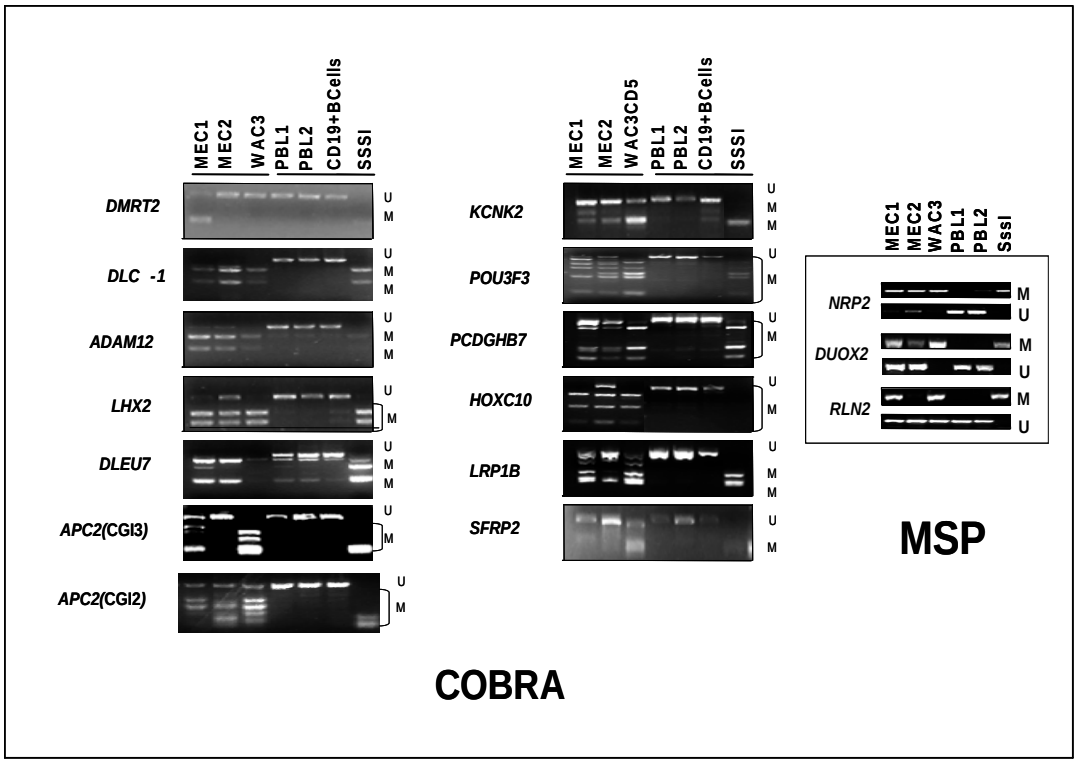

Figure 2.7: COBRA and MSP validation of DNA methylation of 3 cell lines. The left panel illustrates the DNA methylation of *DMRT2, ADAM12, LHX2, DLEU7, APC2 (CGI3), APC2 (CGI2), KCNK2, POU3F3, PCDGHB7, HOXC19, LRP1B, SFRP2* using COBRA primers. Two CGI were interrogated for APC2. The right panel shows the DNA methylation status of *RLN2, NRP2* and *DUOX2* using MSP. These confirmations were conducted on the three cell lines, normal female (PBL1) and male (PBL2) peripheral blood lymphocytes, CD19+ B cells, and in vitro *SssI* treated DNA. Methylated (M) or unmethylated (U) are indicated on a 3% agarose gel.

Analysis of DNA methylation in primary CLL cells

Results from cell lines do not always exactly match those of primary cells. Therefore, we also examined the methylation status of the same 15 candidate genes/regions in primary CLL samples. In Figure 2.8 each row represents a single gene and columns are grouped to represent the results of methylation within 3 groups of patients with increasing levels of CD38 expression. Two fragments were examined for *APC2*: CGI2 and CGI3 located inside and the 3' region respectively. Not every row has an equal number of samples. For instance, 36 samples were successfully examined for *PCDHGB7*, but only 29 samples for *ADAM12*. All samples for which no result is reported were re-examined by COBRA at least 3 times, but all still failed to provide a PCR product for digestion. The reasons are not entirely clear, but most likely this is a result of genomic alterations in the regions under consideration. In the remaining samples the results were grouped by CD38 expression; 0-10%, 11-30%, and 31-91%. The percentage of samples methylated for each gene in each group is shown in Table 2.3.

Gel images, the genomic DNA regions and the chromosomal locations of these genes are depicted in Figures 2.9 to 2.23. Based on our earlier observation suggesting that the 10% CD38 threshold might be best for class separation, contingency tables were generated for each gene based on the methylation results, and the patient samples were stratified into 2 groups based on CD38 surface expression ($CD38^{low}$ and $CD38^{high}$). From these contingency tables, estimates of the odds ratio (OR) and other statistics were computed and are reported in Table 2.3. For example, in the case of *HOXC10*, methylation was present in *HOXC10* in all 19 cases with >10% CD38 expression and 4

out of 10 cases with <10% CD38 expression. The corresponding OR for *HOXC10* was over 28, which implies that the odds of methylation are more than 28 times greater when CD38 > 10%, as compared to odds of methylation when CD38 $\leq$ 10%. Conversely, methylation was present in *DLEU7* for all 12 cases tested with $\leq$ 10% CD38 expression and 7/22 samples with >10% CD38 group, resulting in an OR of 0.02. This implies that the odds of methylation in *DLEU7* are 50 (1/0.02) times greater when CD38 < 10%, as compared to odds of methylation when CD38 $\leq$ 10% . Using Fisher's Exact Test, the *p*-value for the methylation differences between the 2 groups was p=0.00044 for *HOXC10* and 0.000162 for *DLEU7*. Of the remaining genes, only *SFRP2* showed a *p*-value < 0.05 (p=0.01443), with an OR of 7, suggesting more methylation events at higher CD38 levels.

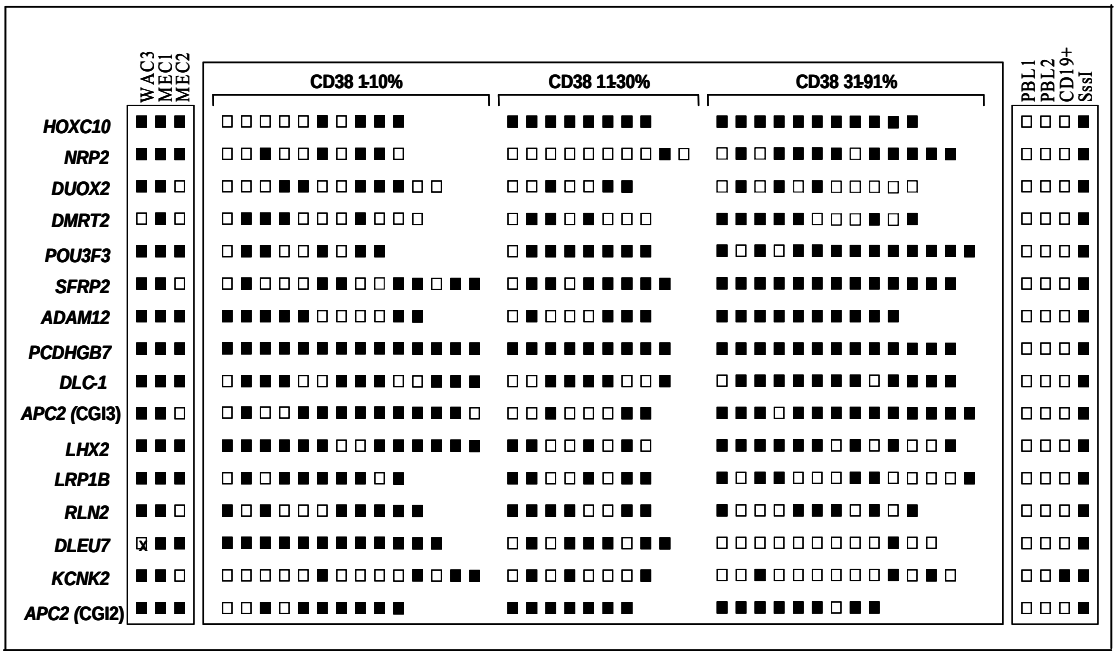

Figure 2.8: The DNA methylation status was validated using either COBRA or MSP from the cell lines as well as the primary CLL samples that were divided into three groups (1-10%, 11-30% and 31-91%) based on CD38 positivity. Results are summarized as methylated (dark square) or unmethylated (open square). Each square represents an individual patient sample and each specific gene. The right side panel represents the DNA methylation status in CLL cell lines.

CD38→									
Genes	M	%	M	%	Exact P	Odds Ratio	Log Odds	LCL Log Odds	UCL Log Odds
HOXC10	4/10	40	19/19	100	0.000442	28.8889	3.36346	1.02291	5.70401
NRP2	4/10	40	11/23	47.83	0.722024	1.3333	0.28768	-1.14768	1.72305
DUOX2	5/12	41.67	6/18	33.33	0.71163	0.734266	-0.30888	-1.74238	1.12461
DMRT2	4/11	36.36	10/19	52.63	0.4664	1.83333	0.60614	-0.84273	2.05500
POU3F3	5/9	55.56	19/22	86.36	0.150433	4.090909	1.40877	-0.23578	3.05332
SFRP2	7/14	50	20/22	90.91	0.002594	11	2.39790	0.63162	4.16417
ADAM12	7/11	63.64	14/18	77.78	0.432745	1.8	0.58799	-0.95825	2.13383
PCDHGB7	14/14	100	22/22	100		0.793103	-0.23180	-3.68959	3.22599
DLC-1	9/14	64.29	16/22	72.73	0.715857	1.406015	0.34076	-1.02948	1.711
LHX2	12/14	85.71	13/21	61.9	0.251643	0.3111	-1.16761	-2.76295	0.42774
LRP1B	7/10	70	11/22	50	0.446063	0.46667	-0.76214	-2.26214	0.73786
RLN2	7/11	63.64	12/19	63.16	1	0.975	-0.02532	-1.48871	1.43808
DLUE7	12/12	100	7/21	33.33	0.000162	0.021333	-3.84748	-6.80155	-0.89342
KCNK2	4/14	28.57	6/21	28.57	1	1.020833	0.02062	-1.39655	1.43779
APC(3')	10/14	71.43	16/22	72.73	1	1.040816	0.04001	-1.37218	1.45219
APC(5')	7/10	70	15/16	93.75	0.326149	2.488889	0.91184	-0.85744	2.68111

Table 2.3: Statistical analysis of COBRA and MSP results . Each of the 15 genes are listed (2 CGIs for *APC2*), along with the number and % of cases confirmed as methylated, the Exact *p*-values and the Odds Ratios using 2 groups (1-10% and 11-92% CD38 expression) as inputs. The right column contains the 95% confidence intervals of the log Odds Ratios. In the case of *PCDHGB7*, since every case tested was methylated, there is no calculated *p*-value.

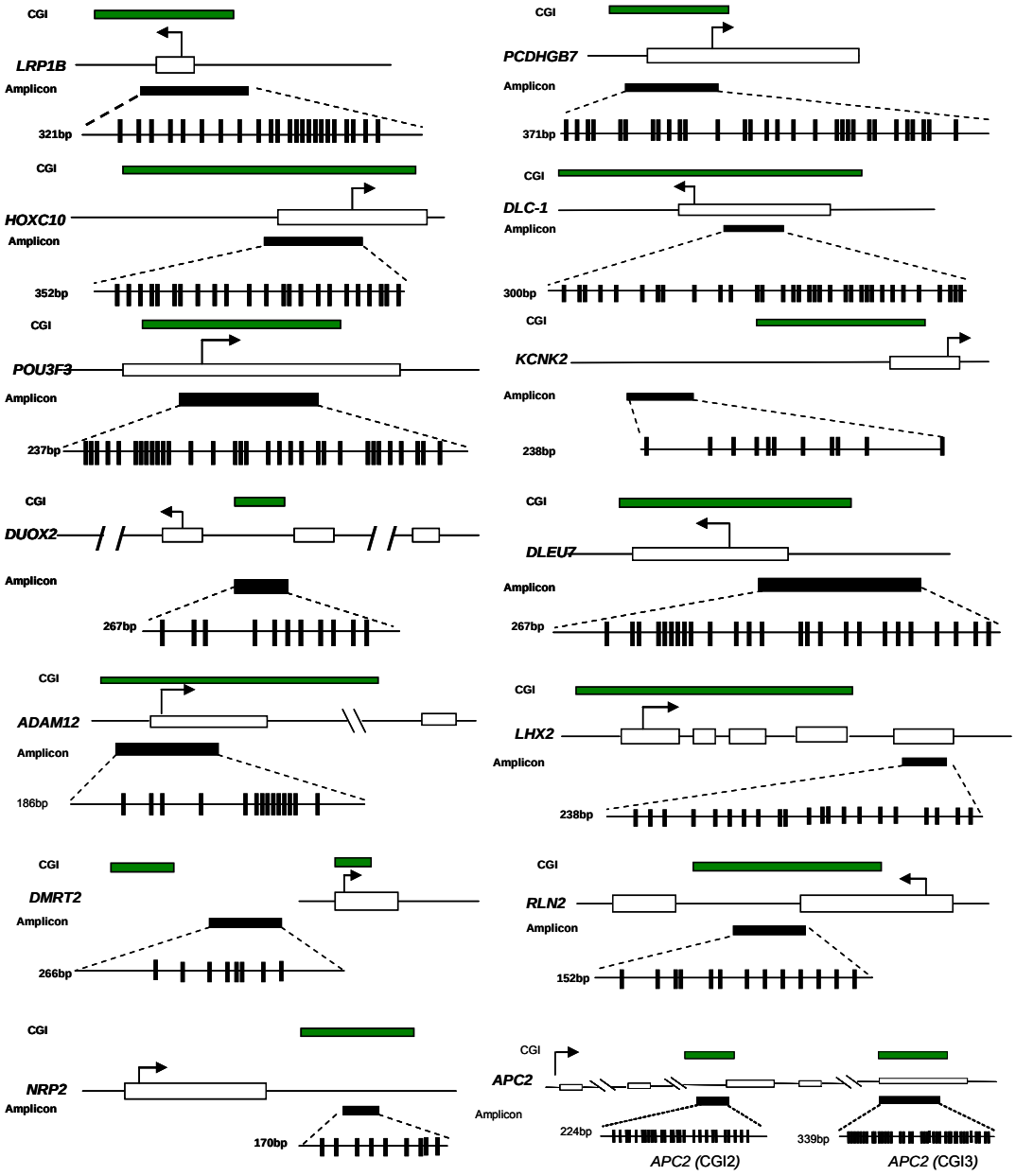

Figure 2.9: Schematic representation of the 16 amplicons. The solid black lines represent the region of interest for which we collected COBRA and MSP data. The green thick bars represent the CGI locations. Short vertical lines represent the position of CpG dinucleotides.

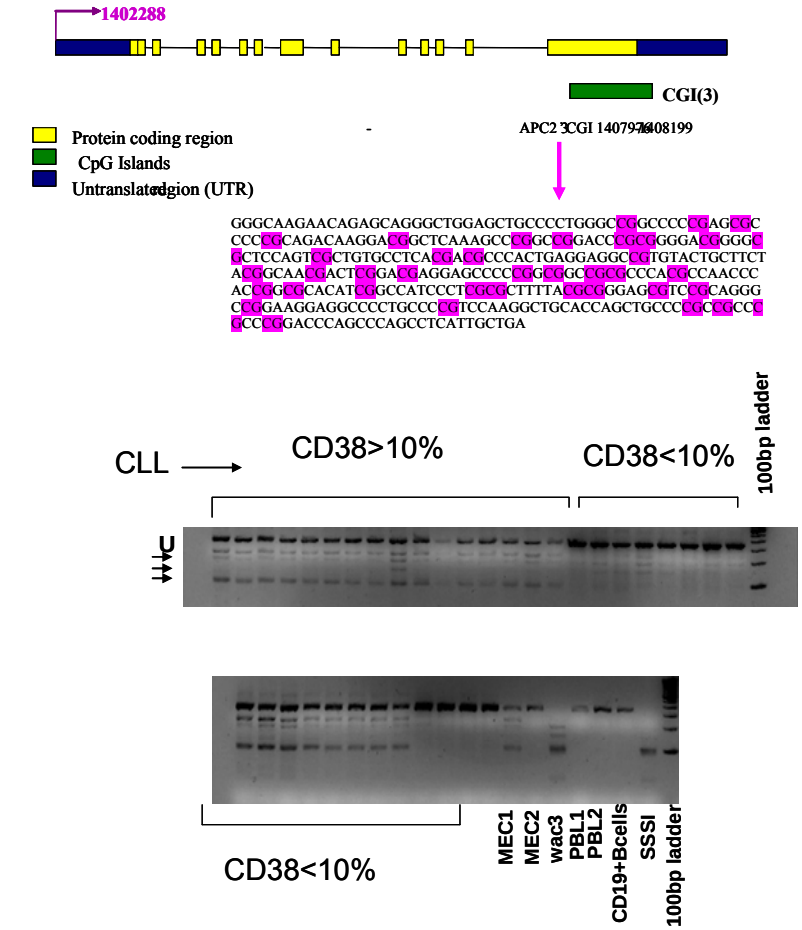

Figure 2.10: *APC2* gene structure and COBRA. *APC2* gene structure and chromosomal location is illustrated. The location of the CpG Island, the genomic DNA sequences and the region analyzed by COBRA are indicated. The gel image presents the COBRA analysis of CGI located in the 3' region of *APC2*. Normal peripheral blood, CD19+ B cells and CLL samples with different CD38 expression levels were digested with *Bstu1*. The 3% agarose gel was utilized to visualize these results. The intensity of the digested DNA bands was quantified using Image analysis software. The arrows represent methylated DNA fragments and U is representing unmethylated DNA fragment.

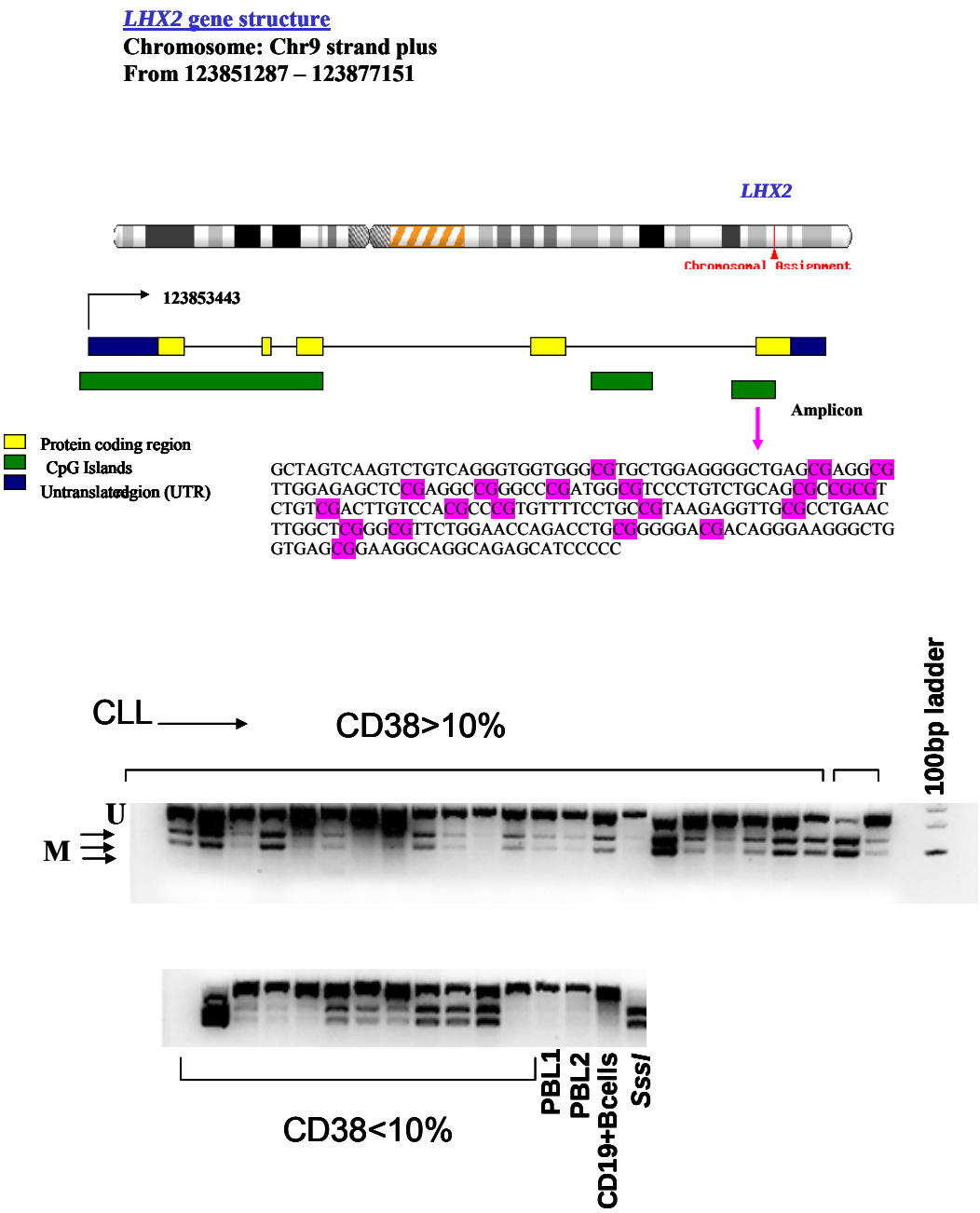

Figure 2. 11: *LHX2* gene structure and COBRA. The DNA methylation status of this gene was validated using COBRA.

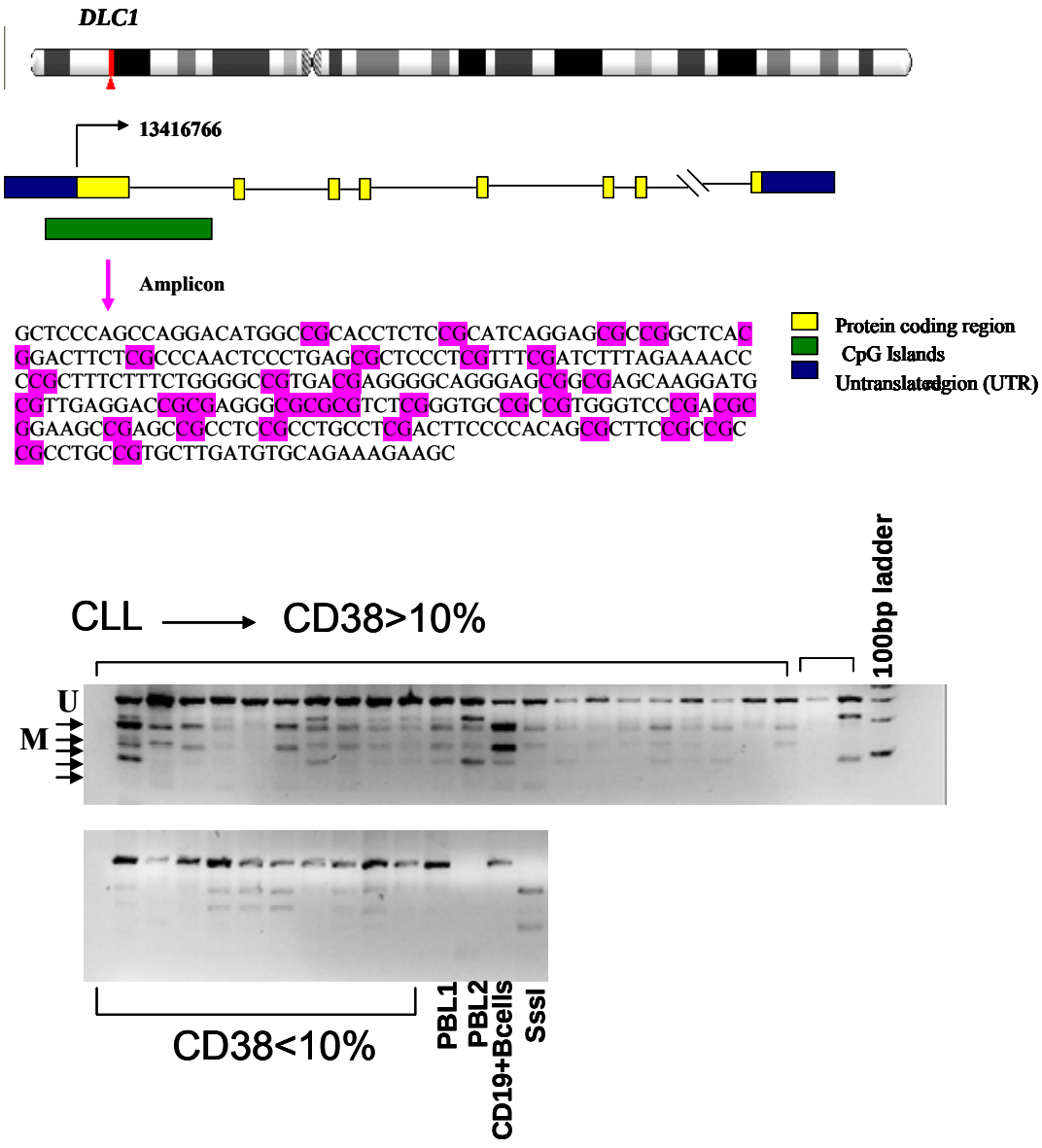

Figure 2.12: *DLC-1* gene structure and COBRA. The location of the CpG island and the region analyzed by COBRA are indicated.

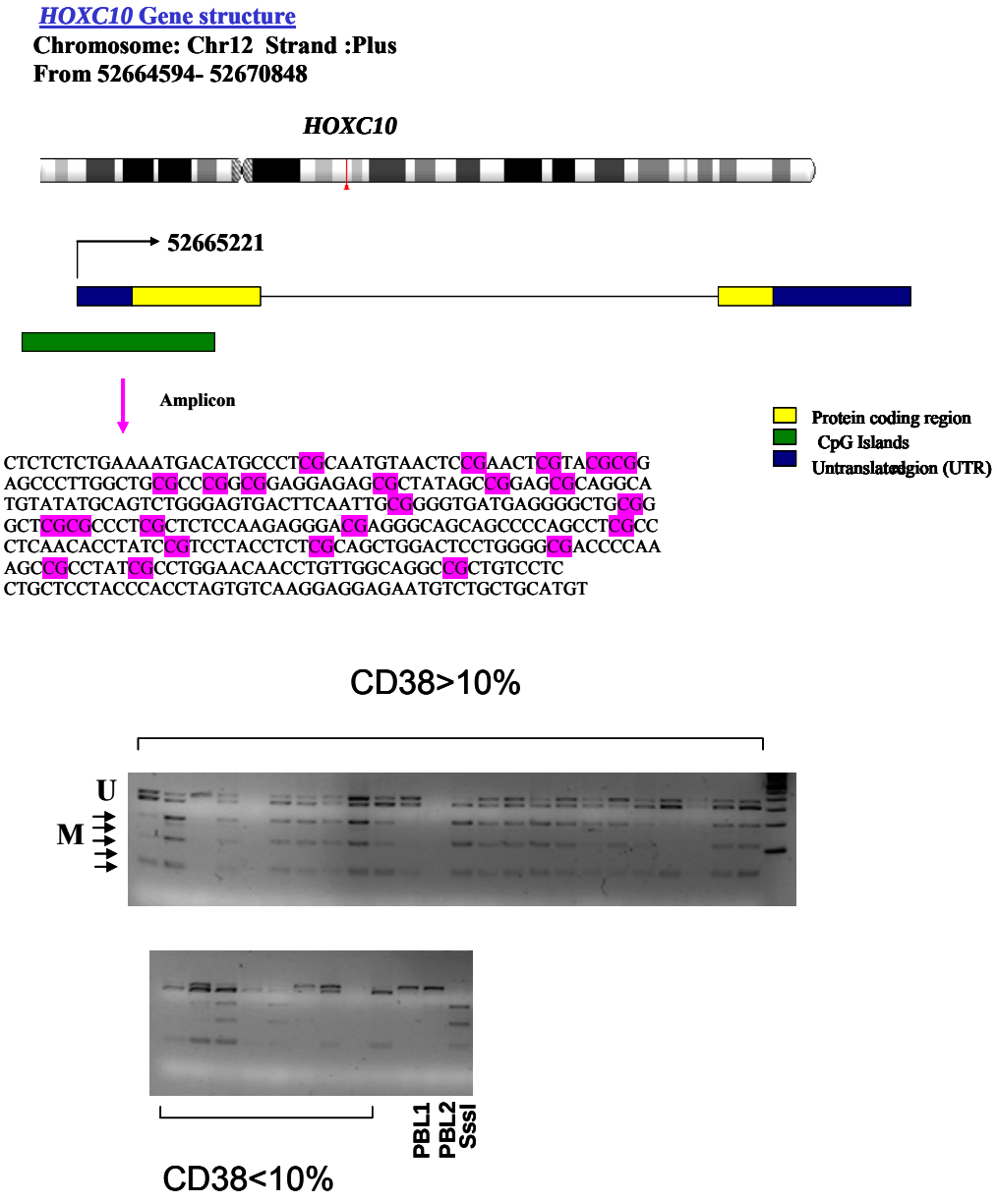

Figure 2.13: ***HOXC10* gene structure and COBRA**. PCR products of *HOXC10* promoter region were digested with *BSTU1* with restriction enzymes with a recognition sequence containing CpG in the original unconverted DNA. Fragmented PCR products indicate the methylated sites, whereas the PCR products that are not fragmented represent unmethylated sites. The DNA sequences represent the region for which we collected COBRA results. The intensity of digested bands is analyzed.

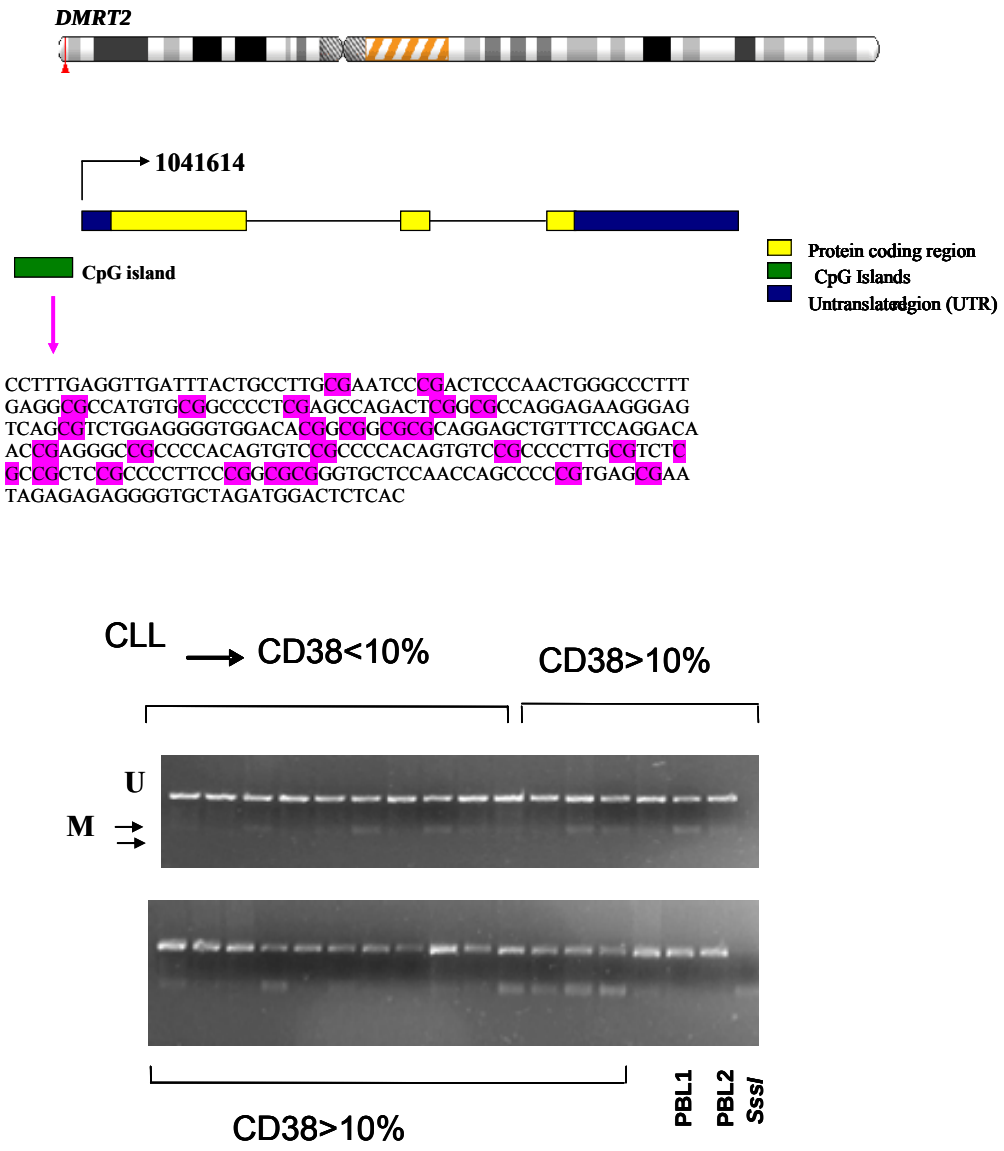

Figure 2.14: *DMRT2* gene structure and COBRA. The DNA methylation status of *DMRT2* was investigated in CLL patient samples with different CD38 expression levels, normal peripheral blood lymphocytes and in vitro treated *SssI* DNA. The DNA methylation was validated using COBRA.

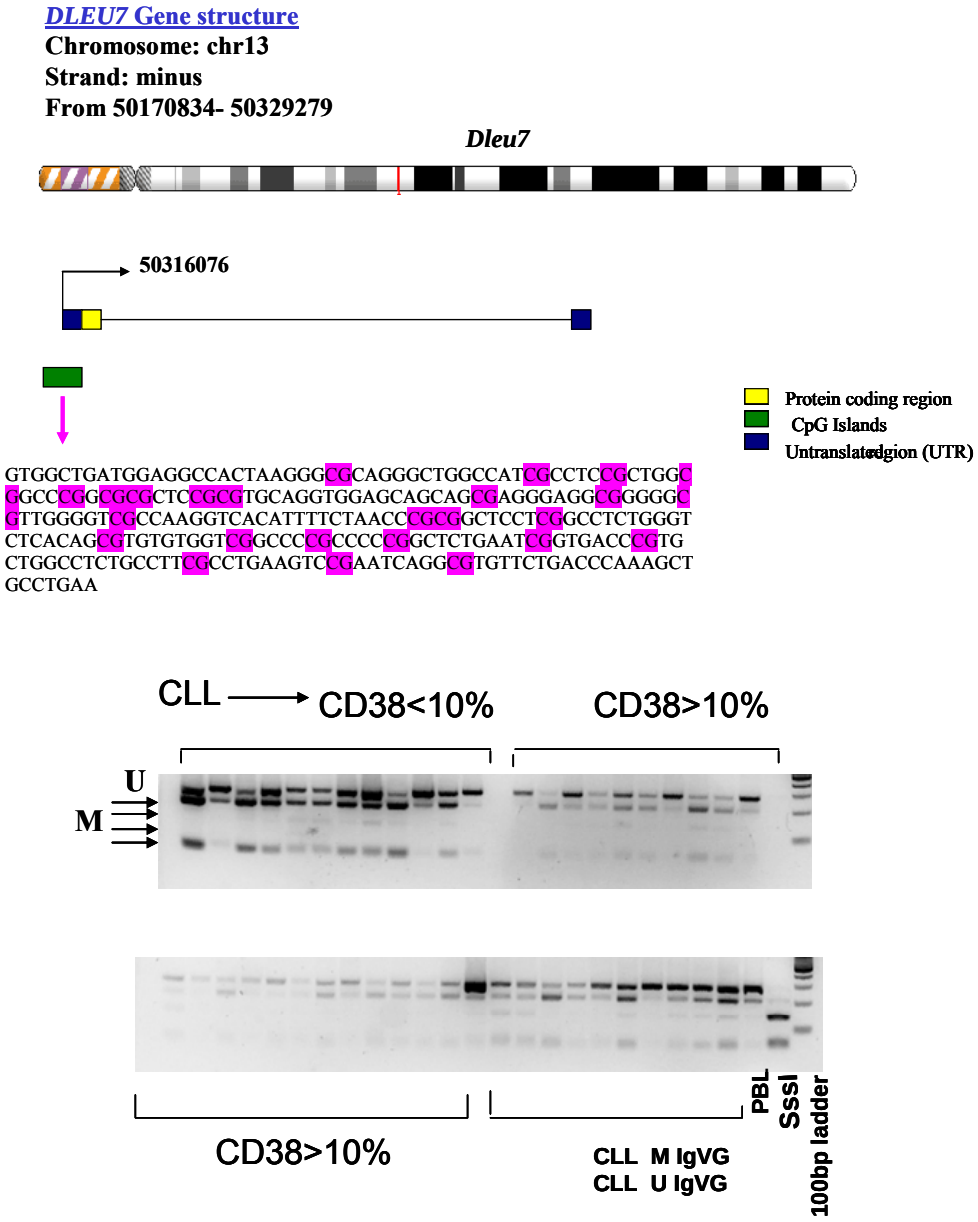

Figure 2.15: *DLEU7* gene structure and COBRA results: A schematic map showing the region of interest that includes the promoter around the transcriptional start site. The methylation status of this region was validated from bisulfite treated DNA of CLL patients with different CD38 expression levels, differing IgVH mutational status, normal PBMC and positive control.

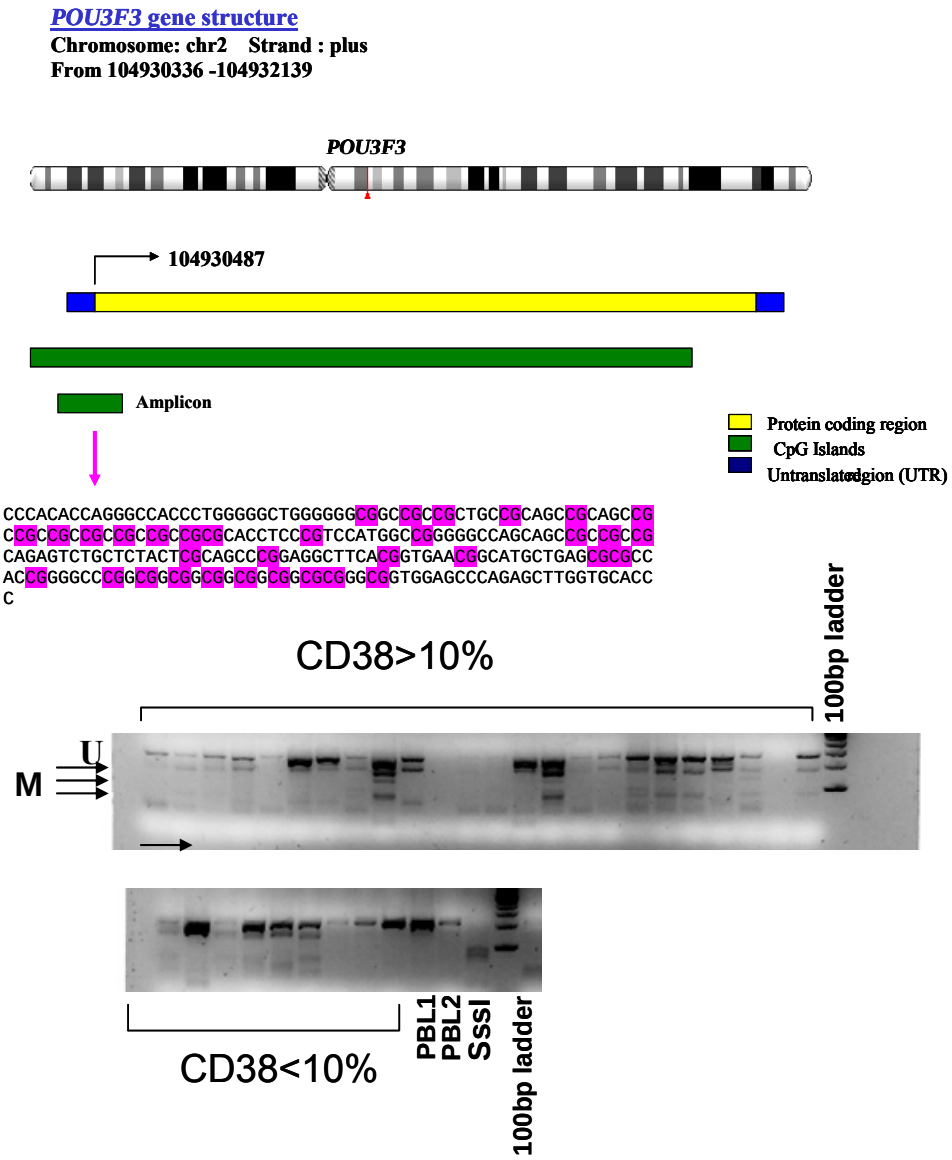

Figure 2.16: *POU3F3* gene structure and COBRA. Genomic DNA was treated with sodium bisulfite, which deaminates unmethylated cytosines to uracil but does not affect 5 methylated cytosine. PCR amplification of differentially methylated regions from the bisulfite treated genomic DNA was carried out using primers that amplify the *POU3F3*.The amplified PCR products were digested with *Bstu1*. The intensity of the digested DNA bands was quantified using ID Image analysis software.

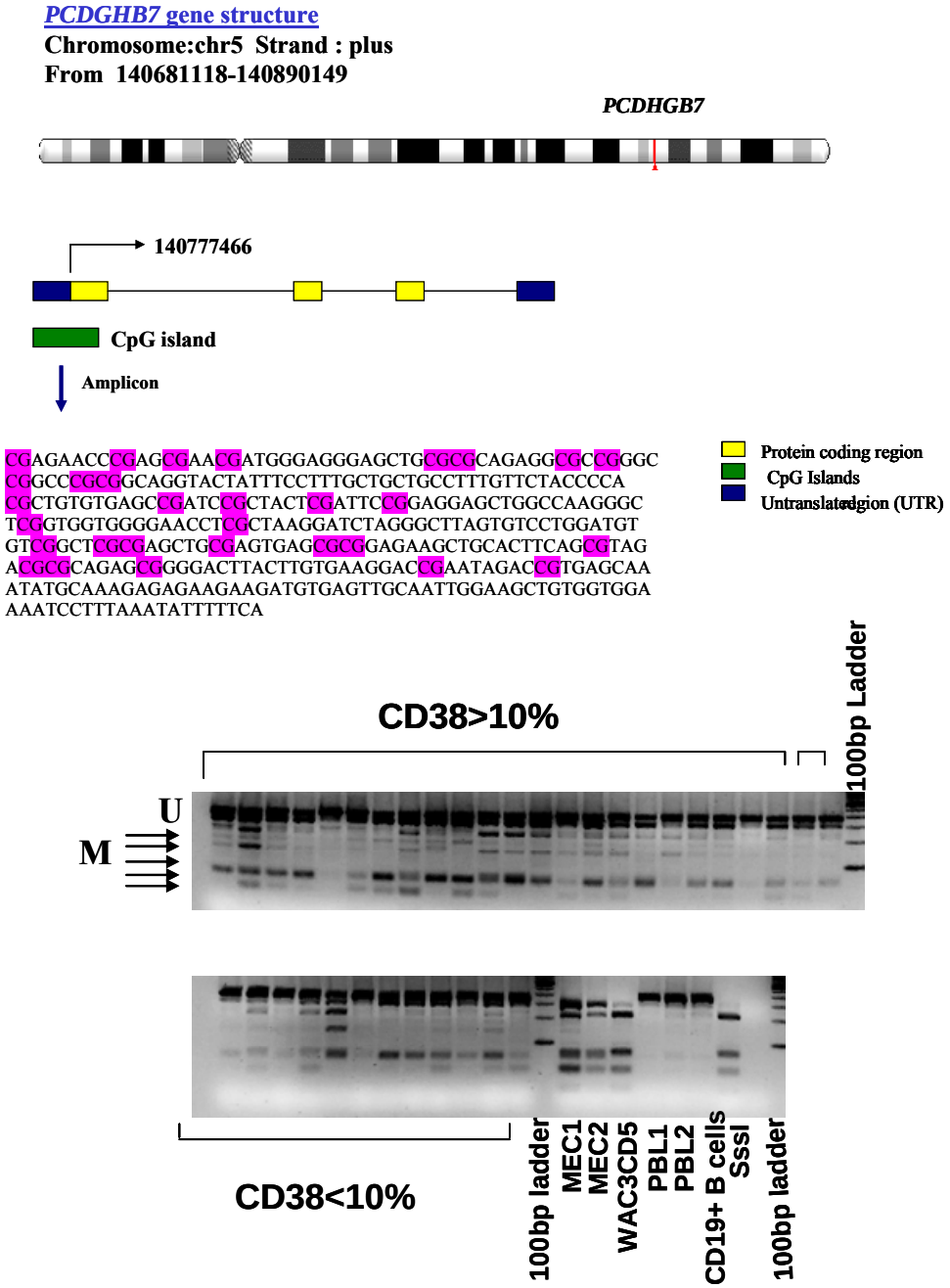

Figure 2.17: *PCDGHB7* gene structure and COBRA. The DNA methylation of *PCDGHB7* was investigated in primary tumor cells as well as the normal controls.

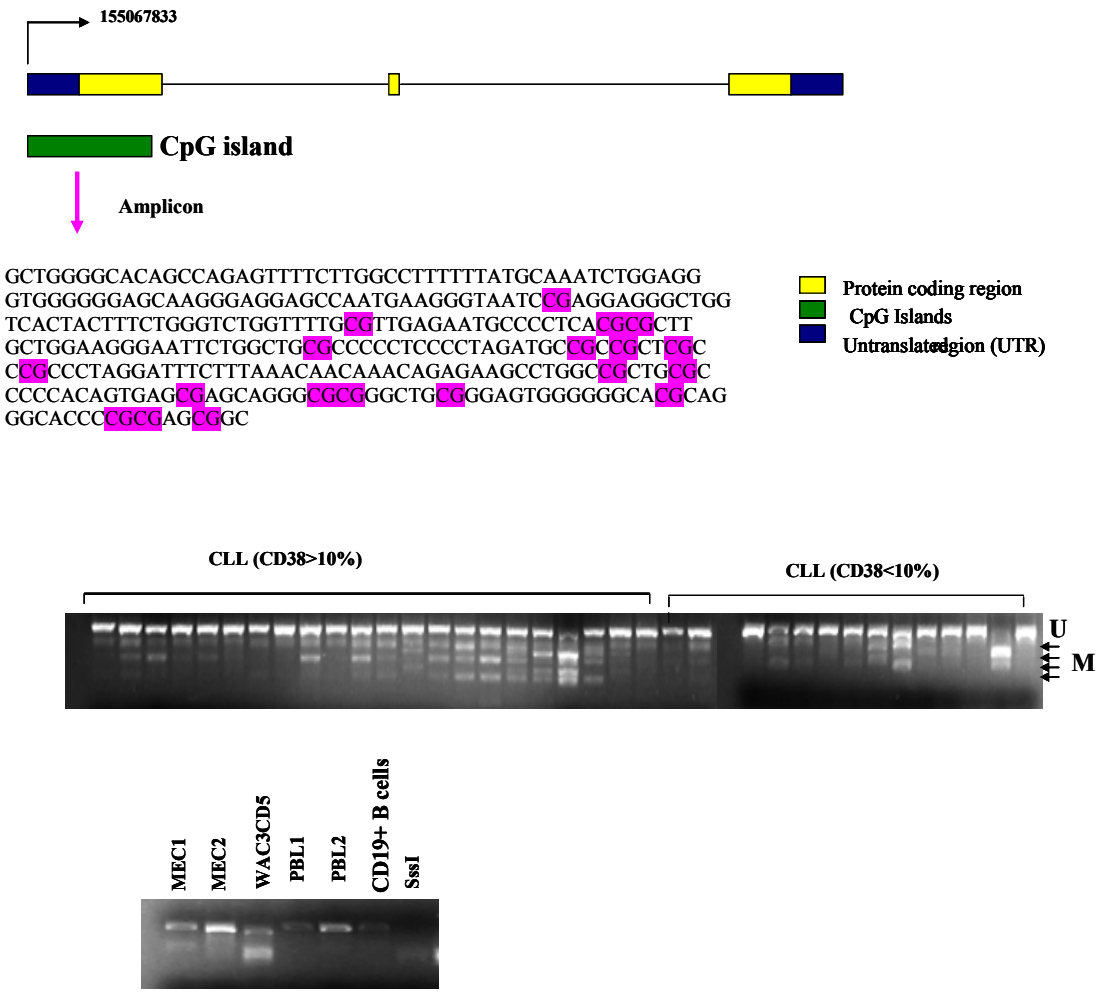

Figure 2.18: *SFRP2* gene structure and COBRA. The PCR product of *SFRP2* was digested with methylation sensitive restriction enzyme *BSTU1*. Fragmented bands represent methylated enzyme cut sites and the undigested bands represent unmethylated sites.

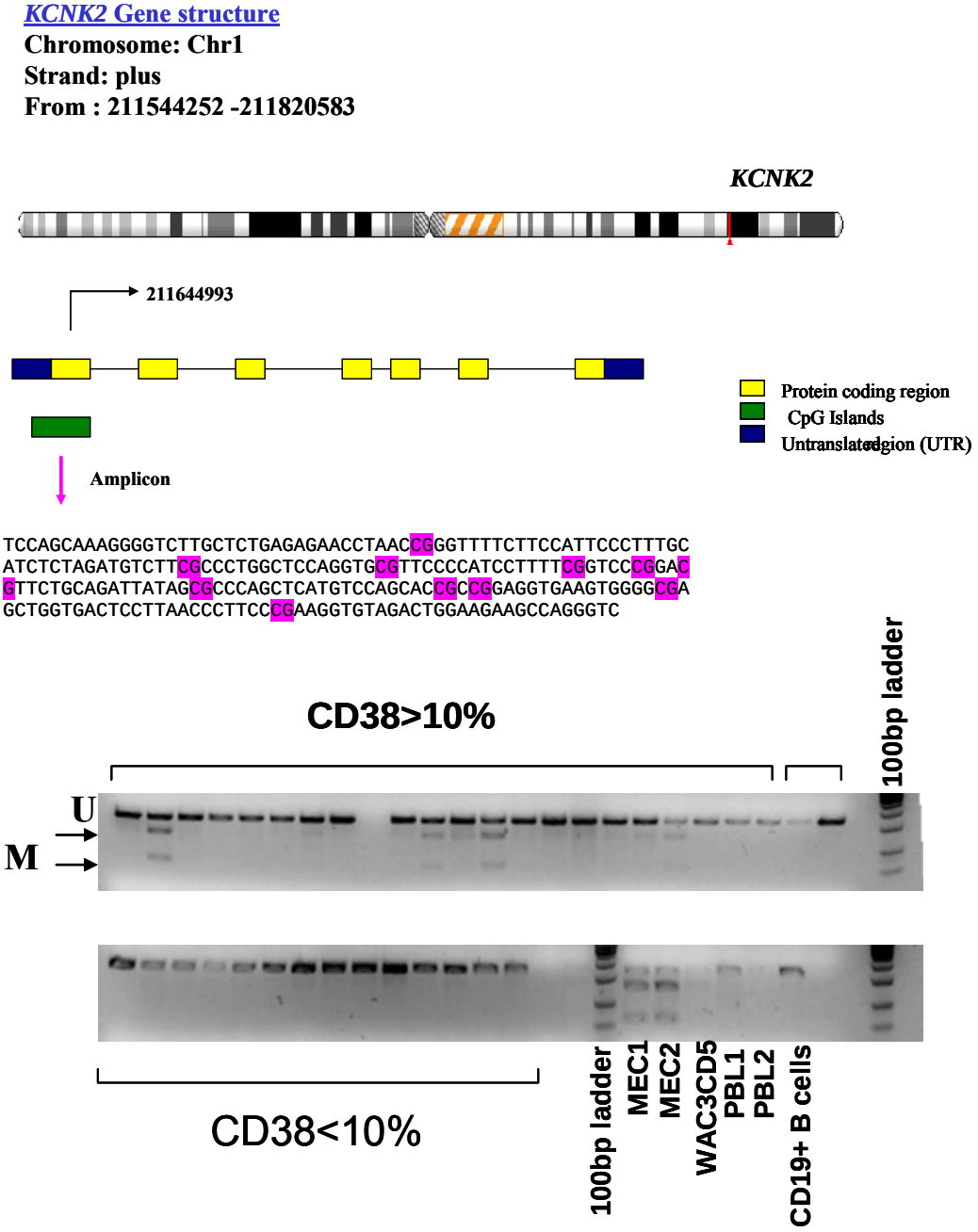

Figure 2.19: *KCNK2* gene structure and COBRA. The PCR product of *KCNK2* was digested with methylation sensitive restriction enzyme *Hpy99I* (CGWCG).

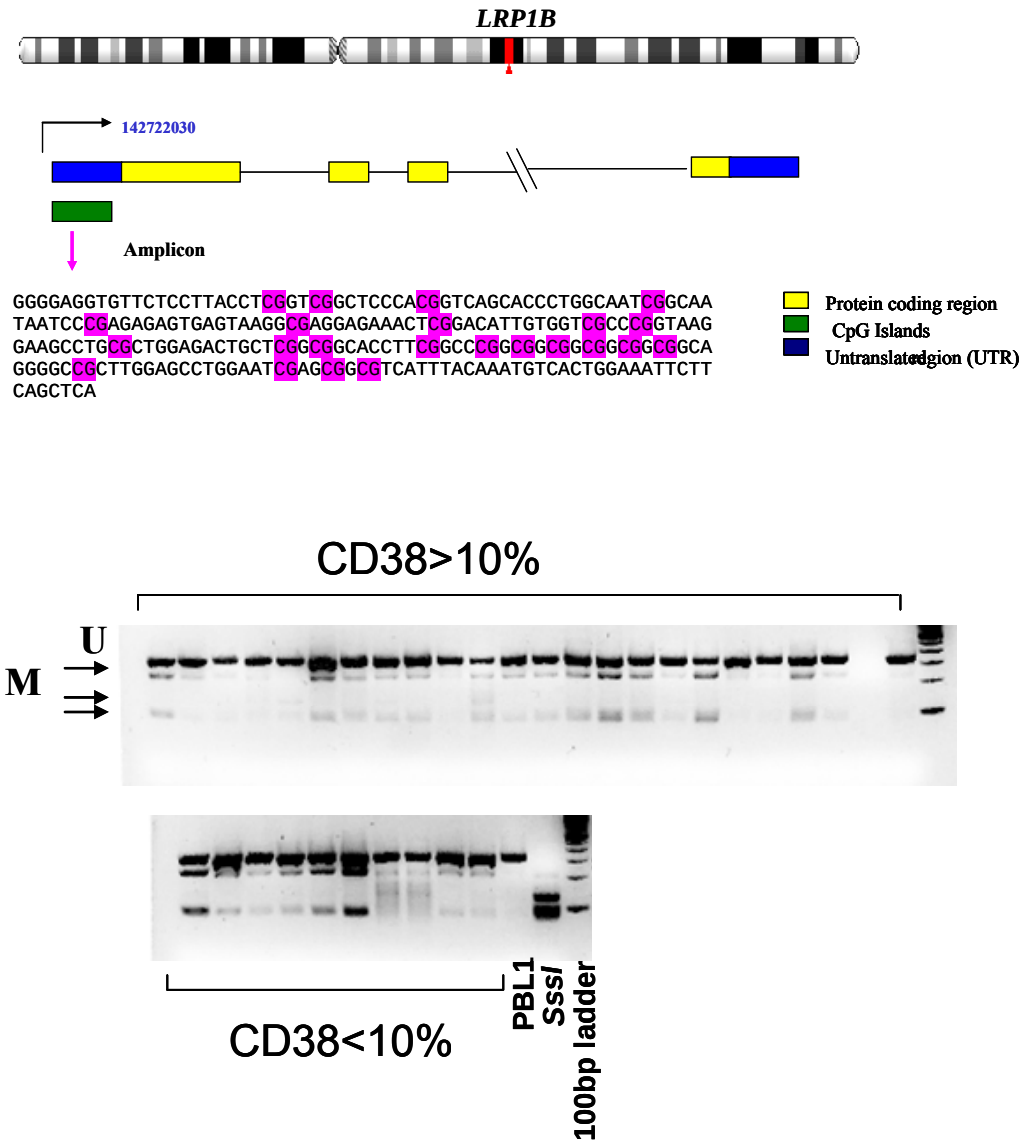

Figure 2.20: *LRP1B* gene structure and COBRA. DNA methylation of *LRP1B* was analyzed using a methylation restriction enzyme (*Taqa1*) which cleaves methylated TCGA sequences. Location of the CpG sites relative to the transcriptional start sites is shown, as well as the interrogated region for the COBRA study.

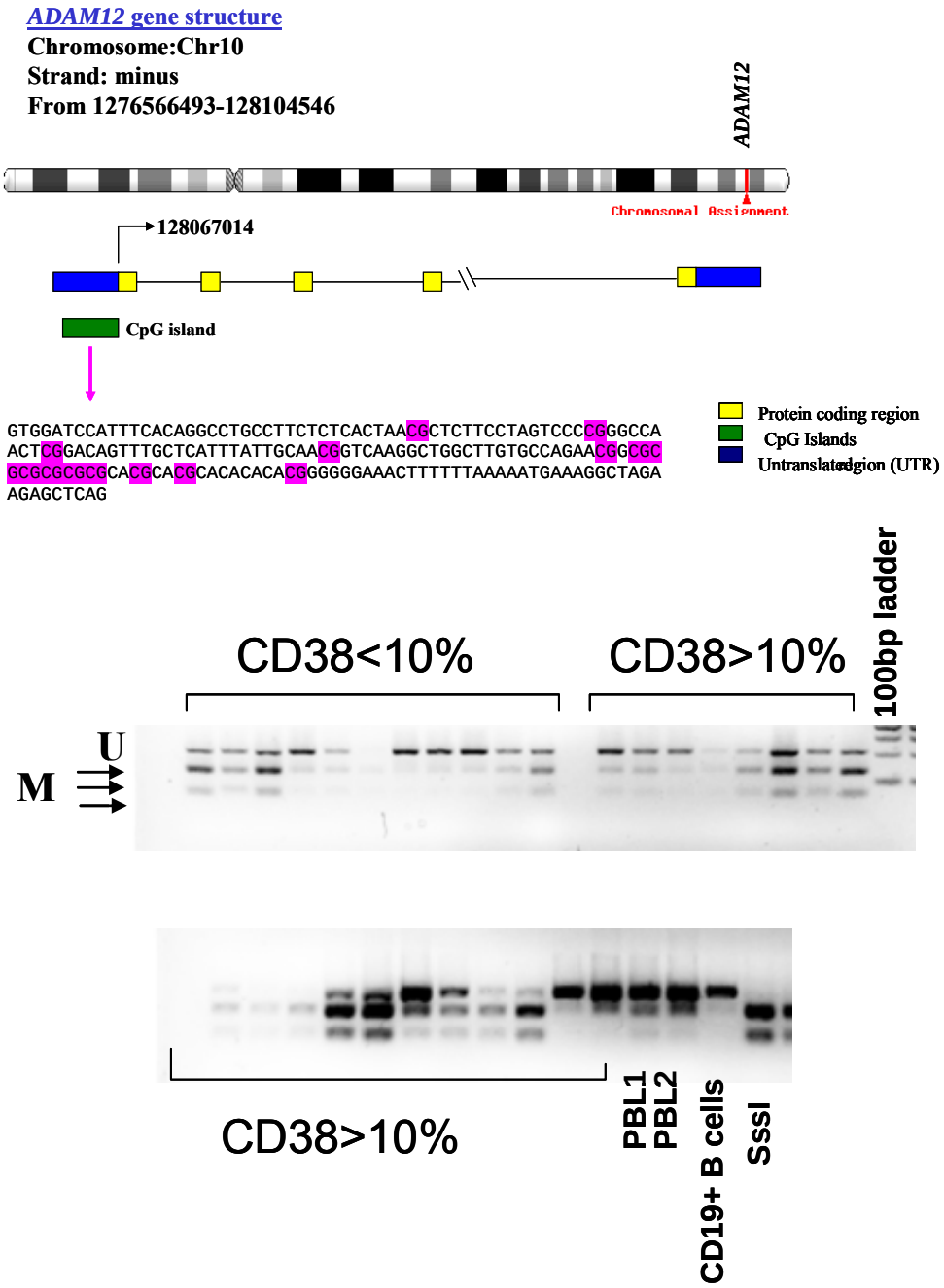

Figure 2.21:*ADAM12* gene structure and COBRA.
Methylation status of *ADAM12* promoter was investigated in B-CLL patients with various CD38 expression levels.

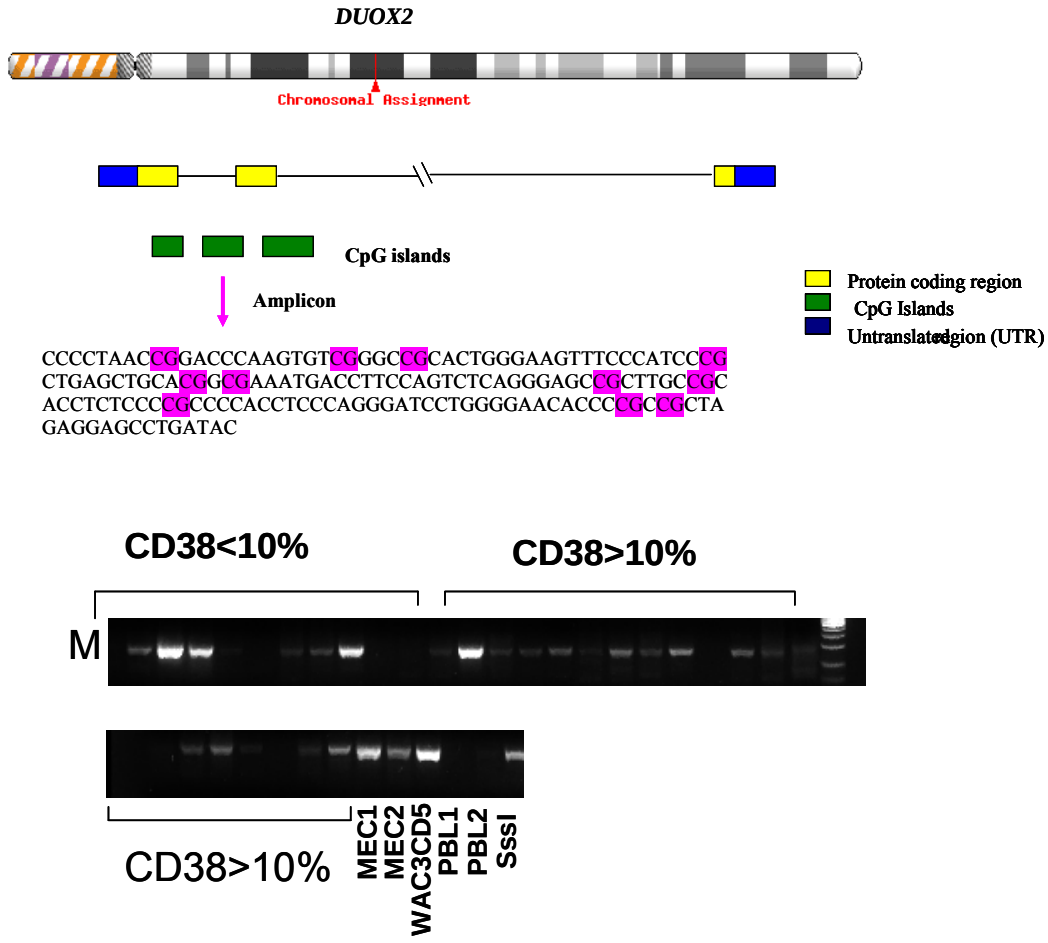

Figure 2.22: *DUOX2* gene structure and MSP. Methylation status of *DUOX2* was investigated using methylation specific PCR. One microgram of genomic DNA was bisulfite treated, then PCR was performed for 35 cycles with primers specific for methylated (M) template, and the products were analyzed on 3% agarose gel. Normal female (PBL1) and normal male (PBL2) peripheral blood lymphocyte DNA was used as negative controls, and in vitro methylated DNA using SssI methyltransferase was the positive control. The presence of a band in the gel image is an indicator of methylation.

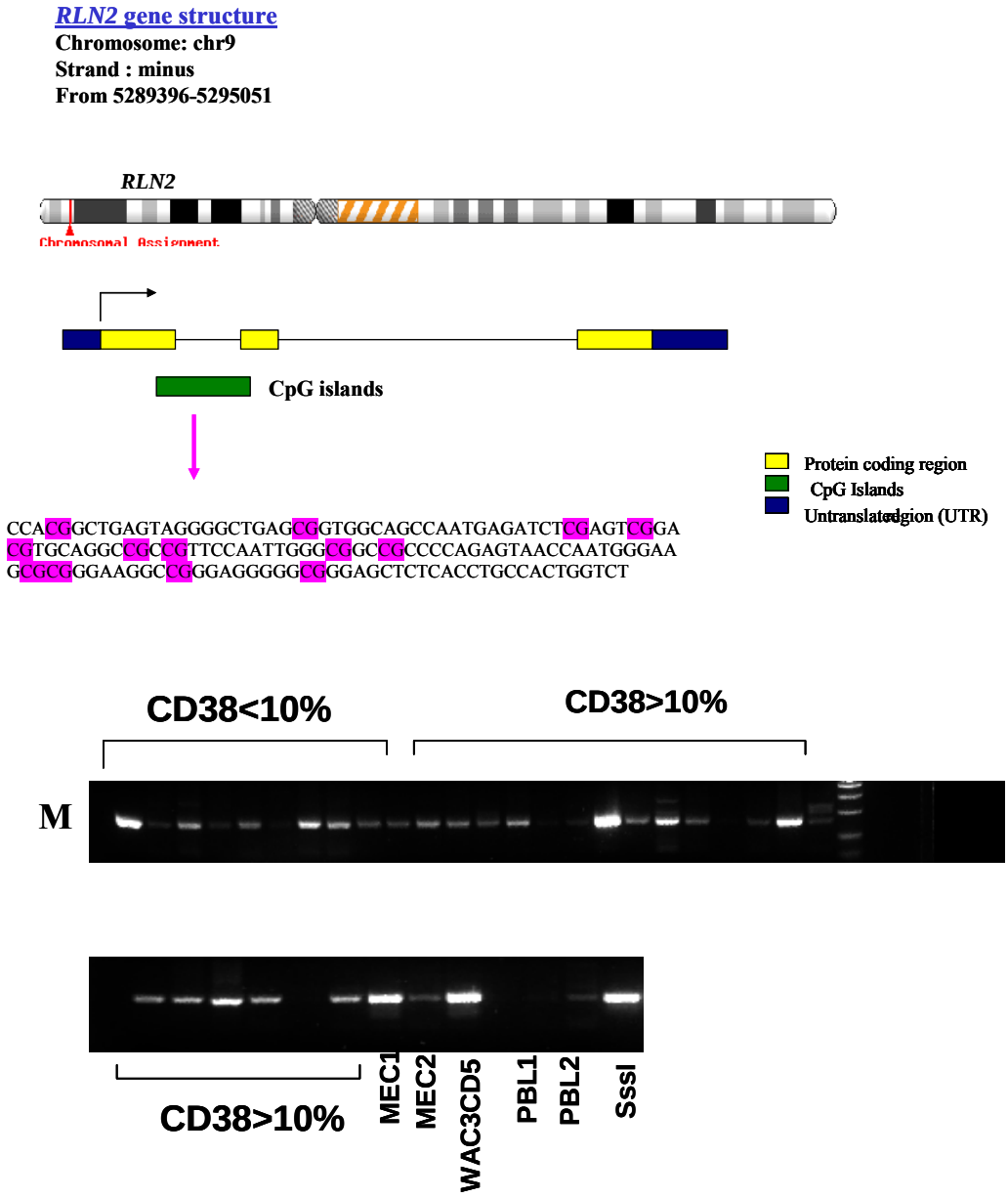

Figure 2.23: *RLN2* gene structure and MSP. The DNA methylation pattern of *RLN2* was investigated in B-CLL samples. Methylated alleles are present in CLL samples but not in the normal lymphocytes.

Bisulfite genomic sequencing of *ADAM12* and *DLEU7*

Qualitative or semi-quantitative estimates of DNA methylation play an important role in epigenetic studies, but in order to define the frequency and specific location of cytosine methylation in regulatory regions of two genes (*ADAM12* and *DLEU7*) we performed bisulfite genomic sequencing from representative primary CLL samples, cell lines, and appropriate controls.

The CGI in *ADAM12* encompasses the promoter region and part of the 5'UTR (Figure 2.24).The relative positions of CG dinucleotides are shown. Bisulfite sequencing demonstrated that, as expected, normal CD19+ B-cells were unmethylated, while the *SssI*-treated positive control was fully methylated. The MEC2 cell line ($CD38^{high}$) was densely methylated in CG positions 4-13 and the WAC3CD5 ($CD38^{low}$) cell line showed dense methylation across the entire region of CG 1-14. Interestingly, the MEC1 cell line, with intermediate levels of CD38, demonstrated a pattern suggesting a dual population of methylated DNA fragments. Four representative samples of primary CLL cells with >10% CD38 expression (15, 44, 50, 82% CD38) showed a dense pattern of methylation similar to that of MEC2 and WAC3CD5. Three additional cases with CD38<10% (1, 3 and 3%) showed a similar patterns which is consistent with the COBRA results showing methylation across the spectrum of CD38 expression levels.

Since it appeared that *DLEU7* was differentially methylated and correlated with CD38 expression levels, we chose to perform detailed bisulfite sequencing to validate this in cases with favorable or unfavorable biological characteristics. The *DLEU7* gene contains a CGI that spans part of the promoter and first exon and includes binding sites for SP1 transcription factors (Figure 2.25). The bisulfite sequencing reaction interrogated

25 CG dinucleotides with reference to potential interactions of binding sites and methylated or unmethylated cytosine. The patterns of methylation in MEC1 and MEC2 cell lines were similar, and showed a region near the middle of the CGI that was unmethylated, while the remainder was densely methylated. CGs from 5' cytosine positions 1-9 and 14-25, that also encompass SP1 binding sites, were methylated. Multiple attempts to perform this analysis on the WAC3CD5 cell line failed due to an inability to generate a PCR product with these primers. Of the primary CLL samples studied with genomic bisulfite sequencing, 5 were $CD38^{low}$ (1 to 3% positive). IgVH mutational status was tested for 3 of these 5 and also found to have mutated IgV_H ($\geq$ 2%). Both $CD38^{low}$ and mutated IgV_H suggest a favorable prognosis. These 5 all showed extensive methylation for CGs from 5' cytosine positions 1-9 and 14-25 similar to that of the CLL cell lines. There was a core region from CGs 10-12 that remained unmethylated, but contained no SP1 transcriptional regulatory protein binding sites. The same pattern was found in the MEC1 cell line, although this cell line remains pretty consistently ~69% positive for CD38. Conversely, *DLEU7* was much less methylated in 2 representative patients with $CD38^{high}$ (50% and 96% CD38) and 2 additional patients with unmutated IgV_H genes (suggestive of poor prognosis). A similar sporadic low level of methylation was observed for normal CD19+ B cells (Figure 2.25). While the pattern of MEC1 methylation was virtually identical to better prognosis cases, its CD38 expression level was not consistent with the primary CLL cells in this group. This cell line was, however, derived from the CLL patient when in a less accelerated clinical phase. Thus, the pattern of preferential methylation in the $CD38^{low}$ group confirmed the findings by COBRA

analysis and also suggests this might be related to the favorable or unfavorable characteristics of the CLL cells.

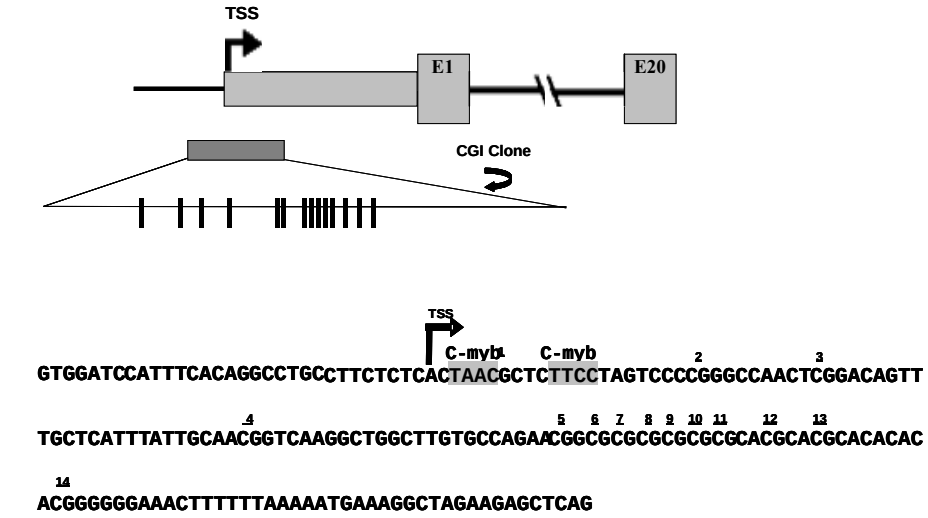

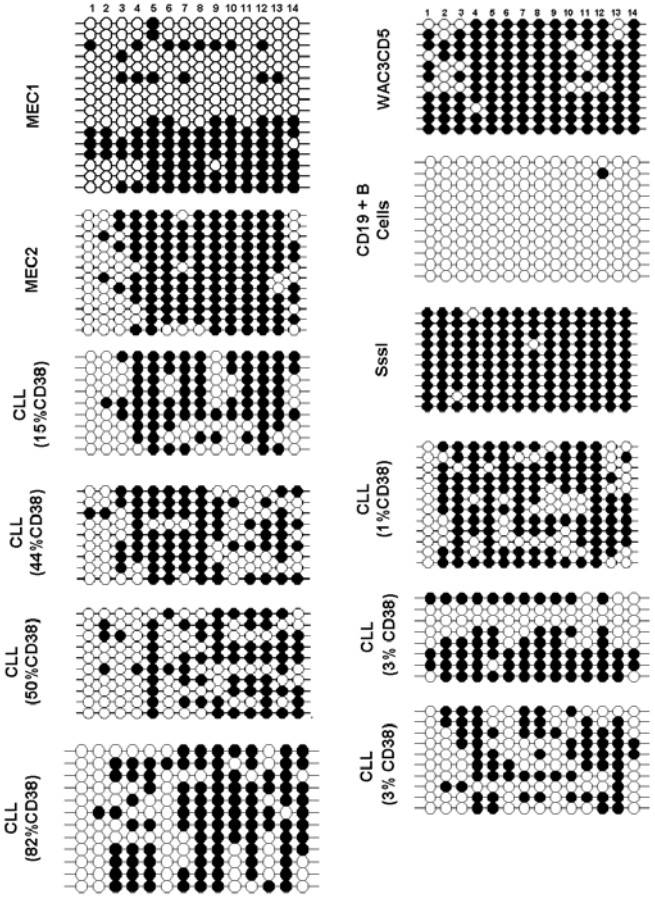

Figure 2.24: Bisulfite sequencing of *ADAM12*. A schematic map showing the region of interest that includes the promoter around the transcriptional start site. The methylated status of 14 CG dinucleotides (1-14) was determined from bisulfite treated DNA of CLL patients with different CD38 expression levels, 2CLL cell lines (MEC2and WAC3), and CD+19 B cells from a healthy donor, along with in vitro methylated DNA (*SssI* treated). Each row represents the results from an individual clone across the 14 CGs. Filled circles indicate methylated cytosine and open circles are unmethylated sites.

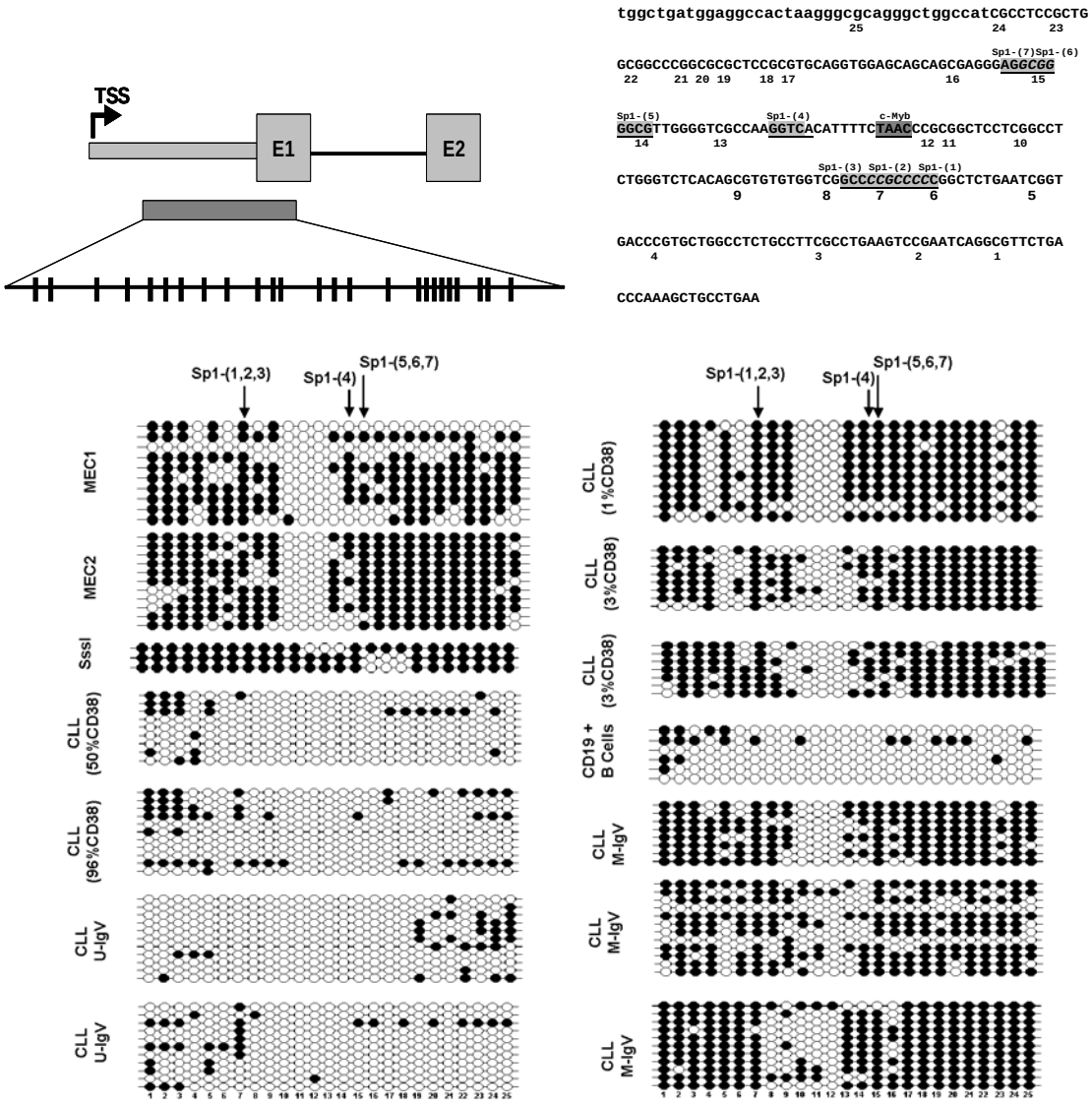

Figure 2.25: Bisulfite sequencing of *DLEU7*. DNA methylation of 25 CG dinucleotides was examined in a 5' region of *DLEU7* that spans a part of a region spanning the predicted 5'UTR and part of the exon; the location of this region with respect to the transcription start site (TSS) is shown. The CG dinucleotides are shown as heavy black lines. The methylated status of 25 CG dinucleotides was determined from bisulfite treated DNA of CLL patients with different CD38 expression levels and differing IgVH mutational status, 2CLL cell lines (MEC1and MEC2) and CD19+ B cells from a healthy donor. Each row is the result from an individual clone across the 25 CG dinucleotides. Filled circles indicate methylated cytosine and open circles are unmethylated sites.

Pharmacologic reactivation of genes in CLL cell lines

In an effort to investigate the functional impact(s) of DNA methylation and/or histone deacetylase inhibition on mRNA expression of selected genes (*LHX2*, *NRP2*, *DLEU7*, *KCNK2*, *DLC-1*, *ADAM12*, *APC2* and, *SFRP2*), we used 3 CLL cell lines before and after treatment using the demethylating agent 5'-Aza, a histone deacetylase inhibitor (TSA), and both in combination. It is quite difficult to perform such studies on primary cells since 5'-Aza is a competitive inhibitor of DNMTs and demethylation seems to require at least a few rounds of cell division. For it to work primary CLL cells are not very amenable to such in vitro conditions.

Quantitative real-time RT-PCR was performed in triplicate, and the median expression level was calculated (Figure 2.26). As shown, the re-expression pattern varied by gene and by cell line, but in all instances pharmacologic reversal was observed to some degree. For instance, treatment of the cell lines with 5'-Aza alone resulted in robust re -expression of *ADAM12* mRNA in all three cell lines, which is in good agreement with the density of methylation shown in MEC1 and WAC3CD5. However, TSA alone and in combination with 5'-Aza, induced up-regulation of *ADAM12* in MEC1 and WAC3CD5. This data, like that from other studies, suggests the involvement of additional mechanism(s) affecting chromatin compaction in addition to DNA methylation.

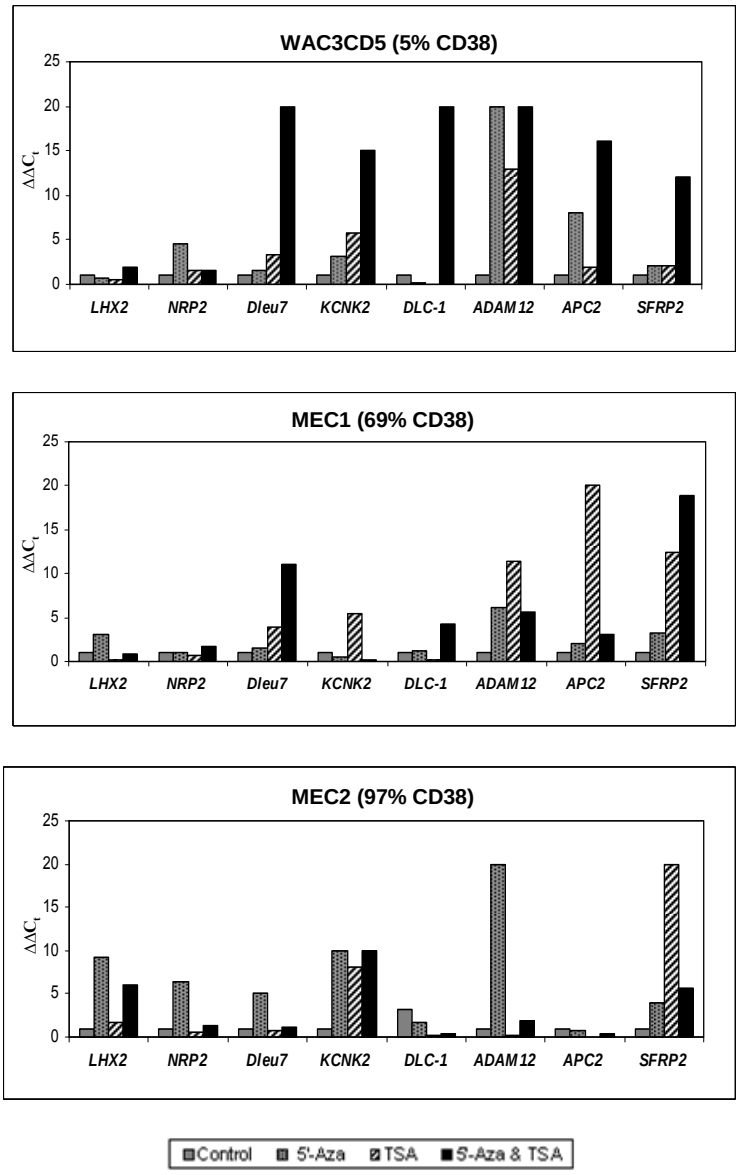

Figure 2.26: Pharmacological reactivation in CLL cell lines. The mRNA expression levels of 8 genes were quantified using real time RT-PCR in untreated WAC3CD5, MEC1 and MEC2 cell lines. These were treated with the demethylating agent 5'Aza, TSA, or the combination of 5-Aza and TSA. A house keeping gene (*HPRT1*) was used as an internal control for all of the above genes, except for *DLC-1* where *GAPDH* was used. The relative expression level of each gene was determined using $2^{-\Delta\Delta Ct}$ where Ct is the cycle threshold for positivity.

Discussion

Aberrant DNA methylation has been reported in virtually every type of human cancer examined (reviewed in [22-26]). Our previous investigations in 3 types of small B-cell NHL identified multiple genes that were differentially methylated [17]. While the number of samples was too small for meaningful statistical analysis by prognostic parameters in the CLL patients, there appeared to be 2 groups that segregated by methylation profile. This initial observation motivated us to ask if methylation status might have some impact on the biological features of CLL subtypes.

Cells of CLL patients exhibit a spectrum of biological features, and surrogate biomarkers such as the IgVH mutational status, p53 alterations, cytogenetic abnormalities, ZAP-70 and CD38 expression; all of which are valuable in distinguishing clinical subsets of CLL [27;28]. Our rationale for focusing the study around CD38 levels derived from the fact that CD38 has recently been actively investigated for its biological functions [7;27-30]. The CD38 protein is thought to function as a co-signaling molecule, along with the B-cell receptor (BCR), and relates to the ability to transduce trans membrane signaling via cross-lineages of BCR and CD38 [9;10;29;31;32]. CLL cells have been thought to have diminished cell cycling capacity, but CD38 (+) and CD38 (-) subclones of individual CLL samples were analyzed for co-expression of molecules associated with cellular activation and protection from apoptosis [29]. Regardless of the size of the CD38 (+) fraction within a sample, the CD38(+) subclones were markedly enriched for expression of Ki-67, CD27, CD62L, CD69, ZAP-70, human telomerase reverse transcriptase, and telomerase activity compared to CD38(-) subclones [29]. These observations may help explain why $CD38^{high}$ cases of CLL are associated with poor

clinical outcome. Further evidence for a central role of CD38 derives from the fact that its activation can trigger proliferation or survival signals through interactions with the CD31 ligand expressed by nurse-like cells and stromal/endothelial components [28] which leads to tyrosine phosphorylation of ZAP-70. These observations may help explain the linkage of CD38 and ZAP-70 and why high levels of these proteins are coordinately associated with poor clinical outcome. While we did not have ZAP-70 data on all our patients, we did have CD38 levels, and although not perfect, their coexpression occurs in the majority of cases [28].

Gene expression analysis suggests that CLL may derive from antigen-stimulated B-cells and the origin of each subset represents a putative stage of normal B-cell differentiation [33]. The cases with $CD38^{high}$ and unmutated IgVH genes are similar to pre-germinal center B-cells and portend a poor prognosis, whereas those cases with mutated IgVH genes and $CD38^{low}$ are reminiscent of post-germinal center B-cells and generally have an indolent course to their disease. We also did not have IgVH mutational results on all of our subjects, but again view the associations of IgVH status and CD38 in a manner that supports using CD38 as a surrogate for IgVH mutations in certain of our experiments [3;34].

We initially chose to base the present study on CD38 expression levels to investigate any potential role(s) for DNA methylation of genes that might affect biological behavior in these subgroups. In this context, we observed that some genes are methylated or unmethylated in most (or all) cases, while others segregate with $CD38^{low}$ or $CD38^{high}$ expression (data not shown). Part of the study also derives from publications suggesting that there has not yet been universal agreement on the precise level of CD38

expression that best segregates patients into clinical groups or what levels comprise $CD38^{low}$ or $CD38^{high}$ cases. Levels of 7%, 20%, and 30% have all been put forward as clinical thresholds [3;27;35].

Previous studies have demonstrated global [36] and gene-specific hypomethylation events in CLL involving genes such as *Erb-A1* [37], *TCL1* [38], and *BCL2* where hypomethylation has been thought to contribute to BCL2 protein over- expression [39]. In the context of gene-specific hypermethylation, we have previously demonstrated DNA methylation involving multiple genes in CLL but did not segregate the data by CD38 expression [17;18]. The genes *ZAP-70* [40], *TWIST2* [41], E-cadherin (*CDH1*) [42], *TERT* [43], and the metabotrobic glutamate receptor 7 (*GRM7*) [44] have been reported as differentially methylated in primary CLL. The *DAPK1* and *PTPRO* genes are also frequently affected by methylation, and this *DAPK1* abnormality has been found in both spontaneous and familial CLL cases [45;46]. Thus, there is an ever-growing literature regarding the CLL methylome that has led us to this investigation of DNA methylation patterns between $CD38^{low}$ or $CD38^{high}$ cases to determine if this epigenetic alteration might contribute to differential biological behavior.

Multiple genes were methylated across all levels of CD38 expression in this study, but there were also genes that were preferentially methylated based on CD38 expression levels. For instance, the *PCDHGB7*, *DLC-1*, *APC2*, *LHX2*, and *ADAM12* genes were methylated across all, or most, levels of CD38 tested and therefore are not very likely to explain differences in biological behaviors between subsets, but the alterations could contribute to the biological behavior of CLL B cells in general. However, there were also genes that were preferentially methylated based on CD38

expression levels. Specifically *HOXC10* and *SFRP2* were methylated in $CD38^{high}$ cases while *DLEU7* was methylated mainly in $CD38^{low}$ cases. Both of these sets, and indeed other differentially methylated genes that we have not yet confirmed, are certainly candidates to explore biological behaviors that may differ between CD38 subtypes and are related to clinical behavior/outcome. These observations point to genes and/or pathways that may be biologically relevant and affected by DNA methylation in CLL. Potentially, some of these methylated genes may be explored for use as diagnostic or prognostic epigenetic biomarkers.

One important caveat is that methylation does not always lead to gene silencing. In the context of pharmacologic reversals, treatment with a demethylating agent generally induced up-regulation of the associated gene mRNA, but not always. In some cases, full re-expression required a combination of de-methylation and inhibition of histone deacetylase(s). These observations are not unexpected, as there are many examples of genes that seem to be more or less sensitive to these treatments. Although CLL cell lines generally recapitulate the methylation patterns in primary CLL cells, the associations with gene expression must be confirmed in primary CLL cells. However, such ex vivo experiments are difficult with current demethylating agents that require cell divisions since CLL cells do not readily divide on in vitro cultures for very long. Thus, there is clearly more to be learned about differential gene susceptibility to initial DNA methylation (and histone modifications) and their sensitivities to pharmacologic interventions. These questions are relevant and important in discussions of clinical epigenetic therapies.

Another caveat relates to site-specific DNA methylation. For example, in the *TERT* gene containing dense methylation across the promoter, a core group of cytosines in the middle of the promoter remain unmethylated and transcription proceeds [47]. Thus, gene expression was present even though prominent methylation was also present, but in a very site-specific manner that did not interfere with binding of certain transcription factors. We observed a similar situation in which bisulfite sequencing in the *DLEU7* promoter demonstrated a methylation pattern similar to that of *TERT*. In this case, however, methylation occurred at SP1 binding sites and mRNA expression was decreased but was then reactivated with pharmacologic treatment. Nevertheless, this illustrates the need for single base pair cytosine methylation analysis in order to fully appreciate the specific focal nature of DNA methylation within regulatory regions and its association with the binding sites of regulatory proteins [21].

A final caveat is that our study is limited by the relatively small numbers of samples from patients with CLL and the lack of longitudinal outcomes data. These factors limited our ability to investigate how the methylation patterns of any of the candidate genes correlates with outcome. Future investigations, either in the context of comparative clinical trials or prospective collections of clinical tissue and outcomes data, will be necessary to confirm the importance of methylated genes as prognostic biomarkers.

Of the gene regions we confirmed as methylated using COBRA and MSP, some have known functions of biological interest in CLL, and others point toward further investigations into groups of genes (HOX clusters) and pathways (WNT) that may be productive. The gene, a disintegrin and metaloprotease 12 (*ADAM12*), has multiple and

diverse functions in normal and malignant cells and is highly expressed in fast growing tissues and some tumor cells such as breast and bladder cancers. However, its role in either normal B-cells or in CLL remains unclear. Since CLL is generally not as rapidly growing as some tumor types, it is tempting to speculate that perhaps down regulation of this gene contributes to less aggressive clinical behavior. The *DLEU7* gene contains a CGI spanning the promoter and first exon regions and includes binding sites for multiple transcriptional enhancing factors. This gene was previously reported to be affected by DNA methylation, but its relationship to CD38 expression was not explored [48]. In our study, *DLEU7* methylation is more common in $CD38^{low}$ than $CD38^{high}$ cases.

The *APC2* and the soluble frizzled member *SFRP2* [49] genes are members of the WNT signaling pathway which is deregulated in CLL [50-53]. WNTs are a large family of secreted glycoproteins involved in cell proliferation, differentiation, and oncogenesis. The classical WNT signaling cascade inhibits the activity of the enzyme glycogen synthase kinase-3β (GSK3β), augmenting β-catenin translocation to the nucleus and transcription of target genes. We have previously shown that GSK3β accumulates in the nucleus of CLL cells, and that inhibition of GSK3β results in epigenetic silencing of nuclear factor KB target genes and induction of apoptosis [53]. Additionally, Lu, et al [51], reported an abundance of mRNA for *WNT16*, *WNT10A*, *WNT3*, and *WNT6* in CLL cells. Thus, epigenetic dysregulation of the Wnt pathway through DNA methylation of specific genes indicates that further studies are warranted and might help elucidate further differences in CLL subsets of patients.

In summary, there are clear alterations in DNA methylation of multiple genes in CLL. Some of these are methylated in cases involving all levels of CD38 and therefore

may affect the general biological behavior of all CLL cases in a similar manner. However, other genes that are differentially methylated and associated with $CD38^{low}$ or $CD38^{high}$ expression are also likely associated with biological characteristics of the disease. Further genome-wide and gene-specific studies will be needed to fully appreciate these alterations and their impact(s) on human CLL.

Reference List

1. Zent CS, Kay NE. Chronic lymphocytic leukemia: biology and current treatment. Curr.Oncol.Rep. 2007;9:345-352.

2. Krober A, Seiler T, Benner A et al. V(H) mutation status, CD38 expression level, genomic aberrations, and survival in chronic lymphocytic leukemia. Blood 2002;100:1410-1416.

3. Damle RN, Wasil T, Fais F et al. Ig V gene mutation status and CD38 expression as novel prognostic indicators in chronic lymphocytic leukemia. Blood 1999;94:1840-1847.

4. Gentile M, Mauro FR, Calabrese E et al. The prognostic value of CD38 expression in chronic lymphocytic leukaemia patients studied prospectively at diagnosis: a single institute experience. Br.J.Haematol. 2005;130:549-557.

5. Hamblin TJ, Orchard JA, Ibbotson RE et al. CD38 expression and immunoglobulin variable region mutations are independent prognostic variables in chronic lymphocytic leukemia, but CD38 expression may vary during the course of the disease. Blood 2002;99:1023-1029.

6. Tobin G, Rosenquist R. Prognostic Usage of VH Gene Mutation Status and Its Surrogate Markers and the Role of Antigen Selection in Chronic Lymphocytic Leukemia. Med.Oncol. 2005;22:217-228.

7. De FA, Zocchi E, Guida L, Franco L, Bruzzone S. Autocrine and paracrine calcium signaling by the CD38/NAD+/cyclic ADP-ribose system. Ann.N.Y.Acad.Sci. 2004;1028:176-191.

8. Deaglio S, Capobianco A, Bergui L et al. CD38 is a signaling molecule in B-cell chronic lymphocytic leukemia cells. Blood 2003;102:2146-2155.

9. Deaglio S, Vaisitti T, Bergui L et al. CD38 and CD100 lead a network of surface receptors relaying positive signals for B-CLL growth and survival. Blood 2005;105:3042-3050.

10. Moreno-Garcia ME, Lopez-Bojorques LN, Zentella A et al. CD38 signaling regulates B lymphocyte activation via a phospholipase C (PLC)-gamma 2-independent, protein kinase C, phosphatidylcholine-PLC, and phospholipase D-dependent signaling cascade. J.Immunol. 2005;174:2687-2695.

11. Pittner BT, Shanafelt TD, Kay NE, Jelinek DF. CD38 expression levels in chronic lymphocytic leukemia B cells are associated with activation marker expression and differential responses to interferon stimulation. Leukemia 2005

12. Guo J, Burger M, Nimmrich I et al. Differential DNA methylation of gene promoters in small B-cell lymphomas. Am.J.Clin.Pathol. 2005;124:430-439.

13. Yang H, Chen CM, Yan P et al. The androgen receptor gene is preferentially hypermethylated in follicular non-Hodgkin's lymphomas. Clin.Cancer Res. 2003;9:4034-4042.

14. Caldwell CW, Patterson WP. Relationship between CD45 antigen expression and putative stages of differentiation in B-cell malignancies. Am.J.Hematol. 1991;36:111-115.

15. Wendel-Hansen V, Sallstrom J, De Campos-Lima PO et al. Epstein-Barr virus (EBV) can immortalize B-cll cells activated by cytokines. Leukemia 1994;8:476-484.

16. Stacchini A, Aragno M, Vallario A et al. MEC1 and MEC2: two new cell lines derived from B-chronic lymphocytic leukaemia in prolymphocytoid transformation. Leuk.Res. 1999;23:127-136.

17. Rahmatpanah FB, Carstens S, Guo J et al. Differential DNA methylation patterns of small B-cell lymphoma subclasses with different clinical behavior. Leukemia 2006;20:1855-1862.

18. Shi H, Guo J, Duff DJ et al. Discovery of novel epigenetic markers in non-Hodgkin's lymphoma. Carcinogenesis 2007;28:60-70.

19. Heisler LE, Torti D, Boutros PC et al. CpG Island microarray probe sequences derived from a physical library are representative of CpG Islands annotated on the human genome. Nucleic Acids Res. 2005;33:2952-2961.

20. Huang TH, Perry MR, Laux DE. Methylation profiling of CpG islands in human breast cancer cells. Hum.Mol.Genet. 1999;8:459-470.

21. Taylor KH, Kramer RS, Davis JW et al. Ultradeep bisulfite sequencing analysis of DNA methylation patterns in multiple gene promoters by 454 sequencing. Cancer Res. 2007;67:8511-8518.

22. Baylin SB. DNA methylation and gene silencing in cancer. Nat.Clin.Pract.Oncol. 2005;2 Suppl 1:S4-11.

23. Esteller M. Cancer epigenomics: DNA methylomes and histone-modification maps. Nat.Rev.Genet. 2007

24. Jair KW, Bachman KE, Suzuki H et al. De novo CpG island methylation in human cancer cells. Cancer Res. 2006;66:682-692.

25. Jones PA, Baylin SB. The fundamental role of epigenetic events in cancer. Nat.Rev.Genet. 2002;3:415-428.

26. Laird PW. Cancer epigenetics. Hum.Mol.Genet. 2005;14 Spec No 1:R65-R76.

27. Deaglio S, Vaisitti T, Aydin S, Ferrero E, Malavasi F. In-tandem insight from basic science combined with clinical research: CD38 as both marker and key component of the pathogenetic network underlying chronic lymphocytic leukemia. Blood 2006;108:1135-1144.

28. Deaglio S, Vaisitti T, Aydin S et al. CD38 and ZAP-70 are functionally linked and mark CLL cells with high migratory potential. Blood 2007

29. Damle RN, Temburni S, Calissano C et al. CD38 expression labels an activated subset within chronic lymphocytic leukemia clones enriched in proliferating B cells. Blood 2007

30. Deaglio S, Vaisitti T, Billington R et al. CD38/CD19: a lipid raft dependent signaling complex in human B cells. Blood 2007

31. Malavasi F, Deaglio S, Ferrero E et al. CD38 and CD157 as Receptors of the Immune System: A Bridge Between Innate and Adaptive Immunity. Mol.Med. 2006;12:334-341.

32. Morabito F, Mangiola M, Stelitano C et al. Simultaneous expression of CD38 and its ligand CD31 by chronic lymphocytic leukemia B-cells: anecdotal observation or pathogenetic hypothesis for the clinical outcome? Haematologica 2003;88:354-355.

33. Chiorazzi N, Rai KR, Ferrarini M. Chronic lymphocytic leukemia. N.Engl.J.Med. 2005;352:804-815.

34. Bagli L, Zucchini A, Innoceta AM et al. Immunoglobulin V(H) genes and CD38 expression analysis in B-cell chronic lymphocytic leukemia. Acta Haematol. 2006;116:72-74.

35. Ibrahim S, Keating M, Do KA et al. CD38 expression as an important prognostic factor in B-cell chronic lymphocytic leukemia. Blood 2001;98:181-186.

36. Wahlfors J, Hiltunen H, Heinonen K et al. Genomic hypomethylation in human chronic lymphocytic leukemia. Blood 1992;80:2074-2080.

37. Lipsanen V, Leinonen P, Alhonen L, Janne J. Hypomethylation of ornithine decarboxylase gene and erb-A1 oncogene in human chronic lymphatic leukemia. Blood 1988;72:2042-2044.

38. Yuille MR, Condie A, Stone EM et al. TCL1 is activated by chromosomal rearrangement or by hypomethylation. Genes Chromosomes.Cancer 2001;30:336-341.

39. Hanada M, Delia D, Aiello A, Stadtmauer E, Reed JC. bcl-2 gene hypomethylation and high-level expression in B-cell chronic lymphocytic leukemia. Blood 1993;82:1820-1828.

40. Corcoran M, Parker A, Orchard J et al. ZAP-70 methylation status is associated with ZAP-70 expression status in chronic lymphocytic leukemia. Haematologica 2005;90:1078-1088.

41. Raval A, Lucas DM, Matkovic JJ et al. TWIST2 demonstrates differential methylation in immunoglobulin variable heavy chain mutated and unmutated chronic lymphocytic leukemia. J.Clin.Oncol. 2005;23:3877-3885.

42. Melki JR, Vincent PC, Brown RD, Clark SJ. Hypermethylation of E-cadherin in leukemia. Blood 2000;95:3208-3213.

43. Bechter OE, Eisterer W, Dlaska M, Kuhr T, Thaler J. CpG island methylation of the hTERT promoter is associated with lower telomerase activity in B-cell lymphocytic leukemia. Exp.Hematol. 2002;30:26-33.

44. Rush LJ, Raval A, Funchain P et al. Epigenetic profiling in chronic lymphocytic leukemia reveals novel methylation targets. Cancer Res. 2004;64:2424-2433.

45. Raval A, Tanner SM, Byrd JC et al. Downregulation of Death-Associated Protein Kinase 1 (DAPK1) in Chronic Lymphocytic Leukemia. Cell 2007;129:879-890.

46. Motiwala T, Majumder S, Kutay H et al. Methylation and Silencing of Protein Tyrosine Phosphatase Receptor Type O in Chronic Lymphocytic Leukemia. Clin.Cancer Res. 2007;13:3174-3181.

47. Zinn RL, Pruitt K, Eguchi S, Baylin SB, Herman JG. hTERT is expressed in cancer cell lines despite promoter DNA methylation by preservation of unmethylated DNA and active chromatin around the transcription start site. Cancer Res. 2007;67:194-201.

48. Hammarsund M, Corcoran MM, Wilson W et al. Characterization of a novel B-CLL candidate gene--DLEU7--located in the 13q14 tumor suppressor locus. FEBS Lett. 2004;556:75-80.

49. Liu TH, Raval A, Chen SS et al. CpG island methylation and expression of the secreted frizzled-related protein gene family in chronic lymphocytic leukemia. Cancer Res. 2006;66:653-658.

50. Howe D, Bromidge T. Variation of LEF-1 mRNA expression in low-grade B-cell non-Hodgkin's lymphoma. Leuk.Res. 2006;30:29-32.

51. Lu D, Zhao Y, Tawatao R et al. Activation of the Wnt signaling pathway in chronic lymphocytic leukemia. Proc.Natl.Acad.Sci.U.S.A 2004;101:3118-3123.

52. Qiang YW, Endo Y, Rubin JS, Rudikoff S. Wnt signaling in B-cell neoplasia. Oncogene 200

53. Ougolkov AV, Bone ND, Fernandez-Zapico ME, Kay NE, Billadeau DD. Inhibition of glycogen synthase kinase-3 activity leads to epigenetic silencing of nuclear factor kappaB target genes and induction of apoptosis in chronic lymphocytic leukemia B cells. Blood 2007;110:735-742.

Chapter 3

Epigenetic regulation of WNT signaling pathway in chronic lymphocytic leukemia

Abstract

B cell chronic lymphocytic leukemia (CLL) is the most common type of adult leukemia characterized by clonal expansion of apoptosis resistant mature B lymphocytes. An increasing body of evidence suggests that the epigenetic alteration of tumor suppressor genes plays significant role in tumorgenesis of CLL. We have used CpG arrays (244K) in combination with methylated CpG island amplification (MCA) technique to investigate methylation of CpG islands genome wide in CLL de nova patient samples with a wide range of CD38 expression as well as the related CLL cell lines MEC1, MEC2, and WAC3CD5. Among hypermethylated genes we found several of the WNT signaling genes, including, *Groucho*/*TLE, FZD2, FZD10, DKK1, AXIN2, SOX* family*, WNT2B, SFRP2, SFRP4,* and *APC2.*

To investigate the expression levels of WNT signaling genes and the possible effects of epigenetic silencing of negative regulators of this pathway, we quantified the gene profiles of 84 genes involved in WNT signaling using real time RT-PCR techniques in nine primary CLL samples. Target genes of β- Catenin-*TCF/LEF* activation and positive regulators of transcription p*300* were highly expressed in CLL cells, compared with normal CD19+ B cells.

Importantly, negative regulators of the WNT pathway (*Groucho/TLE, APC, APC2, NLK, PPP2CA* and *SOX17*) were expressed at significantly lower levels in CLL cells than normal B cell lymphocytes. These genes are viewed as WNT antagonists because of their ability to downregulate WNT signaling. Quantitative real time PCR revealed reactivation of several of the WNT inhibitors in CLL cell lines after treatment with epigenetic modifying drugs, which implies the functional impacts of DNA

methylation and /or histone deacetylase inhibitors on the mRNA expression of these genes. The patterns of DNA methylation and mRNA level of *APC2* were independently confirmed in a large number of CLL B-cells using COBRA, real time RT-PCR, and genomic bisulfite sequencing.

We therefore hypothesize that first, the WNT signaling pathway is active in CLL B cells, and second, that the expression of WNT inhibitors is downregulated due to abnormal DNA methylation. Deregulated WNT signaling pathway through up regulation of oncogenes and down regulation of tumor suppressor genes may contribute to the disrupted apoptosis that characterizes the CLL tumorgenesis.

Introduction

B- cell Chronic lymphocytic leukemia is the most frequent form of adult leukemia in the United States, with an incidence of 17,000 new cases per year. It is characterized by disrupted apoptosis rather than increased proliferation[1]. The aberrant DNA methylation of tumor suppressor genes has been reported in many types of cancers, including CLL. To define the CLL methylome, previously we reported using 9K and 12K genomic DNA microarrays spanning all human chromosomes[2;3]. To further investigate the global CGI methylation in CLL, we used CpG island microarrays containing ~244,000 probes in combination with the CpG island amplification technique (MCA). We found that several of the WNT signaling genes (*APC2*, *FZD2*, *FZD10*, *DKK1*, *DKK2*, *PPP2CA*, *PPP2R3B*, *SFRP2*, *SFRP4*, *LRP5*, *SOX3*, *SOX7*, *SOX9*, *SOX10*, *SOX17*, *NLK*, *TLE2*, *TLE4*, and *AXIN2*) were the preferential targets of DNA methylation in CLL cancer cell lines and primary tumors. Most of these genes are the antagonists of the canonical WNT pathway[4;5].

The WNT signaling pathway is required for embryonic development and has been implicated in promoting many types of cancer including CLL. The WNT signaling pathway is activated through the binding of extracellular glycoprotein WNT to frizzled trans- membrane receptors[6].This interaction leads to the phosphorylation of disheveled protein which associates with *AXIN* and prevents its binding to glycogen synthase kinase 3β(*GSK3β*), and subsequently prevents the phosphorylation of transcriptional factor β-Catenin [7].Therefore, un-phosphorylated β- Catenin cannot be recognized by the components of the E3 ubiquitin ligase β-*TrCP*, and can not be translocated to the nucleus where it interacts with transcriptional factors LEF/TCF, which facilitate transcriptional activation of WNT target genes[8]. On the contrary, in the absence of stimuli, the

destruction complex containing APC/AXIN/CKIα/GSK3β/PPP2CA destabilizes β – Catenin by post-translational modification. At the same time TCF/LEF transcriptional factors interact with repressors of transcription Groucho/TLE, histone deacetylase, to prevent activation of WNT target genes[9].

The main goal of this study was to determine if epigenetic alterations play a role or roles in inactivation of WNT antagonists. We used real time RT-PCR to profile the expression of 84 genes involved in WNT signaling in CLL, normal peripheral blood lymphocytes and normal CD19+ B cells. The gene expression analysis revealed up regulation of several WNT target genes, positive regulators of transcription such as histone acetylase *p300* , *TCF/LEF* transcriptional factors, and the component of the AP-1 transcriptional factor *FOSL1* and *CJUN* in the leukemic B CLL cells and CLL cell lines. With respect to WNT antagonist genes we found at least 10 genes that were under-expressed in CLL compared to normal CD19+ B cells, which had not been previously reported in CLL. We demonstrated that the promoter hypermethylation might be a major cause for the transcriptional silencing of tumor suppressor *APC2* and *SFRP2* supported by genome wide DNA methylation microarray (244K), COBRA and genomic bisulfite sequencing.

Materials and methods

Sample preparation

Blood samples were obtained from six B-CLL patients following diagnostic evaluation at Ellis Fischel Cancer Center in Columbia, MO, in compliance with the local Institutional Review Boards. These patients had blood levels of CD38 expression varying from 1% to 92% as examined by flow cytometry. DNA was isolated as described previously in chapters1 and 2 of this study.

Included in this study were three B-CLL cell lines, namely WAC3CD5, MEC1 and MEC2. The cell lines treatment with epigenetic modifying reagents and their biological characteristics were described in detail in previous chapters.

Methylated CpG island Amplification (MCA)

MCA was performed as described previously[10]. Briefly, 5µg of genomic DNA was digested with 100 units of methylation sensitive restriction enzyme *Sma*1(New England Biolabs) for 6 hours at 25^0C and 20 minutes at 65^0C, followed by digestion with 20 units of *Xma*1 at 37^0C for 16 hours. *Sma*1 is an isoschizomer of *Xma*1 that produces blunt -ended fragments, whereas *Xma*1 produces 5' extensions. DNA fragments were purified using DNA clean and concentrator $^{TM-5}$ from Zymo Research (Orange, CA).RMCA PCR adaptors were prepared by incubating *RMCA24*(5'AGCACTCTCCAGCCTCTCACCGAC 3') and *RMCA12* (5'CCGGGTCGGTGA 3') for 2 minutes at 65^0C , followed by cooling to room temperature for 3 hours. Then 0.5µg of digested DNA was ligated to 0.5 nmol of annealed RMCA oligonucleotide using T4 DNA ligase and incubated at 16^0C for 18 hours. Ligation

PCR was performed using 3µl of ligated DNA as template in 100µl PCR mixture containing 100 ρmole of RMCA24, 2 units of DNA polymerase(vent exo-), and 10mM dNTPs. The reaction mixture was incubated for 5 minutes at 72 ^{0}C and 95 ^{0}C for 3 minutes. Samples were amplified for 25 cycles. The ligation results were verified using 2% agarose gel stained with SYBR Green 1 nucleic acid Gel Stain (Lonza, Rochland, ME). Amplicons that successfully cut with the restriction enzymes (*Sma*1, *Xma*1) produced smears ranging from 300-3kb, with most amplicons at 1kb.
Then we purified the PCR products using a Zymo purification kit. The DNA was quantified using an ND-1000 photometer (Nanodrop Company).

CpG island microarray hybridization and analysis

For CpG island array hybridization, the purified amplicon (2µg) was annealed with random primers and aha dUTP. The high concentration of Klenow enzyme was used to enhance the concentration of DNA 7-10 fold (BioPrime plus array CGH indirect Genomic labeling, Invitrogen) .Fluorescence labeling of DNA was performed using the Alexa fluorescence dye. Fluorescence dyes 647 and 555 were coupled to tumor and normal peripheral blood mono-nucleoside (PBMC) respectively. The labeled material was purified and hybridized to human CpG island microarray containing ~244,000 CpG probes. We performed the hybridization in accordance with the instructions provided by the company. Gene Pix pro 4000A 6.0 (Axon) was utilized to scan the microarrays and the acquired images were analyzed with the Agilent feature extraction software (v9.5). The software uses Loess to normalize background subtracted median intensity of each spot.

CpG island probes that had the 647/555 >2 fold enrichment, and probes that were located within the 500 bases, were selected as hypermethylated signals.

Real Time RT-PCR

Total RNA was extracted from the two cell lines with three different treatments, nine de nova B-CLL patient samples, 2 normal (PBMC) and normal CD19+Bcells according to the protocols described in chapters 1 and 2. The genomic DNA was eliminated from the RNA in two steps; by using on column digestion with the RNase- free DNase kit (Qiagen) and by the genomic elimination reagents provided by RT^2 first strand kit (Super Array Bioscience Corporation). The elimination of DNA contamination is necessary so that the PCR signal intensity reflects the relative level of gene specific mRNA transcript. Reverse transcription was performed with First Strand cDNA Synthesis Kit using 1µg of total RNA. The generated cDNA was used for SYBER green based transcriptase (RT)-PCR amplifications with RT^2 Real Time ^{TM} SYBR Green qPCR master mixes (Super Array) .The generated cDNA from patient samples, 2 CLL cell lines and normal controls were analyzed using Wnt signaling PCR array (Super Array).

The human WNT signaling pathway RT^2 profiler PCR array was utilized to investigate the expression of 84 genes related to WNT mediated signal transduction. This set includes 84 unique genes from WNT pathway that are placed in wells A1-G12. Five housekeeping genes, including *B2M, HPRT1*, *RPL13A*, *GAPDH*, *ACTB*, were placed on wells H1-H5. Well H6 contained the genomic DNA control (GDC), well H7 through H9 contained reverse transcriptional control (RTC), and wells H10 through H12 contained replicate positive PCR control (PPC). The RT^2 First Strand Kit (C-03) includes a built in

external RNA to detect the efficiency of RNA transcription using a primer set in well H7-H9. The positive PCR control (PPC) test the efficiency of PCR itself using a predispensed artificial DNA sequence and the primer set in well H10-H12. The real time RT-PCR was carried out in I -Cycler IQ. We analyzed the data using the ΔΔCt method, where Ct is the cycle number that exceeds the threshold. We also carried out real time RT-PCR reactions with 1µg total RNA of 18 CLL primary tumor samples to analyze the mRNA levels of the *APC2* and *SFRP2* gene on these samples.

DNA methylation analysis of *APC2* using COBRA and bisulfite genomic sequencing

To analyze the DNA methylation of *APC2* and *SFRP2,* in a large number of CLL patients with different CD38 expression levels, the COBRA assay was performed using *Bstu*1 restriction enzyme. The PCR primers and the conditions are summarized in Table 3.1. The Ref Seq Accession # NM_005883 and NM_003013 were used to design primers to amplify the *APC2* and *SFRP2* genes respectively.

Gene	Primer s	Amplicon location	Product size, Tm	
APC2 CGI(1)	(F) ATTGGTTGTTGTTATGGTATTAGTT	Chr19:1,401,0321-1,401,305	273	56
	(R) TAAATCTAAAACCTCCTCCCTCTAC			
APC2 CGI(2)	(F)- TGTTTTTGTTGTTGTAAATTTTTTA	chr19:1,407,976-1,408,199	224	56
	(R) -CAACCAATCCCAACAAATCTC			
APC2 CGI(3*)*	(F)-GGGTAAGAATAGAGTAGGGTTGGAG	chr19:1,418,674-1,419,012	339	56
	(R)-TCAACAATAAAACTAAACTAAATCC			
SFRP2	(F)TTTTTATTTTTTAGATTTGTATAAAAA	chr4:154,929,678-154,929,994	316	54
	(R)-AACCAAAACCCTAACACATC			

Table 3.1: COBRA primers and PCR conditions. Primer sequences and the PCR conditions used for COBRA and genomic bisulfite sequencing are summarized in this table**.**

Results

Methylated gene discovery

To perform a comprehensive analysis of DNA methylation in CLL tumor samples and the three CLL cell lines (WAC3CD5, MEC1, MEC2), we used CpG island arrays containing ~244K probes, which cover most of the CpG islands in entire human chromosome. Our previous study in Small B cell Lymphomas (SBCL) using genomic DNA methylation microarrays containing ~9K CGI demonstrated the heterogeneous patterns of DNA methylation in SBCLs (chapter1 of this dissertation). In chapter 2 of this work we further investigated the global CGI methylation in 38 de nova CLL tumors with the broad range of CD38 expression levels using different sets of genomic methylation microarrays interrogating ~12,000 CGI clones. From previous studies we identified DNA methylation of multiple genes in SBCLs including CLL.

In the present study we utilized the MCA technique to amplify most CpG rich sequences and combine them with CpG island microarrays that span the entire human CpG islands in the genome to profile DNA methylation of CLL. The CpG island microarray covers 237,006 probes; the probes are about 45-60mers in length, with the average probe spacing of 100 bases. Furthermore, a CpG island microarray chip covers about 27,801 Reference Sequence, Ref Seq, genes.

To prepare amplicon, the MCA technique was utilized to enrich the methylated CpG islands through the amplification of methylated *Sma*1 sites. The recognition site for methylation sensitive restriction enzyme *Sma*I is CCC▼GGG, which restricts the genomic DNA into small fragments (<1kb).This recognition sequence occurs frequently within 70-80% of the human CpG islands. The *Sma*1 restriction enzyme cuts only unmethylated

DNA and leaves a blunt end. DNA was then treated with *Sma*1, which cuts methylated C▼CCGGG sites and leaves a sticky end. Then linkers *RMCA12* and *RMCA24* were ligated to the CCGG overhang and the digested DNA served as a template for linker PCR to amplify the methylated DNA fragments. Then the amplified DNA was purified and labeled with labeling dye and hybridized to the human CpG island microarray. The MCA technique and CPG island microarray together provide a complete mapping of DNA methylation patterns along the entire CpG island in the human genome (Figure 3.1).

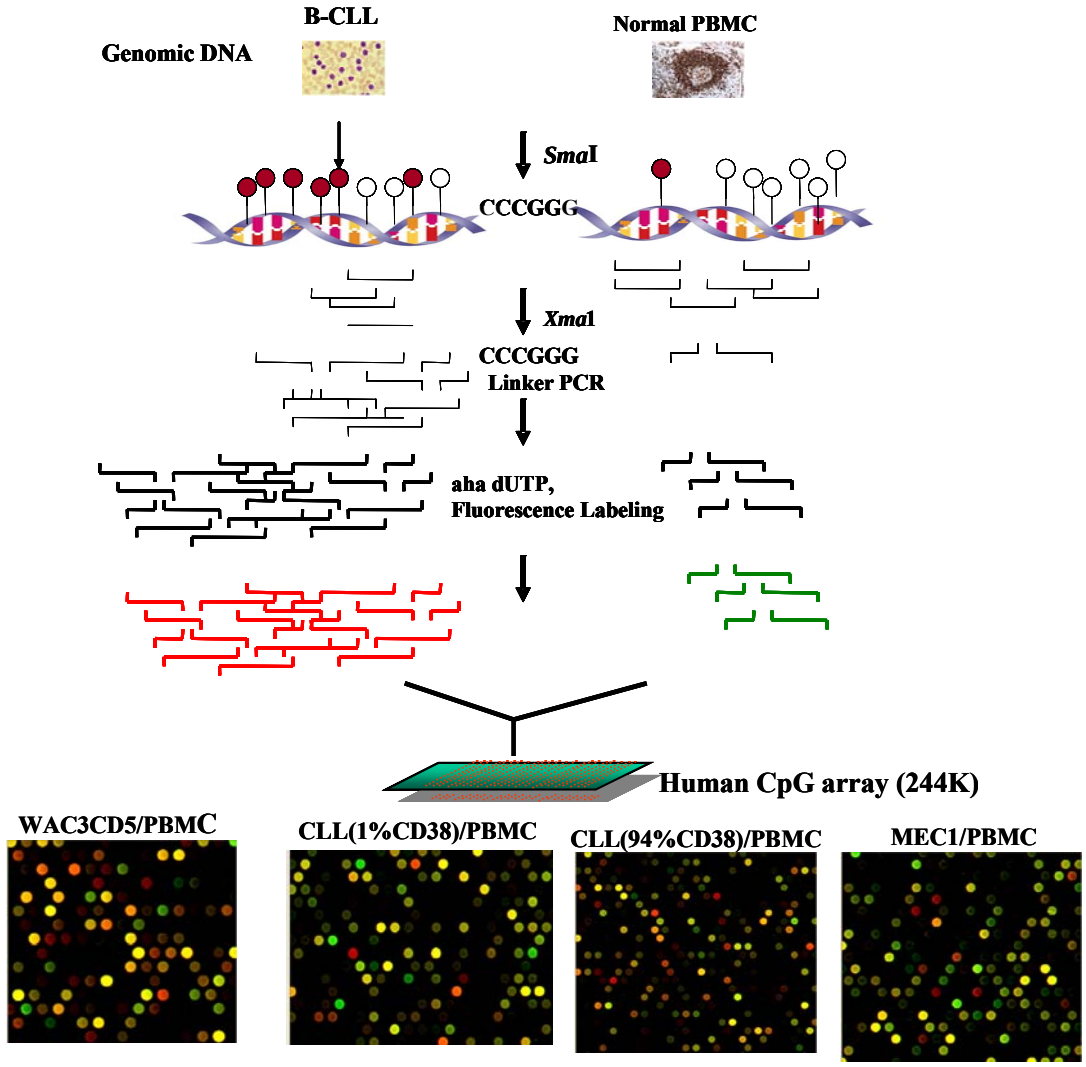

Figure 3.1: **Schematic flow chart of MCA and CpG island microarray**. Approximately 5µg of genomic DNA from CLL primary tumors, CLL cell lines and normal PBMC were digested with methylation sensitive and insensitive restriction enzymes *Sma*1and *Xma*1 respectively. Unmethylated CCCGGG sites are digested by *Sma*I which leaves a blunt ended DNA fragments. The subsequent digestion using *Xma*1 leaves overhang (CCGG) by cutting the methylated CCCGGG sites. Then the digested DNA is purified and ligated with two adaptors. Linker PCR is performed to amplify methylated DNA. The purified amplicons are directly labeled with aha-dUTP. Then tumor DNA is labeled with Alexa 647 and hybridized against Alexa 555 labeled normal PBMC onto a single CpG microarray chip. Arrays are washed, scanned and analyzed with Feature Extraction software using Loess normalization. The Alexa 647/ 555 ratio represents the relative methylation levels for each probe/CpG islands.

Methylation profiles can be useful tools in identifying biological pathways and gene regulatory network that might be disrupted in cancer. Our CpG island microarray profiles led to identification of methylated candidate genes from WNT signal transduction pathway. Aberrant regulation of WNT signaling pathway is a hallmark of many aggressive human cancers, including CLL. We detected methylated CpG islands of several WNT antagonists, *FZD* genes, WNT proteins, and the other negative regulators of the WNT signaling pathway in CLL primary tumors and the CLL cell lines. A total of 20 genes from the WNT pathway were methylated for the three CLL cell lines and primary CLL samples. We used a Venn Diagram Generator (http://www.pangloss.com/seidel/Protocols/venn4.cgi) to identify WNT signaling genes that were exclusively or commonly hypermethylated in each or among the CLL cell lines (Figure 3.2).We found that 8 unique genes were hypermethylated in WAC3CD5 ($CD38^{low}$). Six out of 8 methylated genes (*APC2, CTBP2, SFRP2, SOX21,* and *TLE4, PPP2R1B*) (Table 3.2) are either putative tumor suppressors or the nuclear transcriptional co- repressor of *LEF/TCF* transcriptional factors. We also found 7 and 6 unique hyper methylated genes in MEC1 and MEC2 ($CD38^{high}$), respectively.

Furthermore, we detected several *SOX* genes with high levels of methylation in primary tumors and CLL cell lines. In mammals the SOX family is comprised of twenty members, and several of these are known to be WNT antagonists[11]. A study conducted by Sinner et al. revealed that the SOX proteins can act as both antagonists and agonists of beta –catenin/TCF activity [12]. *SOX21* showed a high level of methylation exclusively in WAC3CD5, whereas *SOX11* and *SOX2* were methylated in MEC1. In addition methylated *SOX3* and *SOX4* were found exclusively in MEC2. Interestingly, only *SOX17* overlaps

between the three CLL cell lines. Moreover, CpG island microarray profiles of WNT signaling genes in primary CLL cancer cells versus normal PBMC were in close agreement with the CLL cell lines microarray results (Figure 3.2, Table3.2). Of the hypermethylated WNT signaling genes in both primary CLL tumors and the three CLL cell lines, *SOX* genes were the most abundant.

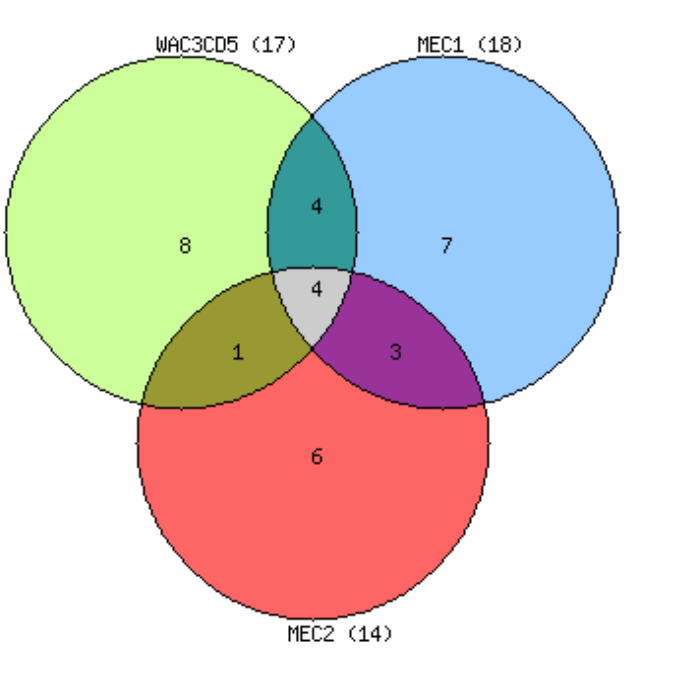

Figure 3.2: Venn diagram representation of hypermethylated genes in CLL cell lines. The representative Venn diagram compares the CpG island methylation of Wnt signaling genes in 3 CLL cell lines, MEC1, MEC2, and WAC3CD5.The overlap indicates the methylated genes in two or all three cell lines.

WAC3CD5	MEC1	MEC2	WAC3CD5,MEC1	MEC1,MEC2	MEC2, WAC3CD5	MEC1,MEC2 WAC3CD5,
APC2	CTBP	PPP1R9B	FZD1	AXIN2	SOX14	FZD10
CTBP2	FZD5	SOX12	SFRP4	PPP2R3B		FZD2
LRP6	NKD1	SOX3	SOX1	SOX9		SOX17
PPP2R1B	SOX11	SOX4	TLE1			WNT5A
SFRP2	SOX2	TLE3				
S0X21	SOX7	WNT2B				
TLE4	WNT7A					
WNT5B						

Table 3.2: Methylated genes in CLL cell lines. CpG island methylation profile in CLL cell line compared to PBMC identified genes from Wnt signaling pathway. The unique genes and those with similar DNA methylation status in CLL cell lines are listed in this table.

WNT signaling pathway in primary CLL cells and the CLL cell lines

Aberrant methylation of tumor suppressor gene in cancer is usually associated with lack of gene expression. Therefore, it has been proposed that DNA methylation in the gene regulatory region serves as an alternative mechanism of gene silencing in cancer .To examine the relationship between DNA methylation and expression of WNT related genes, total RNA samples from CLL patients and normal CD19+ B cells were characterized on the WNT signaling PCR array. The PCR was performed using the real time RT -PCR instrument and the threshold cycle (Ct) was calculated for every gene on each PCR array. To identify genes that were differentially expressed between the CLL tumor cells and normal CD19+ B cells, we used the ΔΔCt method. Thus to classify a gene as being up regulated or down regulated in tumor samples relative to control, fold changes had to be greater than +2 or -2 respectively. The reproducibility of PCR array was evaluated for every plate (Table 3.3). PCR Array data analysis Web Portal was used to analyze the data (http://www.superarray.com/pcrarraydataanalysis.php).

The scatter plot reports from the WNT pathway PCR array experiments were generated for the all 9 primary CLL samples (Figure 3.3 and Table 3.4). These scatter plots indicating the positions of several noteworthy genes based on their large fold changes in gene expression between the CLL primary tumors and the healthy CD19+ B cells. Of the 84 genes, 20 genes, including *FOSL1*, *CJUN*, *p300*, *LEF1, FZD3, WNT9A*, demonstrated at least 5 fold differences in gene expression between the tumor cells and normal lymphocytes. A group of genes (*PP2CA, TLE2, SOX17, FBXW11*) representing WNT inhibitors were down regulated.

1. PCR Array Reproducibility:

					16%CD38		
Well	**exp1**	**exp2**	**exp3**	**exp4**	**exp5**	**exp6**	**exp7**
Average C_t (PPC)	24.00						
ST DEV C_t (PPC)	1.65						
Average C_t (RTC)	24.37						
ST DEV C_t (RTC)	0.21						
					B CELLS		
Well	**exp1**	**exp2**	**exp3**	**exp4**	**exp5**	**exp6**	**exp7**
Average C_t (PPC)	19.73						
ST DEV C_t (PPC)	0.06						
Average C_t (RTC)	23.60						
ST DEV C_t (RTC)	0.10						

2. Reverse Transcription Control (RTC):

				16%CD38			
Well	**exp1**	**exp2**	**exp3**	**exp4**	**exp5**	**exp6**	**exp7**
ΔC_t (AVG RTC - AVG PPC)	0.37						
RT Efficiency	Pass						
				B CELLS			
Well	**exp1**	**exp2**	**exp3**	**exp4**	**exp5**	**exp6**	**exp7**
ΔC_t (AVG RTC - AVG PPC)	3.87						
RT Efficiency	Pass						

3. Genomic DNA Contamination (GDC):

				16%CD38			
Well	**exp1**	**exp2**	**exp3**	**exp4**	**exp5**	**exp6**	**exp7**
ΔC_t (GDC - AVG HKG)	4.58						
Genomic DNA:	OK						
				B CELLS			
Well	**exp1**	**exp2**	**exp3**	**exp4**	**exp5**	**exp6**	**exp7**
AVG ΔC_t (GDC - AVG HKG)	10.24						
Genomic DNA:	OK						

Table 3.3: PCR array reproducibility. RNA quality control parameters, including House Keeping Gene (HKG) expression level, reverse transcription PCR efficiency, and genomic DNA contamination were evaluated for every plate using the Genomic DNA Control (GDC), Reverse Transcription Control (RTC) and Positive PCR Control (PPC), included in the last row of the 96 well plates. PCR Array data analysis Web Portal was used to analyze the data (http://www.superarray.com/pcrarraydataanalysis.php)

Scatter Plot			
		$2^{-\Delta Ct}$	
Well	Symbol	16%CD38	B cells
A01	AES	0.7684	0.5987
A02	APC	0.0224	0.0107
A03	AXIN1	0.1267	0.0374
A04	BCL9	0.0052	0.0008
A05	BTRC	0.0129	0.0142
A06	FZD5	0.0010	0.0008
A07	CCND1	0.0026	0.0009
A08	CCND2	0.0728	0.0201
A09	CCND3	0.0364	0.0567
A10	CSNK1A1	0.0480	0.0698
A11	CSNK1D	0.2207	0.0567
A12	CSNK1G1	0.0257	0.0094
B01	CSNK2A1	0.0591	0.0748
B02	CTBP1	0.1456	0.1604
B03	CTBP2	0.0001	0.0002
B04	CTNNB1	0.5070	0.2432
B05	CTNNBIP1	0.0032	0.0029
B06	CXXC4	0.0001	0.0001
B07	DAAM1	0.0060	0.0215
B08	DIXDC1	0.0001	0.0000
B09	DKK1	0.0001	0.0001
B10	DVL1	0.0085	0.0087
B11	DVL2	0.0224	0.0081
B12	EP300	0.3345	0.0284
C01	FBXW11	0.0728	0.0748
C02	FBXW2	0.0317	0.0247
C03	FGF4	0.0001	0.0000
C04	FOSL1	0.0008	0.0000
C05	FOXN1	0.0001	0.0000
C06	FRAT1	0.0129	0.0230
C07	FRZB	0.0001	0.0001
C08	FSHB	0.0001	0.0000
C09	FZD1	0.0060	0.0005
C10	FZD2	0.0002	0.0018
C11	FZD3	0.0390	0.0022
C12	FZD4	0.0001	0.0000
D01	FZD6	0.0257	0.0041
D02	FZD7	0.0074	0.0009
D03	FZD8	0.0008	0.0038
D04	GSK3A	0.0448	0.0374
D05	GSK3B	0.0836	0.0698
D06	JUN	2.8679	0.6417
D07	KREMEN1	0.0001	0.0001
D08	LEF1	0.0634	0.0062
D09	LRP5	0.0028	0.0022
D10	LRP6	0.0004	0.0003
D11	MYC	0.0052	0.0163
D12	NKD1	0.0011	0.0001
E01	NLK	0.0060	0.0215
E02	PITX2	0.0002	0.0000
E03	PORCN	0.0060	0.0050
E04	PPP2CA	0.0418	0.0921
E05	PPP2R1A	0.1672	0.1303
E06	PYGO1	0.0001	0.0000
E07	RHOU	0.0015	0.0004
E08	SENP2	0.0195	0.0265
E09	SFRP1	0.0056	0.0000
E10	SFRP4	0.0001	0.0000
E11	FBXW4	0.0418	0.0326
E12	SLC9A3R1	0.0961	0.0608
F01	SOX17	0.0003	0.0004
F02	T	0.0004	0.0008
F03	TCF7	0.0091	0.0005
F04	TCF7L1	0.0001	0.0000
F05	TLE1	0.3345	0.0921
F06	TLE2	0.0003	0.0025
F07	WIF1	0.0001	0.0000
F08	WISP1	0.0001	0.0001
F09	WNT1	0.0011	0.0001
F10	WNT10A	0.0028	0.0013
F11	WNT11	0.0003	0.0000
F12	WNT16	0.0028	0.0071
G01	WNT2	0.0001	0.0002
G02	WNT2B	0.0001	0.0004
G03	WNT3	0.0364	0.0017
G04	WNT3A	0.0001	0.0002
G05	WNT4	0.0001	0.0001
G06	WNT5A	0.0001	0.0001
G07	WNT5B	0.0001	0.0002
G08	WNT6	0.0004	0.0009
G09	WNT7A	0.0002	0.0001
G10	WNT7B	0.0001	0.0002
G11	WNT8A	0.0001	0.0004
G12	WNT9A	0.0001	0.0000

Table 3.4: Changes in gene expression for WNT genes between the CLL (1%CD38) and normal CD10+ B cells. The data used to generate the scatter plot. PCR Array data analysis Web Portal was used to analyze the data (http://www.superarray.com/pcrarraydataanalysis.php).

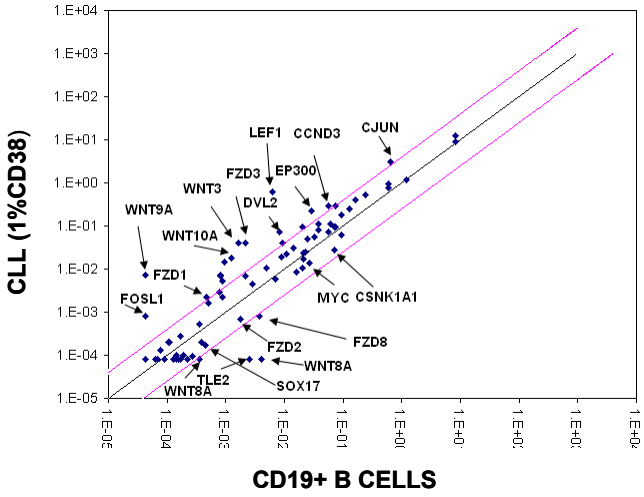
CLL (1%CD38)
CD19+ B CELLS
LEF1
CCND3
CJUN
FZD3
EP300
WNT3
DVL2
WNT9A
WNT10A
FZD1
FOSL1
MYC
CSNK1A1
FZD8
FZD2
WNT8A
TLE2
SOX17
WNT8A

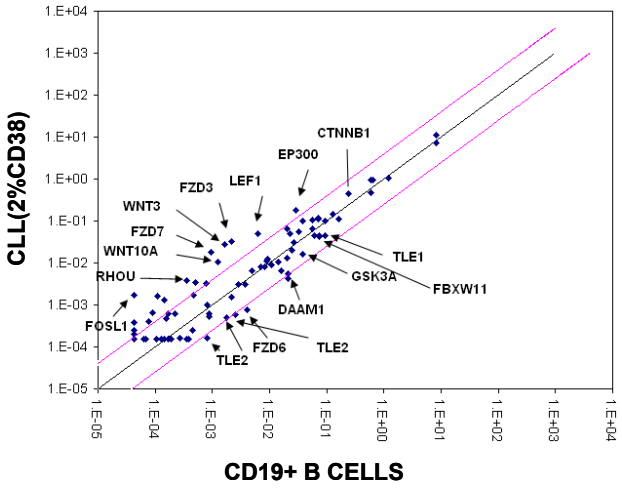
CLL(2%CD38)
CD19+ B CELLS
CTNNB1
EP300
FZD3
LEF1
WNT3
FZD7
WNT10A
TLE1
RHOU
GSK3A
FBXW11
DAAM1
FOSL1
FZD6
TLE2
TLE2

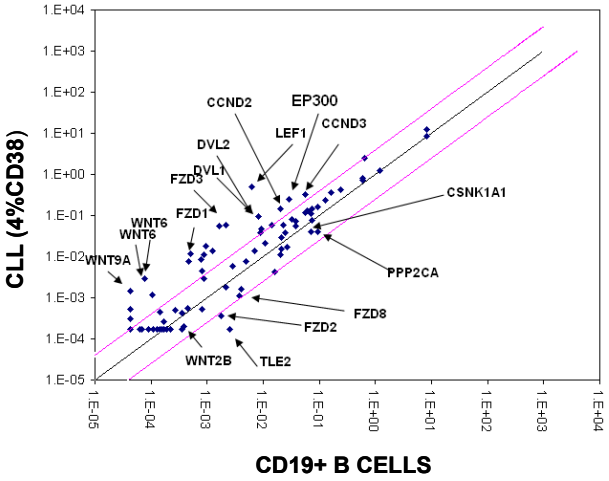
CLL (4%CD38)
CD19+ B CELLS
CCND2
EP300
LEF1
CCND3
DVL2
DVL1
FZD3
CSNK1A1
FZD1
WNT6
WNT6
WNT9A
PPP2CA
FZD8
FZD2
WNT2B
TLE2

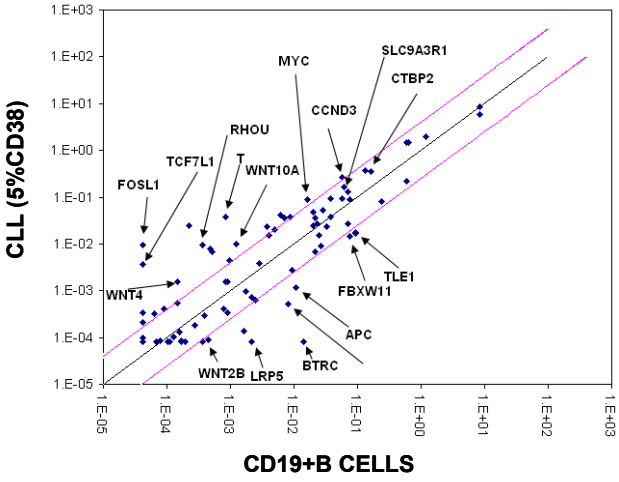
CLL (5%CD38)
CD19+B CELLS
MYC
SLC9A3R1
CTBP2
CCND3
RHOU
TCF7L1
T
WNT10A
FOSL1
TLE1
FBXW11
WNT4
APC
BTRC
WNT2B
LRP5

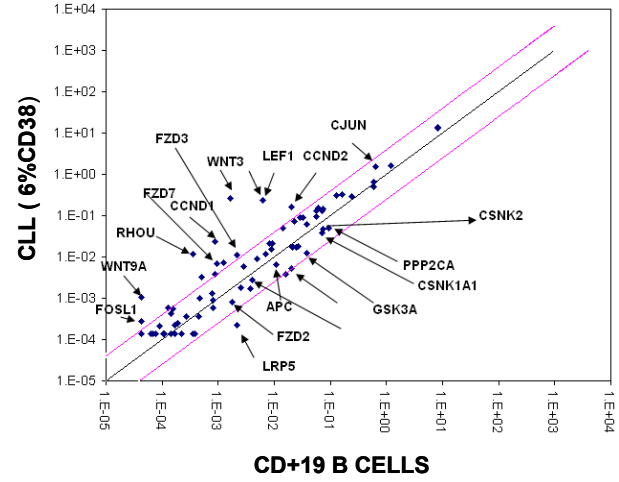
CLL (6%CD38)
CD+19 B CELLS
CJUN
FZD3
WNT3
LEF1
CCND2
FZD7
CCND1
CSNK2
RHOU
PPP2CA
WNT9A
CSNK1A1
FOSL1
APC
GSK3A
FZD2
LRP5

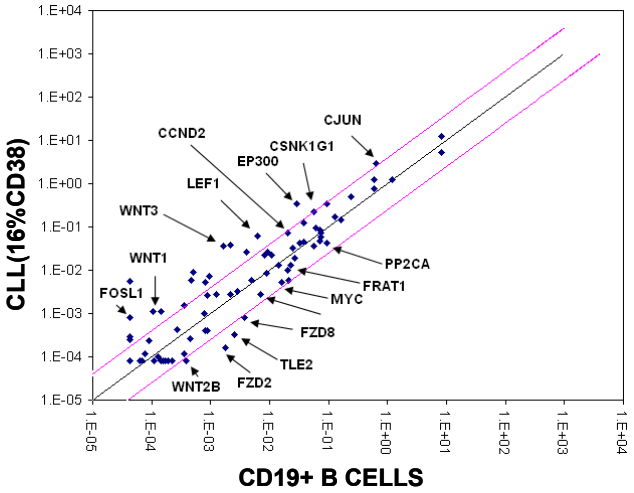
CLL(16%CD38)
CD19+ B CELLS
CJUN
CCND2
CSNK1G1
EP300
LEF1
WNT3
WNT1
PP2CA
FRAT1
FOSL1
MYC
FZD8
TLE2
WNT2B
FZD2

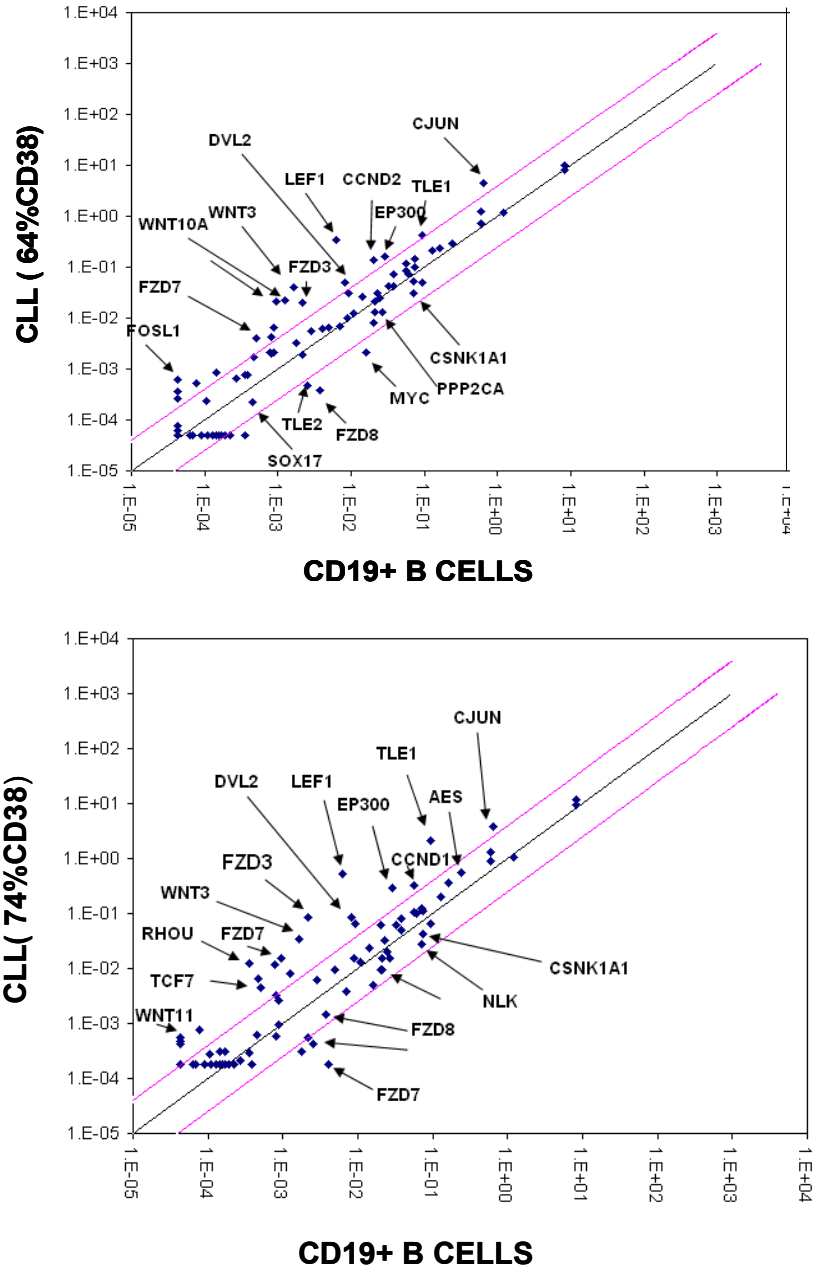

Figure 3.3: Scatter plot analysis of gene expression. The figure depicts a relative expression level of each gene ($2^{-\Delta Ct}$) between the tumor (Y axis) and normal control (X axis). The black line represents the fold change of 1 and the pink line indicates the desired fold changes in gene expression threshold.

Hierarchical clustering analysis was performed using ΔΔCt to visualize the expression levels of Wnt signaling genes on primary CLL samples compared to normal CD19+ B cells (Figure 3.4)

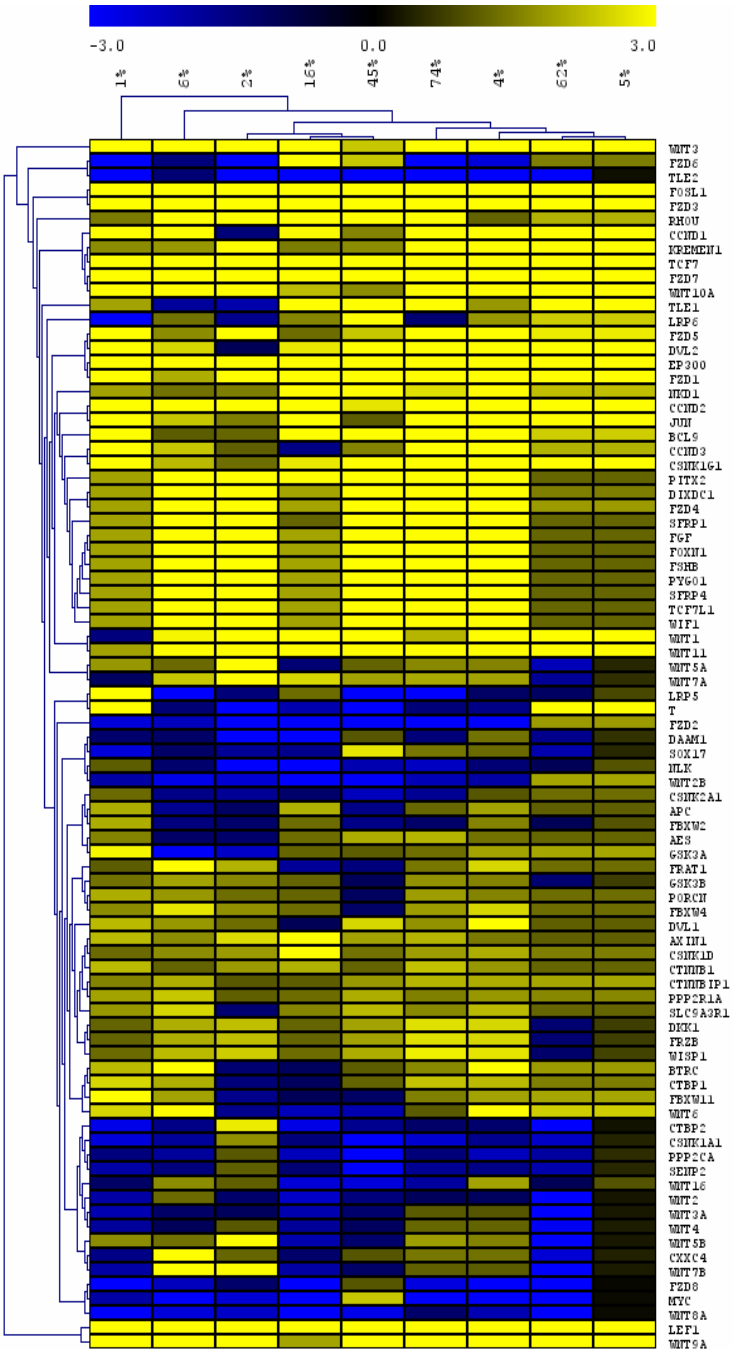

Figure 3.4: Expression analysis of WNT mediated signaling genes in 9 primary B – cell CLL samples. The hierarchical clusters were generated using TIGR *Mev* software based on the similarities in gene expression. Relative expression of each gene compared to normal lymphocyte was measured ($2^{-\Delta Ct}$) then the fold changes were calculated. The numbers on top represent CLL patient samples with various CD38 expression levels. Every row represents a specific gene from the Wnt signaling pathway and color change within each row corresponds to the fold changes in gene expression in CLL cells versus the CD19+ B cells. Yellow indicates genes with higher expression level compared to the normal lymphocyte, blue represents the lower level of expression, and black indicates no changes in gene expression between the tumor and the normal cells.

Of the 84 genes in WNT pathway, 22 genes showed a significant level of gene expression in tumor cells compared with control. In the leukemic B -CLL cells, the WNT target genes, *CCND1, CCND2, CCND3, DVL2*, *CJUN, LEF1, FOXN1, FGF4, FOSL1, WIP-1* and *PITX2* were the most abundant. These genes are associated with the aggressive biological behavior of many types of cancer [13].These genes have been previously identified as direct downstream targets for *LEF1/TCF* and WNT signaling. The up regulated genes included proliferation inducing transcriptional factor such as *CJUN,* nuclear proteins histone acetylase (*p300*), and the fos related antigen1 (*FOSL1*).

For the first time in this work we report the up-regulation of *CJUN* and *FOSL1* in leukemic B CLL cells. The oncogenic nature of AP-1 transcriptional factors *FOSL1* (Fra-1) and *CJUN* has been investigated in many types of solid tumors[14]. In addition, these genes, that are often up regulated in tumor cells, play a role in tumor progression and metastasis. Increase in *FOSL1* expression has been reported in both pulmonary epithelial and mesothelial cells after exposure to crocidolite asbestos fibers[15;16]. Moreover, studies have shown that the transforming activity of *CJUN* in vitro is usually associated with co-expression of Ras and Src[17]; thus, abnormal expression of *CJUN* may promote the malignant transformation of normal mammalian cells[18]. Importantly, the mouse embryonic fibroblast lacking *CJUN* showed elevated p53 level, implying that *CJUN* behaves as a positive regulator of cell cycle by suppressing p53 and, indirectly, its target, p21[19]. Previous studies have demonstrated the activation of *FOSL1*and *CJUN* by the external and internal signals that include the DNA damage, oxidative stress, UV radiation stress and, more importantly, antigen binding by T or B cell lymphocytes[20].

Differential expression of WNT ligands

In the CLL cells, *WNT1, WNT10A,* WNT11, *WNT9A*, *WNT3* were expressed at significantly higher levels compared to normal CD19+ B cells (Figure 3.4). There are 19 WNT ligands that have been identified in human to date. These proteins belong to a large family of intracellular glycoproteins that are conserved throughout the evolution from *Drosophila* to human (reviewed in [21]).

In *Drosophila,* the WNT signaling pathway can be activated through three distinct groups. The first pathway, that engages the stabilized β -Catenin, is canonical [22]. The second pathway, namely the planner cell polarity (PCP), involves RhoA and Jun kinase (JNK) [23], and the third pathway happens through activation of Protein Kinase C (*PKC*)[24;25]. The WNT ligands can be subdivided into the different classes of WNT according to the pathway in which they are involved. For example, *WNT1, WNT3*, *WNT3A*, *WNT7A*, *WNT7B* and *WNT8A* belong to the WNT1 class, whereas, WNT4, WNT5B, and WNT11 are members of WNT5A class. The canonical pathway is activated upon binding of the members of the *WNT1* class to the frizzled receptors. However, members of the *WNT5A* class stimulate the intracellular calcium signaling[26]. In vertebrates, the WNT5A and WNT11 have been suggested to activate the non canonical pathways [24].

Our data demonstrated up-regulation of *WNT1*, *WNT3* and *WNT11*, which may activate the canonical signaling pathway in CLL, at significantly higher level than *WNT5A*, *WNT2, WNT2B* and *WNT8A* in CLL compared to the normal lymphocytes. Studies have shown that WNT proteins provide signals for the renewal and proliferation of hematopoietic stem cells (HSC) (reviewed in[27]) . Although the explicit mechanism

underlying the effects of WNT ligands in development of hematopoietic progenitor remains to be understood, it is clear that WNT signaling plays role in normal hematopoiesis.

FZD2 and *FZD8* were absent from all CLL tumors

We quantified gene expression levels of trans- membrane protein (*FZD*) receptors in CLL primary and cell lines, as well as normal controls. At present, 10 *FZD* receptors have been identified in human samples. Over expression of *FZDs* have been detected in many type of solid tumors and usually are associated with nuclear accumulation of β-Catenin and activation of WNT/ β- Catenin canonical pathway[28;29]. *FZD1*, *FZD3*, *FZD5*, *FZD7* were expressed in both normal CD19+ B cells and the CLL cells; however, the expression levels for all four cases were detected at higher levels in the tumor cells than the normal cells (Figure 3.4). These results are in agreement with the study reported by Lu et al[30]. In contrast the *FZD2* and *FZD8* were expressed at significantly lower levels in B cell CLL samples than the normal CD19+ B cells. Although the *FZD2* has been shown to be up regulated in solid tumors such as colorectal, esophageal and liver cancers in mice[31], up regulation of *FZD2* and *FZD8* has not been reported in hematopoietic malignancies.

LRP6 mRNA level was detected in CLL patients with higher level of CD38

In stimulated cells, upon engagement of WNT ligands and FZD receptors, low density lipoprotein receptor related protein 5-6 (*LR5/LRP6*) forms a complex with *FZD* and WNT ligands (reviewed in [32]). This interaction results in stabilization of cytoplasmic β-Catenin and its nuclear transformation by nuclear transport proteins. *LRP5* mRNA was

detected in one out of nine CLL patient samples; however, *LRP6* was abundantly expressed in CLL patients with high CD38 expression levels (Figure 3.4).

Differential regulation of disheveled genes

Disheveled proteins (*Dsh* in *Drosophila* and *DVL1* 1-3 in mammals) are the immediate down stream molecule of *FZD* receptors. Several lines of evidence indicate that in stimulated cells *DVL1* recruits *AXIN* to the frizzled/ *LRP* complex to dissociate *AXIN* from the destruction complex [33]. This recruitment induces the stabilization of β –Catenin and ultimately leads to the transcription of WNT target genes[34]. Although the function of disheveled proteins is not fully elucidated, DVL proteins may play important roles in all three WNT signaling pathways. Up regulation of disheveled proteins was reported in non-small cell lung cancer, mesothelioma and cervical cancer[35-37]. Human DVL1 has been reported to be over expressed in prostate cancer as well[38]. In this study we report over expression of *DVL1*and *DVL2* in 7/9 CLL primary tumors compared to normal control (Figure3.4).

Up regulation of histone acetylase E1 binding protein *p300*

Cellular protein *p300* interacts with phosphorylated *CREB1* and functions as histone acetyltransferase that regulates the gene transcription through chromatin remodeling[39]. Studies have shown that in human *CBP/p300* functions as a β- Catenin binding transcriptional activator[40]. Moreover, *p300* acts as a co activator of hypoxia –inducible factor1 alpha (HIF1α) and plays a role in stimulation of *VEGF* which is a hypoxia induced gene[41].

We detected the *p300* mRNA transcript at higher levels in the primary tumor cells compared to the normal CD19+ B cells and normal PBMC (Figure 3.5).

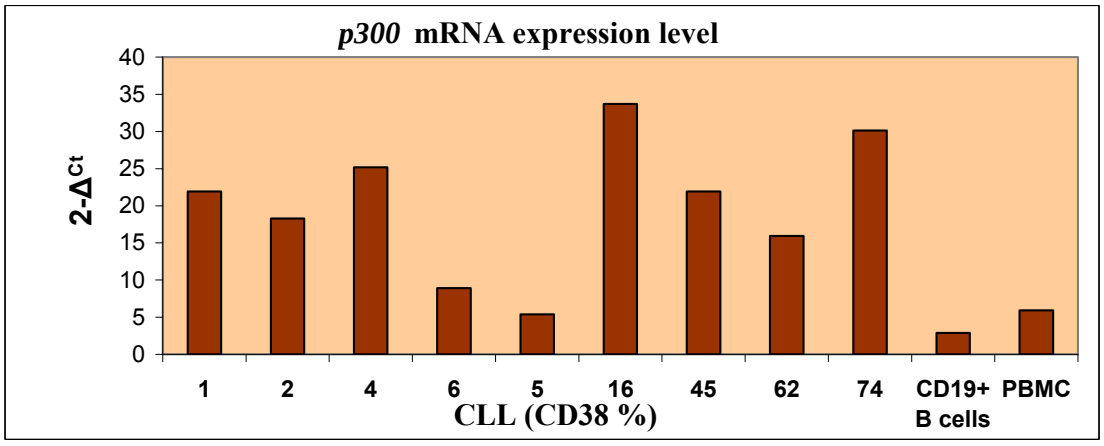

Figure 3.5 Relative expression of *p300* in CLL cells. The relative expression levels of *p300* was measured in 12 CLL cells with different expression level of CD38, normal CD19+B cells, and PBMC using real-time RT-PCR. The numbers in the X axis represent the CD38 expression levels in CLL patient samples.

Up regulation of transcriptional factor *LEF1* and *TCF7* in CLL

Transcriptional factor LEF1 and TCF7 have been proposed to mediate the canonical WNT signaling pathway through co- expression with β –Catenin , since LEF/TCF transcriptional factors are not able to activate gene transcription independently, the association with β- Catenin provides additional cofactors for transcriptional activity. Although both *LEF1* and *TCF7* exhibited significantly increased expression in CLL patients compared to CD19+ B cells and normal PBMC, *LEF1* transcript detected at significant higher level than *TCF7* (Figure 3.6). The leukemic B cells had >4 fold higher expression level of *LEF1/TCF* than the normal lymphocytes. The over expression of *LEF1*

has been reported previously; however, its biological role in tumorigenesis of CLL remains unclear.

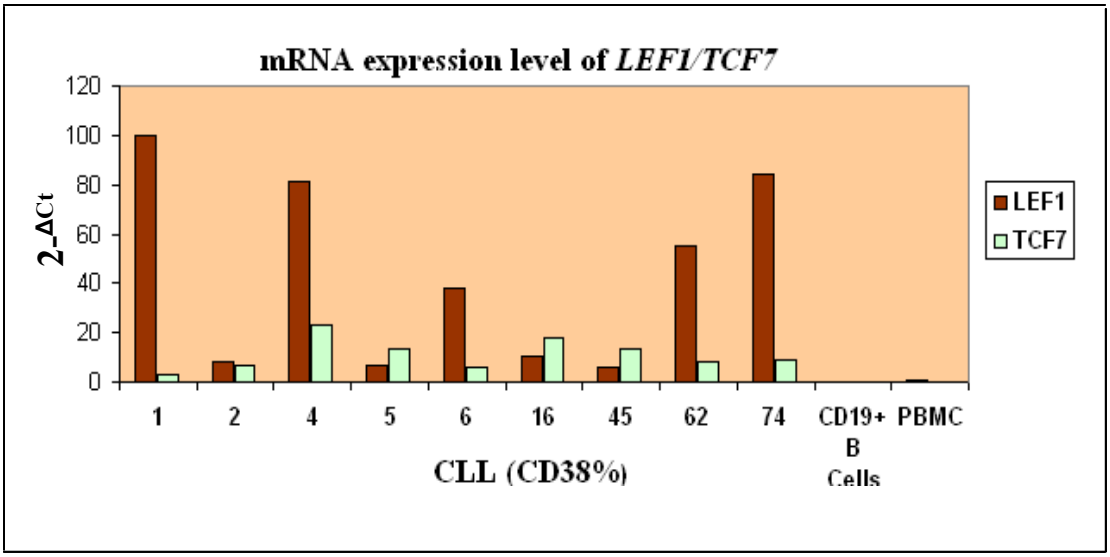

Figure 3.6: Real time RT-PCR expression analysis of *LEF1*and *TCF7* in tumor cells and normal controls. Although both genes are expressed at higher levels in the tumor cells compared to the normal control, increases in *LEF1* mRNA level were dramatic compared to *TCF7.* The CD38 expression levels are shown in the X axis.

Destruction complex in WNT signaling pathway

The expression of multiple genes that negatively regulate the WNT signaling pathway including *APC/APC2, PPP2CA, CKIα, AXIN, GSK3β*, *SOX17*, and genes involved in ubiqutination and degradation of β -Catenin was examined. β- Catenin, the central component of the WNT signaling pathway, is regulated through ubiquitin proteasome system and the phosphorylation by *GSK3β* [42;43]. In the absence of WNT stimulation, the multi component destruction complex including *GSK3β, AXIN* [44], *APC* [45], *PPP2CA* and the *CK1α* come together to promote phosphorylation of

β- Catenin and thereby target it for degradation by the β-*TrCP* and the components of the ubiquitin proteosome pathway such as *FBXW2, FBXW4* and *FBXW11.* The mRNA levels of these genes were examined in CLL cells as well as the normal controls. Our data revealed under expression of the protein phosphatase 2A catalytic subunit (*PPP2CA*) in a majority of the B-cells CLL patients (Figure 3.7). The tumor suppressor PP2A is one of the four major Ser/Thr phosphatases that negatively regulate cell growth and division. PPP2CA associates with a variety of regulatory subunits.

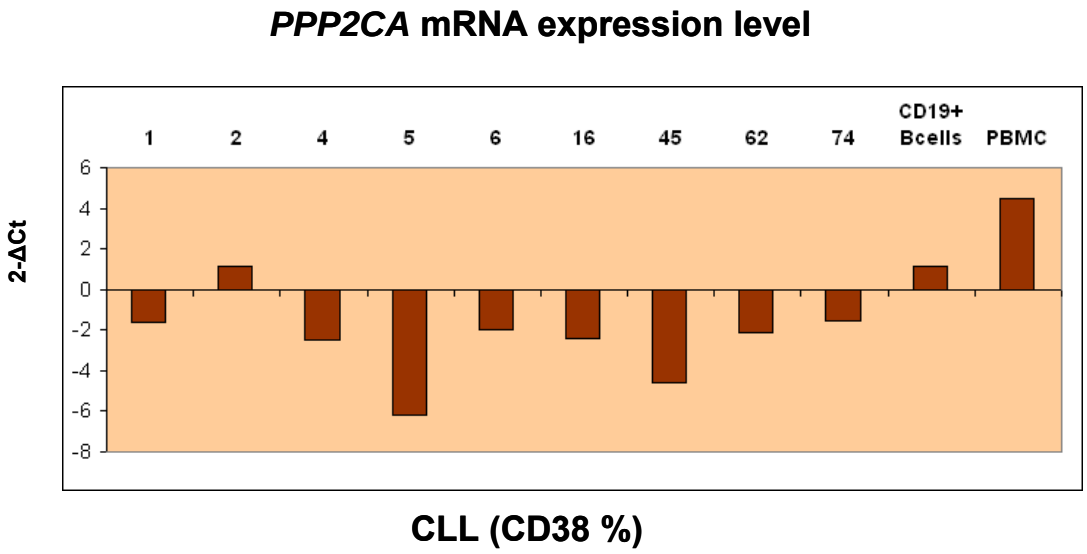

Figure 3.7: *PPP2CA* mRNA detected at very low level in CLL tumor cells compared to normal cells. *PPP2CA* transcript was not detected in B cells CLL samples using real time RT-PCR. The X axis represents the CD38 expression levels in CLL patient samples.

***APC/APC2* expression level in CLL primary tumors**

APC is a tumor suppressor gene that plays an important role in cytoplasmic destabilization and nuclear transport of β- Catenin [22]. *APC* regulates β -Catenin through interaction with the component of the destruction complex, namely *AXIN* at three binding sites that are located in the central region of the *APC* protein .Studies have shown that the majority of colon cancer patients carry a truncated form of *APC* tumor suppressor gene.Our quantitative real time PCR experiment showed down regulation of the *APC* gene in primary CLL patient samples, as well as the CLL cell lines examined in this work.

We also investigated expression of the *APC2* gene by real time RT-PCR in a different panel of CLL tumor cells and the related cancer cell lines (Figure 3.8). *APC*2, also known as *APCL* (located on chromosome 19p13.3), is functionally related to the *APC* gene[46]. Similar to the *APC* gene, *APC2* can destabilize the cytoplasmic β- Catenin and ultimately prevents activation of WNT target genes. Study has shown that the over expression of *APC2* mediates reduction of β- Catenin level in *SW40* colon cancer cell line, suggesting that *APCL* also may function as a negative regulator of WNT signaling pathway[47]. We found down regulation of *APC2* in CLL patient samples compared with the CD19+ B cells and PBMC (Figure3. 8). It is important to mention that *APC2* is not among the 84 gene primer sets on RT^2 Profiler PCR Array that we examined.

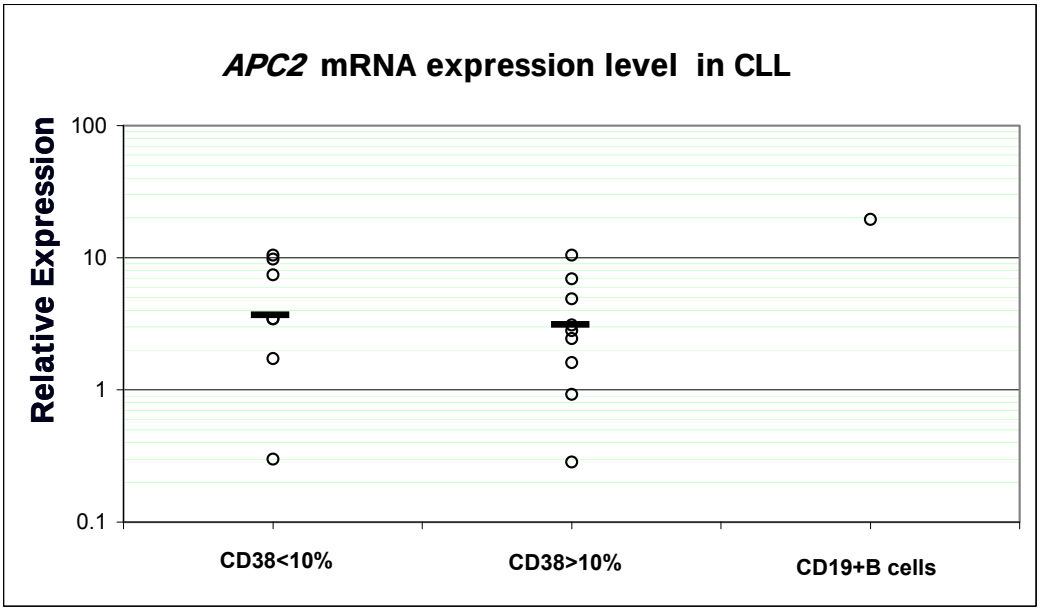

Figure 3.8: Expression analysis of *APC2* in CLL patient samples. Expression of *APC2* transcript quantified using real time RT-PCR in CLL patients with CD38 expression level less than 10%(CD38<10%) and CD38 higher than 10% (CD38>10%) as well as normal CD19+ B cells using real time RT-PCR. *HPRT1* (house keeping gene) used as an internal control. The relative expression was determined using $2^{-\Delta Ct,}$ where Ct is the cycle threshold. Every experiment was repeated three times. Each circle represents a unique sample and the solid horizontal bar indicates the median.

The association between transcriptional silencing of tumor suppressor genes and the CpG island methylation has been well established in the literature. Our CpG island microarray profiling led to the identification of *APC2* among the hypermethylated genes in examined samples. We investigated the association between the transcriptional silencing of *APC2* and CpG island methylation in the primary CLL samples, and the related cell lines using COBRA and genomic bisulfite sequencing.

Three fragments were examined for *APC2*: a CpG island located in the 3'end region CGI(3) , a CpG island located in the coding region CGI (2), and a CpG island in the 5'end outside of the gene CGI (1) (Figure 3.9).This gene was selected for further study because (a) *APC2* mRNA level was decreased significantly in CLL cells compared to normal lymphocytes; (b) the expression of this gene was restored after treatment with epigenetic modifying reagents in CLL cell lines (data is shown in chapter 2) ;and (c) this gene is biologically significant ; it is a tumor suppressor in human cancer and its aberrant regulation relates to the regulation of β -Catenin.

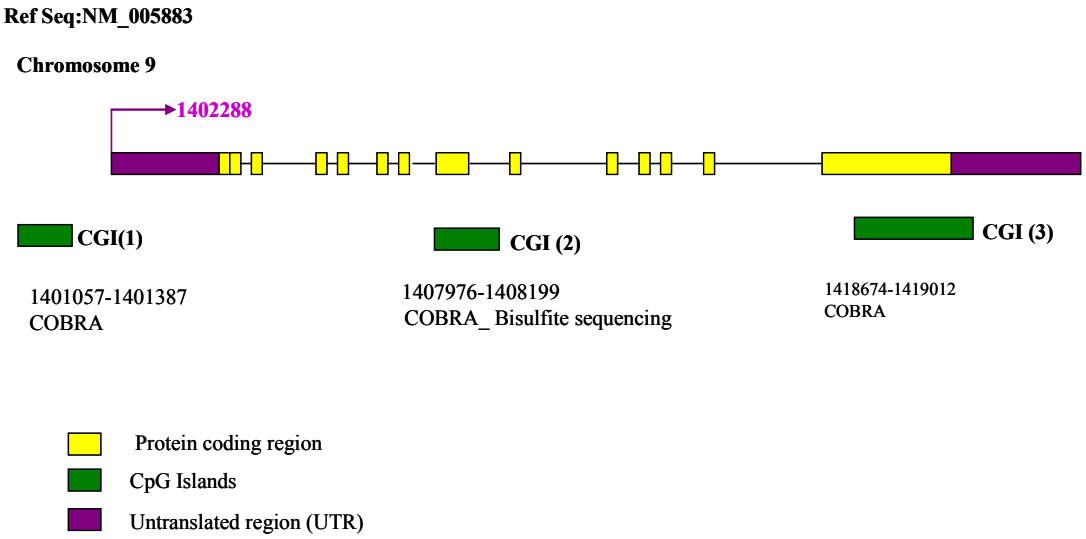

Figure 3.9: Genomic map of *APC2*
The DNA methylation status of 3 CGI encompassing the 3'end region , coding region and the 5'region of the *APC2* gene was investigated in a large numbers of primary CLL cells and three CLL cell lines using COBRA and bisulfite sequencing. The location of these regions relative to the transcriptional start site is shown in this figure. The numbers below each CGI represent the genomic region selected for COBRA or genomic bisulfite analysis.

We found DNA methylation of *APC2* CGI (3) in 25/36 CLL patients as well as MEC1 and WAC3CD5 cell lines (Figure3.10).

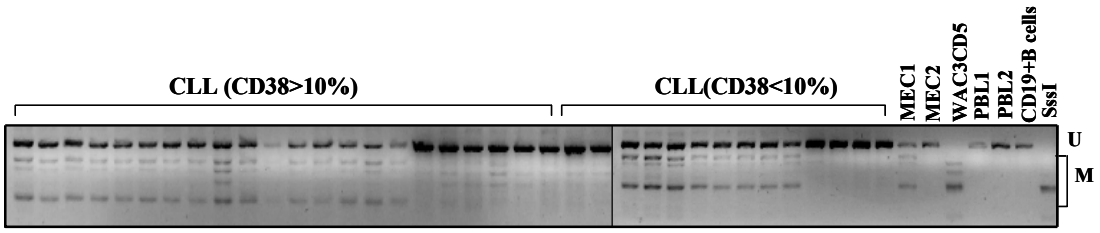

Figure 3.10: DNA Methylation status of *APC2* CGI (3). DNA methylation status of *APC2* CGI (3*)* was investigated in 36 CLL patient samples, three CLL cell lines, normal female (PBL1), normal male (PBL2) peripheral blood lymphocytes, normal CD19+B cells and in vitro *SssI*-treated DNA. Methylated (M) or unmethylated (U) are indicated on 3% agarose gel. The presence of methylated and unmethylated bands reflects the fact that these tumor cells are not 100% neoplastic cells and the various amounts of normal cells may be present.

To further investigate the DNA methylation status of *APC2* in CLL patient samples, we examined the CGI (2) located in the coding region of this gene. Our COBRA results showed the homogenous pattern of methylation across the examined tumor cells (3.11). In addition, we investigated the DNA methylation status of the CpG island located upstream of the *APC2* gene, and we performed COBRA on CLL cell lines as well as the CLL tumor cells. Normal blood lymphocytes and CD19+ B cells had no DNA methylation, whereas cell lines and the patient samples showed different degree of methylation (Figure3.12 and 3.13).

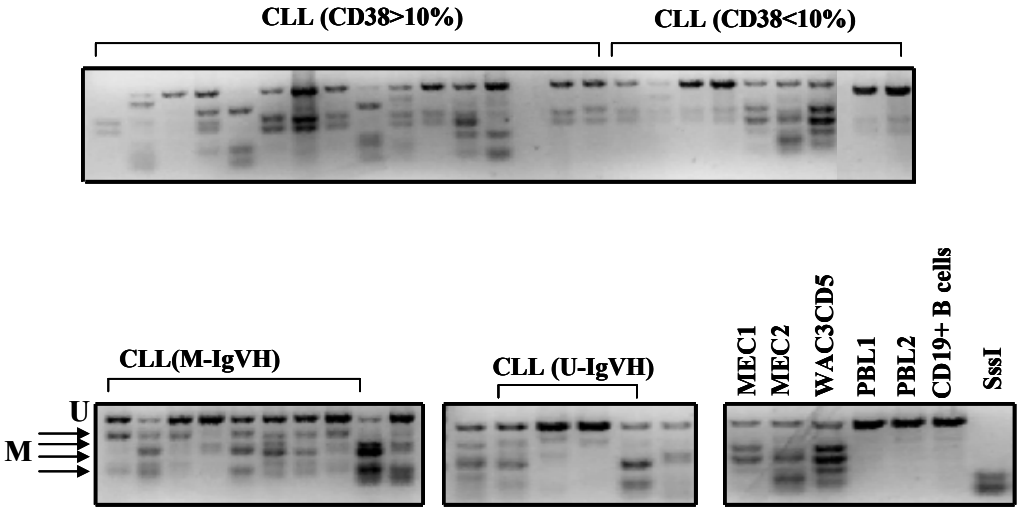

Figure 3.11: **Methylation present in *APC2* CGI (2).**Detection of DNA methylation by COBRA. Genomic DNA was treated with bisulfite and amplified with primers specific to *APC2* CGI(2) and products are digested with *Bst*U1 and electrophoresed in 3% agarose gel .Arrows indicate methylated *Bst*U1sites. This restriction enzyme cleaves only methylated alleles, producing different DNA fragments.

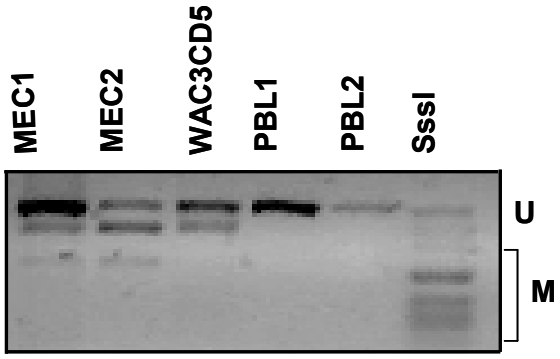

Figure 3.12, **hyper methylation of *APC2* CGI (1) in CLL cell lines.** COBRA analysis of DNA from normal female lymphocytes (PBL1), normal male (PBL2),*SssI* treated PBL, MEC1, MEC2, and WAC3CD5.Undigested and digested fragments correspond to unmethylated (U)and methylated(M) DNA respectively

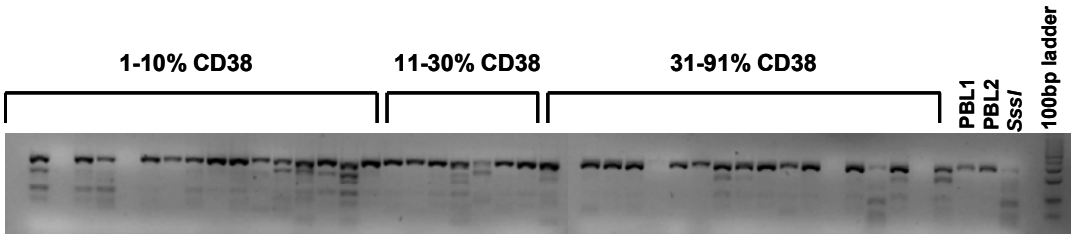

Figure 3.13: Hypermethylation of the *APC2* CGI (1) gene in primary CLL cells.

To get a more complete picture of the specific location and intensity of methylated cytosine in the *APC2* CGI (2), we performed bisulfite genomic sequencing on primary CLL cells with diverse clinical behavior, the three related CLL cell lines, and appropriate controls. We examined the region from1407976-1408199 on chromosome 9. The relative positing of CG dinucleotides is shown in (Figure 3.9). In complete agreement with the COBRA data, normal CD19+ cells and normal PBMC had no or very low levels of DNA methylation, whereas the *SssI* treated positive control were completely methylated (Figure 3.14). Although methylated CG dinucleotides from different patients and cell lines were partially over lapping, the WAC3CD5($CD38^{low}$) cell line ,and three CLL patients with $CD38^{low}$ (3,6,9 %CD38) were densely methylated across the entire region of CG 1-27(Figure 3.15). Interestingly, four patients representing poor prognosis ($CD38^{high}$ and unmutated IgVH gene) demonstrated a pattern of methylation similar to that of MEC1 and MEC2, with intermediate and high levels of CD38, respectively (Figure 3.16)

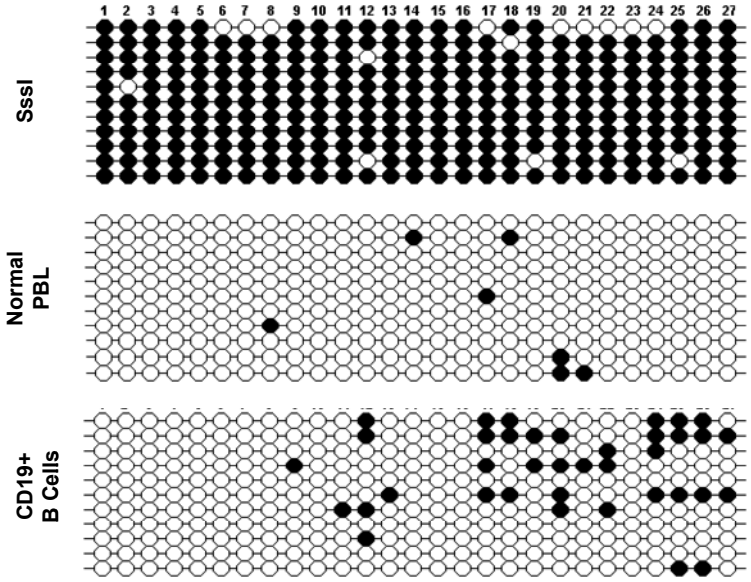

Figure 3.14 Genomic Bisulfite sequencing of *APC2* CGI (2). DNA methylation of CG dinucleotides was examined in healthy CD19+ B cells, normal PBMC and in vitro treated *SssI*. Each row represents an individual clone across the 27 CG dinucleotides. Filled circles indicate methylated cytosine and open circles are unmethylated cytosines.

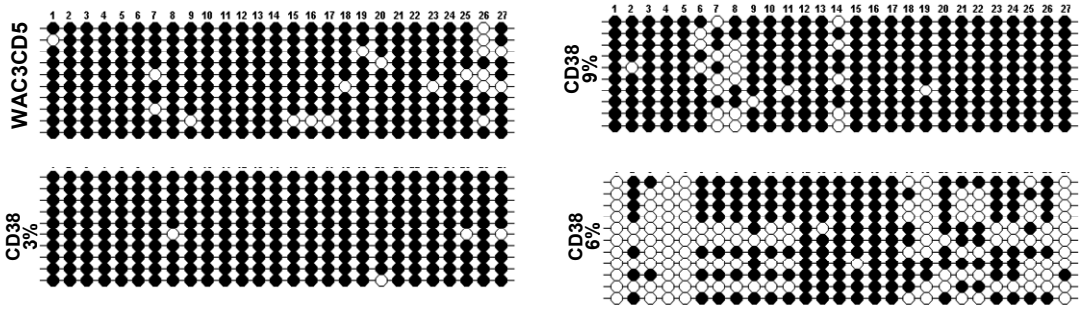

Figure 3.15: Methylation analysis of *APC2* (CGI2) in WAC3CD5 and primary CLL tumor cells with low CD38 expression level. Bisulfite sequencing was performed to examine 27 CG in the coding region of *APC2* from WAC3CD5 ($CD38^{low}$) and patient samples with CD38 expression level less than 10%. Each row of circles represents the sequence of an individual clone.

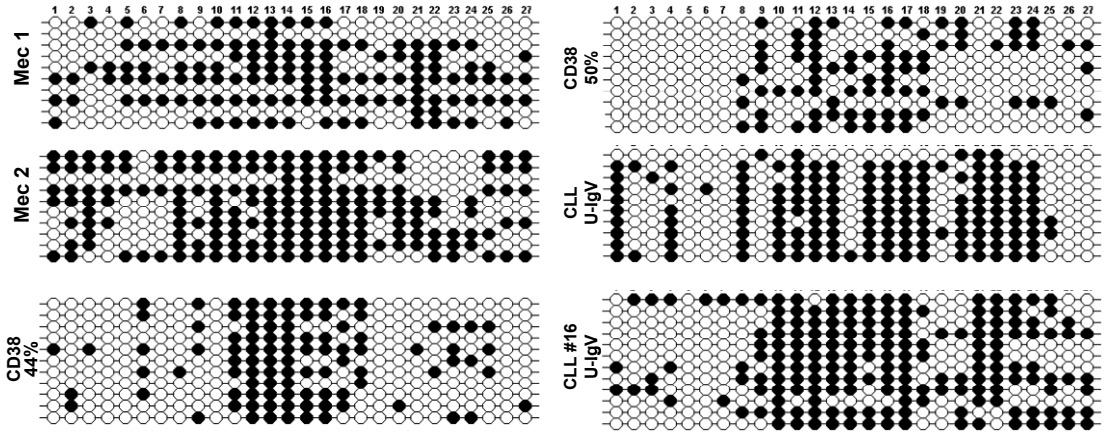

Figure 3.16: Bisulfite sequencing of *APC2* CGI (2) in CLL patients with poor prognosis. The confirmation of tumor associated methylation by genomic bisulfite sequencing is shown in CLL patients with unmutated IgVH gene and high level of CD38 (CD38 ^{high}) representing aggressive types of the disease.

Down regulation of *SFRP2* in CLL patients with high CD38 expression levels

Secreted frizzled related proteins (*SFRP)* are homologues of FZD proteins; therefore, they can bind to WNT ligands and inhibit WNT signaling by acting as competitive inhibitors of *FZD*s. Down regulation of *SFRPs* have been reported in colorectal, gastric, and esophageal cancer [48] . The expressions of *SFRPs* are mainly regulated through DNA methylation in colorectal cancer [49] as well as the chronic lymphocytic leukemia [5]. Although the association between DNA methylation and silencing of *SFRP2* has been studied in tumorigenesis of CLL by others, we decided to include this gene in our study to find out if there is an association between *SFRP2* expression and the level of CD38 expression, which is a predictor of poor prognosis in CLL patients. We investigated the CpG island methylation and expression of *SFRP2* in a series of CLL patient samples with various CD38 expression levels. Indeed, our data

revealed the differential expression of *SFRP2* between the two CLL subtypes. Expression of *SFRP2* was down regulated in patients with CD38>10% when compared with patients with CD38 <10% (Figure 3.17). In addition, we investigated the association between the DNA methylation and the CD38 expression in examined CLL cells. Interestingly, we found marked differences between the DNA methylation of CLL patients with $CD38^{high}$ and $CD38^{low}$ (Figure3.18). Leukemic B CLL patients with $CD38^{high}$ (20/22) showed significant level of methylation compared to patients with $CD38^{low}$ (7/14). However, the DNA methylation patterns of CLL cell line were quite different from the primary tumor cells. WAC3CD5 ($CD38^{low}$) showed higher level of methylation compared to MEC1 and MEC2 with 69.6%, 96% CD38 expression respectively. This discrepancy could be explained by the nature of the cultured cell lines. It has been demonstrated that the cancer cell lines undergo expression and methylation changes in culture.

Similar to the *APC2* gene, the *SFRP2* was not among the 84 gene primer sets on RT^2 Profiler PCR array that utilized in this study. The *SFRP2* gene structure is illustrated in Figure 3. 19.

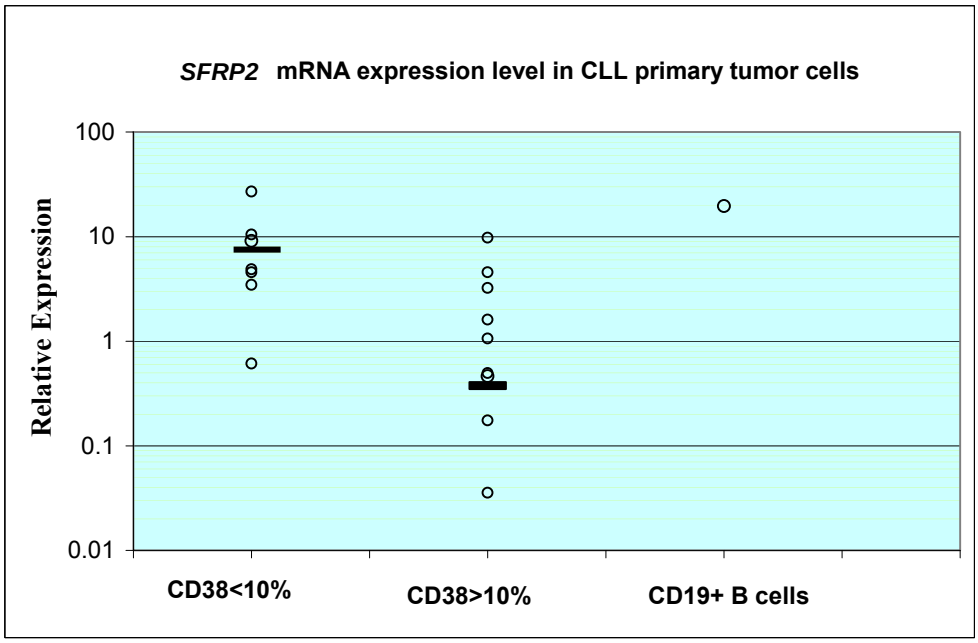

Figure 3.17: Expression analysis of *SFRP2* in CLL patient samples. Expression of *SFRP2* transcript quantified using real time RT-PCR in CLL patients with CD38 expression level less than 10%(CD38<10%) and CD38 higher than 10% (CD38>10%) as well as normal CD19+ B cells using real time RT-PCR. *HPRT1* (house keeping gene) used as an internal control. The relative expression was determined using $2^{-\Delta Ct,}$ where Ct is the cycle threshold. Every experiment was repeated three times. Each circle represents a unique sample and the solid horizontal bar indicates the median.

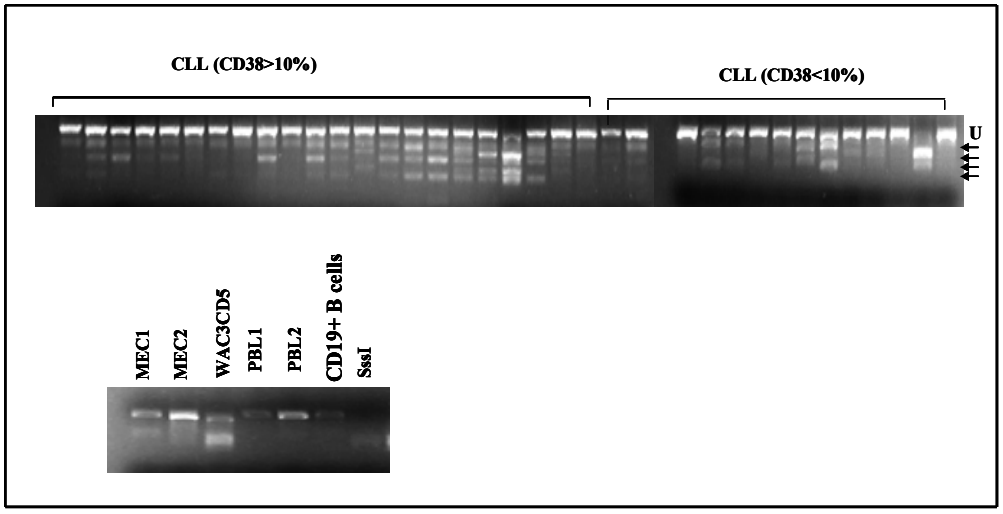

Figure 3.18: Analysis of DNA methylation of the *SFRP2* in primary and CLL cancer cell lines. We used 36CLL tumor samples, three CLL cell lines and the normal controls for analyzing the DNA methylation status of *SFRP2* CpG island, located in the promoter region. The arrows represent the methylated sites.*Bst*U1 restriction sites used in COBRA assay.

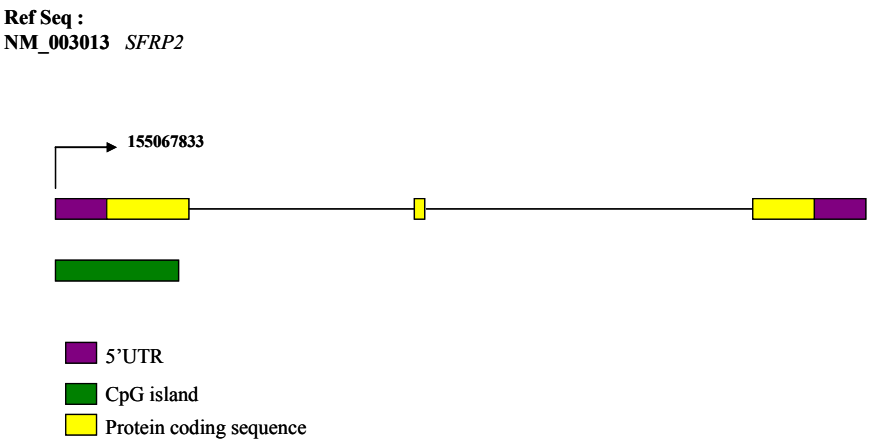

Figure 3.19: *SFRP2* gene structure. The location of CpG island relative to the transcriptional start site , protein coding region and the un translated UTR sites are shown.

Pharmacological reactivation of WNT signaling genes in CLL cell

To determine whether the expression of WNT mediated signaling genes in two CLL cell lines (WAC3CD5 and MEC2) is regulated by epigenetic modification, mainly DNA methylation and chromatin remodeling, we examined the expression of WNT mediated signaling genes (RT^2PCR profiler array) in untreated, 5'-Aza ,TSA and the combination of TSA and 5'-Aza treated CLL cell lines. 5'-Aza depletes DNA methyltransferase (*DNMT1*) by incorporating into DNA directly. Previous studies have shown that 0.5μM of 5'-Aza decreases the whole cellular content of *DNMT1* in WAC3CD5 cell line[50]. Hypermethylation of Wnt inhibitors was associated with down regulation of gene transcription as demonstrated by reactivation of gene expression after treatment with epigenetic modifiers.

Quantitative real time RT-PCR showed induction of *CK1α*, *FZD2, APC, FBXW2, GSK3β* genes after treatment with 5'-Aza, TSA and the combination of both drugs (Figure 3.20). *FZD2* expression increased in both WAC3CD5 and MEC2 up to 9 fold and reached the normal level after treatment with epigenetic modifying drugs. In a previous section of this chapter, we showed significant reduction in the expression of *FZD2* in primary tumor cells compared to normal PBMC and CD19+ B cells. These data demonstrate that re-expression of these genes may be regulated, directly or indirectly, by DNA methylation and histone modification, and that expression level can be modified using inhibitors of DNA methyltransferase and histone deacetylase inhibitor.

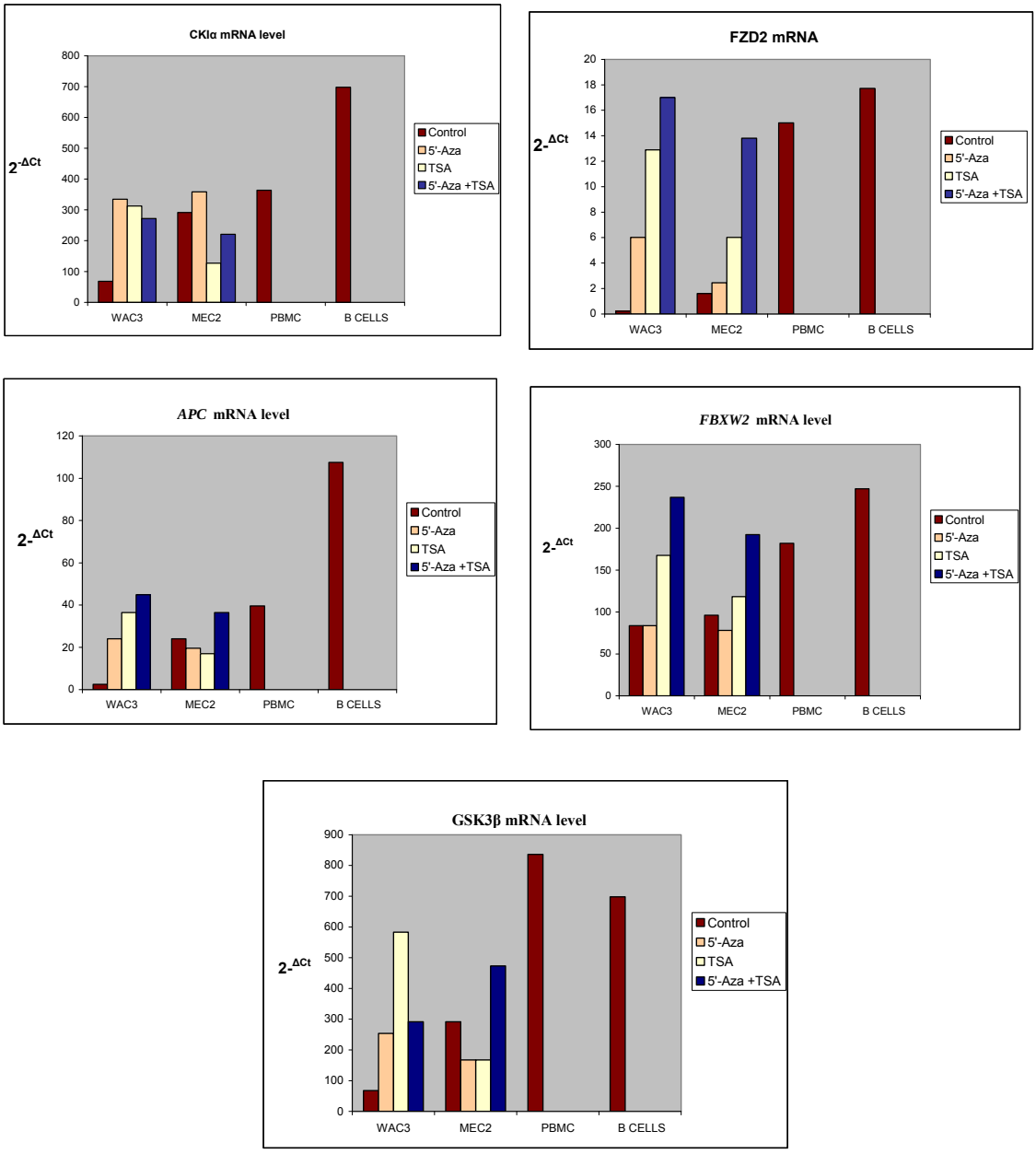

Figure 3.20: Expression analysis of WNT signaling genes in WAC3CD5, MEC2 and normal lymphocytes following treatment with epigenetic modifying reagents. Alteration in gene expression in *WAC3CD5* and MEC2 following treatment with a demethylating agent and a histone deacetylase inhibitor was investigated. The *CKIα, FZD2, APC* and *FBXW2* and *GSK3β* mRNA levels were measured using WNT signaling pathway RT^2 profiler PCR array before the treatment (control), expression after treatment with demethylating agent (5'-Aza), histone deacetylase inhibitor(TSA) and the combination of both drugs (5'-Aza+ TSA).

Treatment by the demethylating agent and histone deacetylase inhibitor were able to induce *Groucho/TLE2* in two CLL cell lines. Interestingly, we found by real time PCR differences in the expression of *Groucho*/*TLE*2 in the normal cells. Although this gene was prominent in both normal controls, however, higher level of transcript was detected in the CD19+ B cells than the normal PBMC. Moreover, *Groucho*/*TLE2* was not detectable in the examined primary CLL tumor samples by real time RT PCR. *Groucho*/*TLEs* (transducing-like enhancer of split) are the co repressors of transcription [51], *Groucho* is a *Drosophila* protein and *TLEs* are its mammalian homologue. Human *TLE* molecules interact with DNA through *LEF1/TCF* transcriptional factors and mediate transcriptional inhibition of WNT target genes [52] . Our CpG island methylation microarray analysis of CLL and the three related CLL cell lines identified *TLEs* among the hypermethylated genes. Moreover, the analysis of gene expression showed no detectable mRNA transcript for *TLE2* in the examined primary tumors and the untreated CLL cell lines. In addition we demonstrated the induction of *TLE2 m*RNA after treatment with epigenetic modifying drugs (Figure 3.21). These data suggest that DNA methylation may be involved, at least in part, in gene regulation of *TLEs* in CLL.

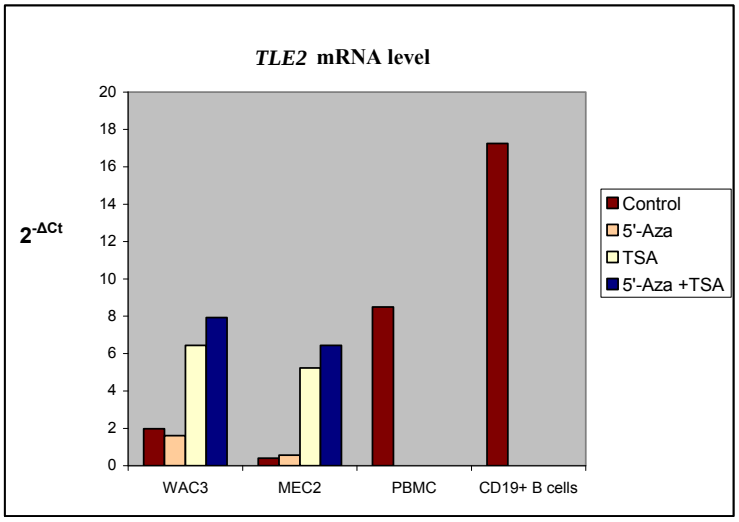

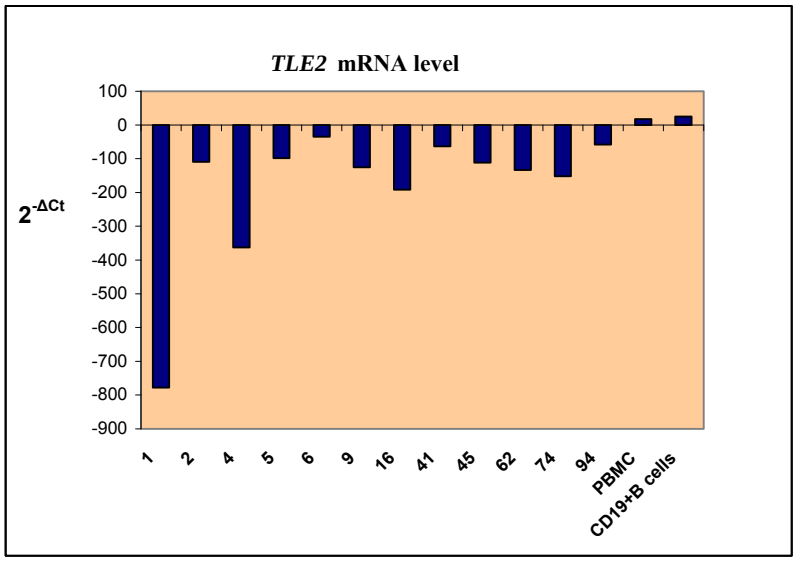

Figure 3.21: Expression analysis of *Groucho*/*TLE2* in CLL cell lines and primary tumors. Expression of the WNT signaling pathway antagonist *TLE2* before and after treatment with 5'-Aza and TSA and the combination of both (5'Aza+TSA) compared to healthy lymphocytes was measured in 2 CLL cell lines. *TLE2* mRNA expression level B cell CLL patient samples, CD19+ B cells and PBMC are illustrated. The X axis represents the CD38 expression levels in the examined CLL patient samples.

Real time RT PCR analysis of Nemo -Like Kinase (*NLK*), a negative regulator of the WNT signaling pathway[53], showed that expression of *NLK* was down regulated in majority of the examined CLL primary tumors as well as the two CLL cell lines. In addition, the expression of *NLK* was restored after treatment of WAC3CD5 ($CD38^{low}$) with 5-'Aza, TSA and both in combination (TSA& 5'Aza), which represents the association between aberrant DNA methylation and histone deacetylation in expression of *NLK*. In contrast, TSA alone induced up- regulation of *NLK* in MEC2 cell line to the same level of this gene in CD19+ B cells (Figure 3.22). These results suggest the involvement of chromatin remodeling in transcriptional regulation of *NLK* in MEC2 ($CD38^{high}$) cell line.

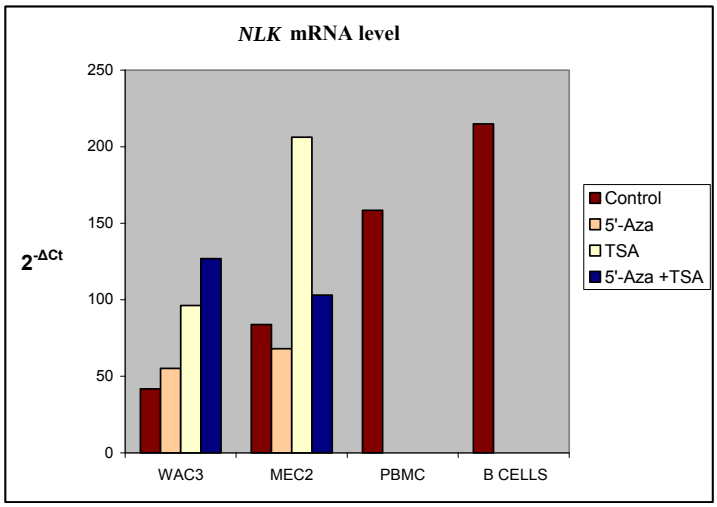

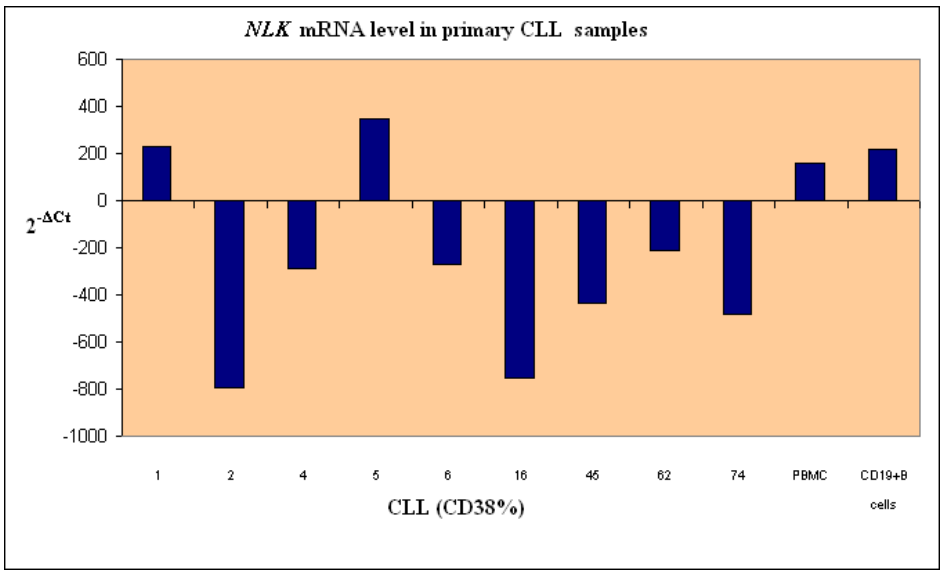

Figure 3.22 Change in mRNA expression level in primary CLL B cells and the CLL cell lines after treatment with the demethylating agents and histone deacetylase inhibitor. Low level of *NLK* transcript was detected on the primary CLL tumor cells compared to the normal PBMC and B cells. Epigenetic modifying reagents were able to induce the expression of *NLK* in WAC3CD5 ($CD38^{low}$), whereas the expression of *NLK* induced in MEC2 after treatment with TSA only. The X axis represents the CD38 expression levels in CLL patient samples.

Discussion

For the first time, in this study we have utilized the MCA technique to enrich methylated DNA in combination with CpG island microarray containing ~244,000 probes that covers the entire human CpG island to profile the aberrant CpG island methylation in B cell CLL primary tumors and the three related cell lines WAC3CD5, MEC1 and MEC2. The role of de novo CpG island methylation in tumorigenesis has been well documented [54]. The de novo CpG island methylation is a part of silencing mechanism that affects a wide variety of different genes, such as tumor suppressor, DNA repair, genes involved in apoptosis and cell growth[55]. There are two hypotheses regarding the relationship between the DNA methylation and gene silencing. One group suggested that the DNA methylation might silence transcription either by disrupting the binding site of the transcriptional factors or through the recruitment of the repressors of the transcription. On the other hand, the other group believes that the heterochromatin may serve as a target for de novo methylation and recruitment of the DNA methyl transferases (*DNMT*s) to the transcriptional active sites [56;57]. In spite of these two different views, it is clear that the de novo CpG island methylation is at least one way of gene transcriptional regulation.

Studies by our group and others have documented the CpG island methylation of many genes involved in hematological malignancies[3;58]. Our CpG island microarray (244K) profiles of primary CLL samples and CLL cancer cell lines identified hypermethylated genes involved in WNT signaling pathway, such as *APC2, AXIN2, PPP2CA, FZD2, SFRP2, SFRP4, Groucho/TLEs, DKK1, SOX* family, *LRP5, NLK,* and *PPP2R1B.*

The WNT signaling pathway controls cell fate determination through

transducing signal to the canonical pathway and the cell movement and polarity via the non canonical pathway. WNT signals are transduced by the WNT factors that bind to a class of seven transmembrane receptors encoded by the frizzled genes[59].Upon the engagement of the WNT ligand and the frizzled receptor, the cytosolic protein "disheveled" are recruited to the membrane. The phosphorylated disheveled protein associates with *AXIN* and subsequently antagonizes the *GSK3β* by a mechanism that is not fully understood. As a result, un-phosphorylated β-Catenin, a central component of the canonical pathway, is no longer targeted for degradation by β-*TrCP*, a component of an E3 ubiquitin ligase. Moreover, the stabilized β-Catenin trans -locates to the nucleus, where it engages the *TCF/LEF* family of transcriptional factor to activate the expression of WNT target genes [8]. These genes are involved in a variety of developmental processes such as differentiation and proliferation of hematopoietic progenitors. Furthermore, *WNT2A, WNT3A , WNT5A* and *WNT10B* and their cognate receptors *FZD3*, *FZD4*, *FZD5*, and *FZD7* are present in the hematopoietic cells, such as bone marrow as well as its non hematopoietic component, stromal cells [60-62].

The mechanism underlying the effects of WNT proteins in maturation of hematopoietic progenitors is not fully understood; however, the significance of WNT signaling in normal hematopoiesis is well known. Inappropriate inactivation of the WNT signaling pathway is a hallmark of a variety of tumors, including myeloid and lymphoid malignancies[63]. In the present study we utilized the WNT signaling pathway focused array to compare the gene expression profiles in leukemic B CLL cells, normal CD19+ B cell, normal PBMC and two CLL cell lines WAC3CD5, MEC2 by real time RT-PCR PCR. The gene expression analysis revealed that WNT target genes *CCND1, CCND2, EP300,*

C-JUN, FGF, FOXN1, *LEF1,FOSL1 (*Fra-1*), PITX2*, were elevated in the primary tumor cells compared to the normal B cells (Figure 3.23).

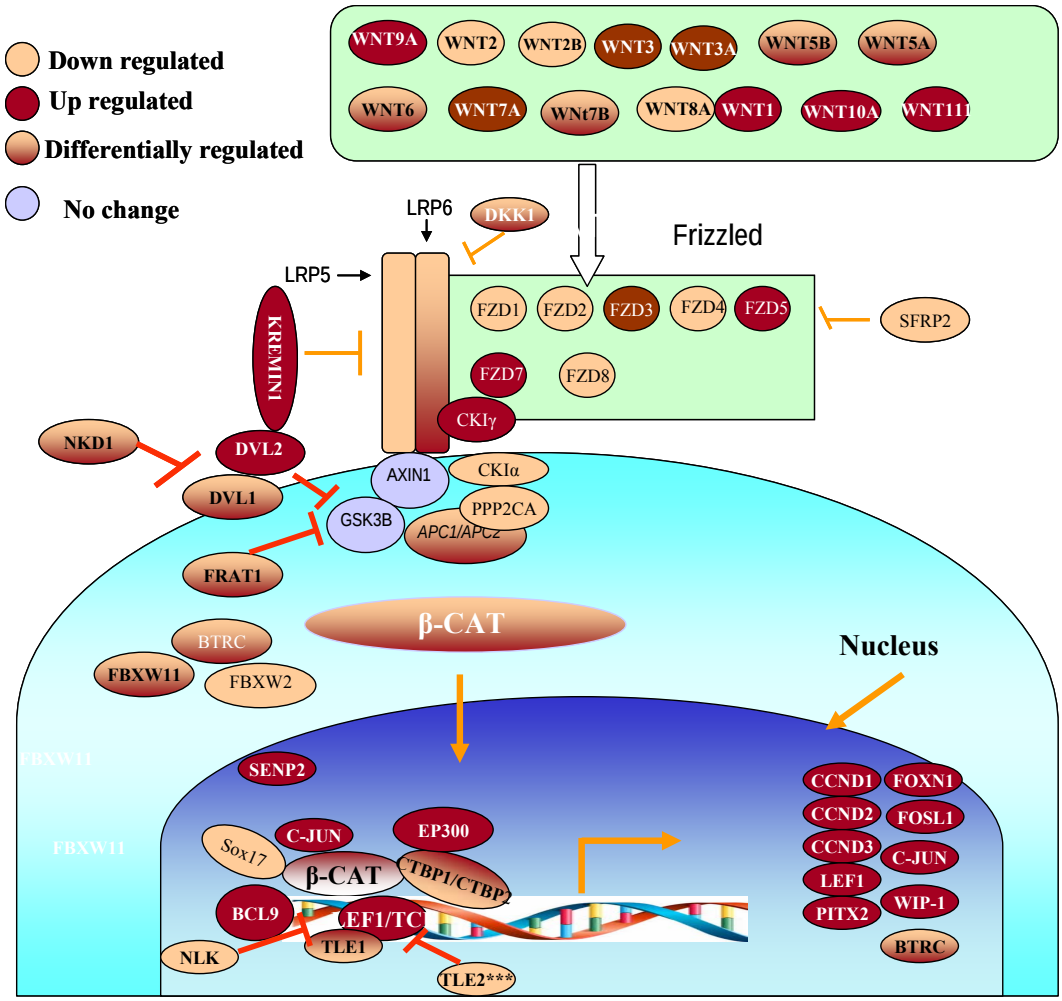

Figure 3.23: Gene expression modeling of WNT signaling pathway in CLL cells. This figure demonstrates a model of WNT signaling pathway in CLL cells that examined in this study. Aberrant expressions of Wnt signaling genes (up-regulated, down regulated and differentially expressed genes) are presented by different colors. This figure also provides information regarding the role of each gene (positive or negative regulator) and its location in the Wnt pathway in respect to other genes

For the first time in this work we report elevated expression level of *p300*, *CJUN* and *FOSL1* (Fra-1) in leukemic CLL B cells compared to the normal B cells by at least 10 fold. These genes are associated with a number of interesting biological functions whose abnormal expression has not been previously reported in CLL. Fos related antigen-1 (*FOSL1* refers to the gene and Fra-1 refers to the protein) and *CJUN* are members of the AP-1 transcriptional factors that their mRNA and protein levels are elevated in multiple primary and metastatic tumors such as brain, breast, lung and colon cancer [15;64]. Data from different laboratories have implicated the oncogenic potential of *CJUN* in malignant transformation of normal mammalian cells. Over expression C*JUN* in MCF-7 breast cancer cells produces a tumorigenic, invasive and hormone resistant phenotype[65]. Moreover, it has been suggested that activation of PI3K/AKT and ERK/MAPK pathway, directly or indirectly, is responsible for elevated *FOSL1* and *C-JUN* mRNA levels in tumor cells. Interestingly, activation of these signaling pathways plays a pivotal role in the proliferation and survival of normal lymphoid cells in response to different stimuli. In spite of extensive impairment of several of these signaling pathways in leukemic B CLL cells, the functional role of PI3K/AKT and ERK/MAPK pathway in tumorgenesis of B-CLL has been documented [66;67]. Therefore, it is tempting to speculate that the increased ERK signaling can affect mRNA expression of *FOSL1*and *CJUN* in CLL cells. Although the role of *FOSL1*and *CJUN* in the pathobiology of B-CLL is not clear, however, the association between increased expression of these genes and tumorgenesis of several solid tumors has been documented.

Furthermore, histone acetylase *p300* appeared to be over expressed in the majority of examined tumor cells. In vertebrates, *p300* has been shown to play an essential role in

mediating the activity of β- Catenin and acts as a positive regulator of transcription in WNT signaling pathway. We demonstrate over expression of WNT target genes in B-CLL cells compared to the healthy B cells, which indicates the active WNT signaling.

Leukemic B- CLL cells exhibit aberrant expression of WNT factors and the frizzled receptor transcripts compared to normal B lymphocytes. It is important to mention that the hematopoietic tissues (bone marrow) and non hematopoieteic tissues such as stromal cells, express *WNT3*, *WNT3A*, *WNT2B*, *WNT 5A* and their receptors *FZD3*, *FZD4*, and *FZD5* and *FZD7* [68]. This suggests that WNT ligands and their *FZD* receptors play a role in initiating WNT signaling in hematopoietic cells. We demonstrated in this study that there are significant differences in the expression of *WNT* ligands and *FZD* receptors in patients with CLL compared to normal PBMC and CD19+ B cells .We found over expression of WNT genes *WNT1, WNT10A*, *WNT11*, *WNT3*, *WNT3A*, *WNT9A* and their cognate receptors *FZD3*, *FZD4*, *FZD5, and FZD7* in CLL primary tumors compared with the normal control. Interestingly *FZD2* and *FZD8* were under expressed in primary tumor cells and the two CLL cell lines.

Treatment of CLL cell lines with a demethylating agent and a histone deacetylase inhibitor resulted in the up regulation of *FZD2* in two CLL cell line. The biological function of WNT factors and FZD receptors in pathobiology of CLL is not clear; therefore, it is difficult to speculate what functional significance these differences in expression play in the course of CLL tumorgenesis.

The increase in the expression of positive regulators of WNT such as disheveled proteins, BCL9*,* pygopus (nuclear co- activator of β-Catenin –LEF/TCF), Casein kinase, gamma1 (CKIγ) suggests that the WNT signaling is critically important in the CLL

malignancy. While CK1γ disrupts the *APC/AXIN/GSK3β/PP2CA/CK1α* destruction complex by phosphorylating co- receptor *LRP5/LRP6* which binds to *AXIN* and sequestering it away from the destruction complex, the other member of CK1 family protein (*CK1α*) plays completely different role in WNT signaling[69;70]. It associates with the destruction complex and facilitates the phosphorylation and stabilization of β- Catenin and ultimately leads to inactivation of WNT pathway. Our analysis of gene expression revealed divergent expression of *CK1* gene family in CLL patients. Furthermore, our experiment showed abundant expression of WNT regulated transcriptional factor *LEF1* in leukemic B CLL cells. Studies in *LEF1*$^{-/-}$ mouse have been shown that the *LEF1* expression is restricted to the pro and pre B cell compartment; however, once cells differentiate to IgM positive mature and immature B cells, *LEF1* is no longer can be detected in these cells (reviewed in [27]). These findings have implicated the role of WNT pathway in the regulation of immature B cell development.

In this work we found down regulation of negative regulators of WNT signaling both cytoplasmic and the nuclear proteins. We found down regulation of *Groucho/TLE* and *SOX17* in CLL tumor cells and CLL cell lines. We correlated the hypermethylation and expression of *TLE1* and *TLE2* in CLL cell lines. We found substantial decreases in the expression levels of these genes using real time RT-PCR. Treatment of *TLE1* and *TLE2* with epigenetic modifying reagents in vitro resulted in up-regulation of these genes, suggesting that these genes are regulated to some extent by DNA methylation and histone modification.

In summary, for the first time in this study we combined the three powerful techniques, 1) MCA to detect changes in DNA methylation genome -wide, 2) CpG island

microarray with 244,000 probes that covers the entire human CpG island to identify methylated genes associated with specific signaling pathway 3) The RT^2 profiler PCR array to profile the expression of genes involve in WNT signaling pathway. We demonstrated that the WNT target genes are expressed at high levels in leukemic CLL B cells compared to the normal lymphocytes. We showed up regulation of nuclear complex consisting of *LEF/TCF, FOSL1*, *CJUN* and *p300* as well as the cytoplasmic proteins such as *DVLs* and CK1γ in CLL cells. Furthermore, the leukemic CLL cells expressed WNT ligands and their cognate receptors as well as the other major component of the canonical pathway.

In addition, we showed the epigenetic silencing of negative regulators of the canonical Wnt pathway including *APC2, Groucho/TLEs*, *NLK*, *SOX* genes family in CLL primary tumors and the CLL cell lines. The association between the methylation patterns of these genes and their expression has not been reported previously in CLL tumorgenesis. These findings demonstrate that the epigenetic regulation of WNT antagonists is another mechanism that activates WNT signaling in CLL. We hypothesize that the over expression of the positive regulators of the WNT pathway together with the epigenetic down regulation of the negative regulators of the pathway are responsible, at least in a part, for the active WNT pathway in CLL tumorgenesis. Moreover, the activation of WNT signaling may play a role in accumulation of mature and incompetent leukemic B cells. Pharmacological antagonists such as human monoclonal antibodies and derivatives of small molecule compound that target the over expressed *WNTs, FZDs, DVL, FOSL1,C-JUN a*nd *p300* in CLL might be used for future investigation in cancer medicine.

Reference List

1. Bannerji R, Byrd JC. Update on the biology of chronic lymphocytic leukemia. Curr.Opin.Oncol. 2000;12:22-29.

2. Rahmatpanah FB, Carstens S, Guo J et al. Differential DNA methylation patterns of small B-cell lymphoma subclasses with different clinical behavior. Leukemia 2006;20:1855-1862.

3. Taylor KH, Pena-Hernandez KE, Davis JW et al. Large-scale CpG methylation analysis identifies novel candidate genes and reveals methylation hotspots in acute lymphoblastic leukemia. Cancer Res. 2007;67:2617-2625.

4. Gonzalez-Sancho JM, Aguilera O, Garcia JM et al. The Wnt antagonist DICKKOPF-1 gene is a downstream target of beta-catenin/TCF and is downregulated in human colon cancer. Oncogene 2005;24:1098-1103.

5. Liu TH, Raval A, Chen SS et al. CpG island methylation and expression of the secreted frizzled-related protein gene family in chronic lymphocytic leukemia. Cancer Res. 2006;66:653-658.

6. Bhanot P, Brink M, Samos CH et al. A new member of the frizzled family from Drosophila functions as a Wingless receptor. Nature 1996;382:225-230.

7. Itoh K, Krupnik VE, Sokol SY. Axis determination in Xenopus involves biochemical interactions of axin, glycogen synthase kinase 3 and beta-catenin. Curr.Biol. 1998;8:591-594.

8. Behrens J, Lustig B. The Wnt connection to tumorigenesis. Int.J.Dev.Biol. 2004;48:477-487.

9. Roose J, Molenaar M, Peterson J et al. The Xenopus Wnt effector XTcf-3 interacts with Groucho-related transcriptional repressors. Nature 1998;395:608-612.

10. Toyota M, Ho C, Ahuja N et al. Identification of differentially methylated sequences in colorectal cancer by methylated CpG island amplification. Cancer Res. 1999;59:2307-2312.

11. Zorn AM, Barish GD, Williams BO et al. Regulation of Wnt signaling by Sox proteins: XSox17 alpha/beta and XSox3 physically interact with beta-catenin. Mol.Cell 1999;4:487-498.

12. Sinner D, Kordich JJ, Spence JR et al. Sox17 and Sox4 differentially regulate beta-catenin/T-cell factor activity and proliferation of colon carcinoma cells. Mol.Cell Biol. 2007;27:7802-7815.

13. Staal FJ, Weerkamp F, Baert MR et al. Wnt target genes identified by DNA microarrays in immature CD34+ thymocytes regulate proliferation and cell adhesion. J.Immunol. 2004;172:1099-1108.

14. Young MR, Colburn NH. Fra-1 a target for cancer prevention or intervention. Gene 2006;379:1-11.

15. Ramos-Nino ME, Blumen SR, Pass H, Mossman BT. Fra-1 governs cell migration via modulation of CD44 expression in human mesotheliomas. Mol.Cancer 2007;6:81.

16. Debinski W, Gibo DM. Fos-related antigen 1 modulates malignant features of glioma cells. Mol.Cancer Res. 2005;3:237-249.

17. Johnson R, Spiegelman B, Hanahan D, Wisdom R. Cellular transformation and malignancy induced by ras require c-jun. Mol.Cell Biol. 1996;16:4504-4511.

18. Schutte J, Viallet J, Nau M et al. jun-B inhibits and c-fos stimulates the transforming and trans-activating activities of c-jun. Cell 1989;59:987-997.

19. Stepniak E, Ricci R, Eferl R et al. c-Jun/AP-1 controls liver regeneration by repressing p53/p21 and p38 MAPK activity. Genes Dev. 2006;20:2306-2314.

20. Young MR, Nair R, Bucheimer N et al. Transactivation of Fra-1 and consequent activation of AP-1 occur extracellular signal-regulated kinase dependently. Mol.Cell Biol. 2002;22:587-598.

21. Lee HC, Kim M, Wands JR. Wnt/Frizzled signaling in hepatocellular carcinoma. Front Biosci. 2006;11:1901-1915.

22. Logan CY, Nusse R. The Wnt signaling pathway in development and disease. Annu.Rev.Cell Dev.Biol. 2004;20:781-810.

23. Veeman MT, Axelrod JD, Moon RT. A second canon. Functions and mechanisms of beta-catenin-independent Wnt signaling. Dev.Cell 2003;5:367-377.

24. Lustig B, Behrens J. The Wnt signaling pathway and its role in tumor development. J.Cancer Res.Clin.Oncol. 2003;129:199-221.

25. Slusarski DC, Yang-Snyder J, Busa WB, Moon RT. Modulation of embryonic intracellular Ca2+ signaling by Wnt-5A. Dev.Biol. 1997;182:114-120.

26. Du SJ, Purcell SM, Christian JL, McGrew LL, Moon RT. Identification of distinct classes and functional domains of Wnts through expression of wild-type and chimeric proteins in Xenopus embryos. Mol.Cell Biol. 1995;15:2625-2634.

27. Khan NI, Bendall LJ. Role of WNT signaling in normal and malignant hematopoiesis. Histol.Histopathol. 2006;21:761-774.

28. Kirikoshi H, Katoh M. Expression of WNT7A in human normal tissues and cancer, and regulation of WNT7A and WNT7B in human cancer. Int.J.Oncol. 2002;21:895-900.

29. Kirikoshi H, Sekihara H, Katoh M. Expression profiles of 10 members of Frizzled gene family in human gastric cancer. Int.J.Oncol. 2001;19:767-771.

30. Lu D, Zhao Y, Tawatao R et al. Activation of the Wnt signaling pathway in chronic lymphocytic leukemia. Proc.Natl.Acad.Sci.U.S.A 2004;101:3118-3123.

31. Calvisi DF, Conner EA, Ladu S et al. Activation of the canonical Wnt/beta-catenin pathway confers growth advantages in c-Myc/E2F1 transgenic mouse model of liver cancer. J.Hepatol. 2005;42:842-849.

32. Willert K, Jones KA. Wnt signaling: is the party in the nucleus? Genes Dev. 2006;20:1394-1404.

33. Cliffe A, Hamada F, Bienz M. A role of Dishevelled in relocating Axin to the plasma membrane during wingless signaling. Curr.Biol. 2003;13:960-966.

34. Cong F, Varmus H. Nuclear-cytoplasmic shuttling of Axin regulates subcellular localization of beta-catenin. Proc.Natl.Acad.Sci.U.S.A 2004;101:2882-2887.

35. Uematsu K, He B, You L et al. Activation of the Wnt pathway in non small cell lung cancer: evidence of dishevelled overexpression. Oncogene 2003;22:7218-7221.

36. Okino K, Nagai H, Hatta M et al. Up-regulation and overproduction of DVL-1, the human counterpart of the Drosophila dishevelled gene, in cervical squamous cell carcinoma. Oncol.Rep. 2003;10:1219-1223.

37. Uematsu K, Kanazawa S, You L et al. Wnt pathway activation in mesothelioma: evidence of Dishevelled overexpression and transcriptional activity of beta-catenin. Cancer Res. 2003;63:4547-4551.

38. Mizutani K, Miyamoto S, Nagahata T et al. Upregulation and overexpression of DVL1, the human counterpart of the Drosophila dishevelled gene, in prostate cancer. Tumori 2005;91:546-551.

39. Snowden AW, Perkins ND. Cell cycle regulation of the transcriptional coactivators p300 and CREB binding protein. Biochem.Pharmacol. 1998;55:1947-1954.

40. Li J, Sutter C, Parker DS et al. CBP/p300 are bimodal regulators of Wnt signaling. EMBO J. 2007;26:2284-2294.

41. Arany Z, Huang LE, Eckner R et al. An essential role for p300/CBP in the cellular response to hypoxia. Proc.Natl.Acad.Sci.U.S.A 1996;93:12969-12973.

42. Price MA. CKI, there's more than one: casein kinase I family members in Wnt and Hedgehog signaling. Genes Dev. 2006;20:399-410.

43. Yost C, Torres M, Miller JR et al. The axis-inducing activity, stability, and subcellular distribution of beta-catenin is regulated in Xenopus embryos by glycogen synthase kinase 3. Genes Dev. 1996;10:1443-1454.

44. Hart MJ, de los SR, Albert IN, Rubinfeld B, Polakis P. Downregulation of beta-catenin by human Axin and its association with the APC tumor suppressor, beta-catenin and GSK3 beta. Curr.Biol. 1998;8:573-581.

45. Kinzler KW, Vogelstein B. Lessons from hereditary colorectal cancer. Cell 1996;87:159-170.

46. Nakagawa H, Murata Y, Koyama K et al. Identification of a brain-specific APC homologue, APCL, and its interaction with beta-catenin. Cancer Res. 1998;58:5176-5181.

47. van Es JH, Kirkpatrick C, van de WM et al. Identification of APC2, a homologue of the adenomatous polyposis coli tumour suppressor. Curr.Biol. 1999;9:105-108.

48. Zou H, Molina JR, Harrington JJ et al. Aberrant methylation of secreted frizzled-related protein genes in esophageal adenocarcinoma and Barrett's esophagus. Int.J.Cancer 2005;116:584-591.

49. Suzuki H, Toyota M, Nojima M, Mori M, Imai K. [SFRP, a family of new colorectal tumor suppressor candidate genes]. Nippon Rinsho 2005;63:707-719.

50. Rush LJ, Raval A, Funchain P et al. Epigenetic profiling in chronic lymphocytic leukemia reveals novel methylation targets. Cancer Res. 2004;64:2424-2433.

51. Gasperowicz M, Otto F. Mammalian Groucho homologs: redundancy or specificity? J.Cell Biochem. 2005;95:670-687.

52. Cavallo RA, Cox RT, Moline MM et al. Drosophila Tcf and Groucho interact to repress Wingless signalling activity. Nature 1998;395:604-608.

53. Yamada M, Ohnishi J, Ohkawara B et al. NARF, an nemo-like kinase (NLK)-associated ring finger protein regulates the ubiquitylation and degradation of T cell factor/lymphoid enhancer factor (TCF/LEF). J.Biol.Chem. 2006;281:20749-20760.

54. Baylin SB, Belinsky SA, Herman JG. Aberrant methylation of gene promoters in cancer---concepts, misconcepts, and promise. J.Natl.Cancer Inst. 2000;92:1460-1461.

55. Zardo G, Tiirikainen MI, Hong C et al. Integrated genomic and epigenomic analyses pinpoint biallelic gene inactivation in tumors. Nat.Genet. 2002;32:453-458.

56. Klose RJ, Sarraf SA, Schmiedeberg L et al. DNA binding selectivity of MeCP2 due to a requirement for A/T sequences adjacent to methyl-CpG. Mol.Cell 2005;19:667-678.

57. Bird A, Macleod D. Reading the DNA methylation signal. Cold Spring Harb.Symp.Quant.Biol. 2004;69:113-118.

58. Shi H, Guo J, Duff DJ et al. Discovery of novel epigenetic markers in non-Hodgkin's lymphoma. Carcinogenesis 2007;28:60-70.

59. Yang-Snyder J, Miller JR, Brown JD, Lai CJ, Moon RT. A frizzled homolog functions in a vertebrate Wnt signaling pathway. Curr.Biol. 1996;6:1302-1306.

60. Austin TW, Solar GP, Ziegler FC, Liem L, Matthews W. A role for the Wnt gene family in hematopoiesis: expansion of multilineage progenitor cells. Blood 1997;89:3624-3635.

61. Van Den Berg DJ, Sharma AK, Bruno E, Hoffman R. Role of members of the Wnt gene family in human hematopoiesis. Blood 1998;92:3189-3202.

62. Reya T, O'Riordan M, Okamura R et al. Wnt signaling regulates B lymphocyte proliferation through a LEF-1 dependent mechanism. Immunity. 2000;13:15-24.

63. Baba Y, Garrett KP, Kincade PW. Constitutively active beta-catenin confers multilineage differentiation potential on lymphoid and myeloid progenitors. Immunity. 2005;23:599-609.

64. Wang HL, Wang J, Xiao SY et al. Elevated protein expression of cyclin D1 and Fra-1 but decreased expression of c-Myc in human colorectal adenocarcinomas overexpressing beta-catenin. Int.J.Cancer 2002;101:301-310.

65. Smith LM, Wise SC, Hendricks DT et al. cJun overexpression in MCF-7 breast cancer cells produces a tumorigenic, invasive and hormone resistant phenotype. Oncogene 1999;18:6063-6070.

66. Kawauchi K, Ogasawara T, Yasuyama M. Activation of extracellular signal-regulated kinase through B-cell antigen receptor in B-cell chronic lymphocytic leukemia. Int.J.Hematol. 2002;75:508-513.

67. Ogasawara T, Yasuyama M, Kawauchi K. Constitutive activation of extracellular signal-regulated kinase and p38 mitogen-activated protein kinase in B-cell lymphoproliferative disorders. Int.J.Hematol. 2003;77:364-370.

68. Chiba H, Kobune M, Kato J et al. Wnt3 modulates the characteristics and cobblestone area-supporting activity of human stromal cells. Exp.Hematol. 2004;32:1194-1203.

69. Bustos VH, Ferrarese A, Venerando A et al. The first armadillo repeat is involved in the recognition and regulation of beta-catenin phosphorylation by protein kinase CK1. Proc.Natl.Acad.Sci.U.S.A 2006;103:19725-19730.

70. Bustos VH, Marin O, Meggio F et al. Generation of protein kinase Ck1alpha mutants which discriminate between canonical and non-canonical substrates. Biochem.J. 2005;391:417-424.

APPENDIX 1

Gene Name	Assession no.	Chromosome	CpG Island	Gene Function
AAK1	**NM_014911**	**2p13.3**	**YES**	AP2 associated Kinase 1
ABCG1	**NM_207630**	**21q22.3**	**NO**	ATP binding cassette transporter G1
ACTR6	**NM_022496**	**12q23.1**	**YES**	Activated protein 6
ALX4	**AB058691**	**11p11.2**	**YES**	Aristaless-like homoebox 4
ANX4	**NM_001153**	**2p13.3**	**YES**	Annexin A4
ARF4	**BC016325**	**3p21.2-p21.1**	**YES**	ADP-ribosylation factor 4
ARX	**AY038071**	**Xp22.1-p21.3**	**YES**	Aristaless related homeobox
ATOX2	**NM_004045**	**5q33.1**	**YES**	Antioxidant protein 1
BLK	**NM_001715**	**8p23.1**	**NO**	B lymphoid tyrosine kinase
BZW1	**NM_014670**	**2q33.1**	**YES**	Basic leucine zipper and W2 domains 1
CG1-150	**AF177342**	**17p13.3**	**NO**	Hypothetical protein
CHODL	**AF257472**	**12q12.1**	**YES**	Chondrolectin
CHP	**NM_007236**	**15q15.1**	**YES**	Calcium binding protein
CROC4	**NM_006365**	**1q22**	**YES**	Transcriptional activator
CSDA	**BC021926**	**12q13.2**	**YES**	Cold Shock Domain Protein A
CYP27B1	**NM_000785**	**12q14.1**	**YES**	Cytochrome P450
DBC1	**AF027734**	**9q32-q33**	**NO**	Deleted in Bladder Cancer 1
DEDD	**BC046149**	**1q23.3**	**YES**	Death factor domain containing
DKFZP586D0919	**BC016395**	**12q14.1**	**YES**	Hepatocellular carcinoma-associated
DDX54	**BC005848**	**12q24.13**	**NO**	Dead box polypeptide 54
EIF2AK3	**NM_004836**	**2p11.2**	**YES**	Eukaryotic translation initiation factor 2-alphakinase 3
EIF3S8	**BC001571**	**16p11.2**	**YES**	Eukaryotic translation initiation factor 3
EIF4E	**NM_001968**	**4q23**	**YES**	Eukaryotic translation initiation factor
EN2	**NM_001427**	**7q36.3**	**YES**	engrailed homolog 2
ENSA	**NM_207042**	**1q21.2**	**YES**	Endosulfine alpha isoform 3
FOXD2	**NM_004474**	**1p33**	**YES**	Forkhead box D2
GSH1	**AB044157**	**13q12.2**	**YES**	GS homeobox 1
GSTA4	**NM_001512**	**6p12.1**	**NO**	Glutatione S-transferase A4
GSTM5	**LO2321**	**1p13.3**	**NO**	Glutathione s-transferase M5
GTF3C1	**U02619**	**16p12**	**YES**	General transcription factor IIIC
H3F3A	**NM_002107**	**1q41**	**YES**	H3 histones family 3A
HAS2	**NM_005328**	**8q24.13**	**YES**	Hyaluronan synthase 2
HIRIP3	BC000588	16p11.2	YES	HIRA interacting protein 3

Gene Name	Assession no.	Chromosome	CpG Island	Gene Function
HIST1H4F	NM_003540	6p22.2	NO	Histone1,H2ad
HMGCS1	NM_002130	5p12	YES	3 hydroxy 3-methylglutaryl-coenzymeA synthase
HNRPM	NM_005968	19p13.2	NO	M4 protein deletion mutant
HOXC10	BC001293	12q13.3	YES	HomeoboxC10
IDE	M21188	10q23-q25	YES	Insulin-degrading enzyme
INFK	NM_020124	9p21.2	YES	Interferon like protein precursor
ITM2C	AF271781	2q37.1	YES	Integral membrane Protein 2C
KCN2	NM_021614	5q22.3	YES	Potassium intermediate/ small conductance
KCNK2	NM_001017424	1q41	NO	Potassium channel superfamily K membrane 2 isoform
KCNK4	NM_016611	11q13.1	YES	Potassium channel superfamily K member 4 isoform
KIAA0152	D63486	12q24.31	YES	Hypothetical protein KIAA0152
KIF23	NM_004856	15q23	YES	Kinesin family member 23
KLHL2	NM_007246	4q32.3	YES	Kelch-like 2
LHX2	AF124735	9q33-q34.1	YES	LIM homeobox 2
LRP1B	AF176832	2q21.2	YES	Low Density lipoprotein receptor
MAGEF1	BC010056	3q13	YES	Melanoma-associated antigen F1
MGC21416	BC012469	Xq13.1	YES	Hypothetical protein LOC286451
MLLT2	L13773	4q21	YES	Myeloid/lymphoid or mixed-lineage leukemia
MT2A	NM_005953	16q12.2	YES	Metallothionein 2A
MYBBP1A	NM_014520	17q13.2	YES	MYB binding protein (P160) 1 A
MYLK	NM_053030	3q21.1	NO	Myosin light chain kinase isoform 5
NAV1	NM_020443	1q32.1	YES	Neuron navigator
NF-IL3A	NM_005384	9q22.31	NO	Nuclear factor, interleukin 3 regulated
NGEF	BC031573	2q37	NO	Neuronal guanine nucleotide exchange factor
NKX6-1	NM_006168	4q21.2-q22	NO	NK6 transcription factor related, locus 1
NLGN1	AB028993	3q26.31	NO	Neuroligin 1
NNT	AL831822	5p13.1-5cen	YES	Nicotinamide nucleotide transhydrogenase
NRP2	BC009222	2q33.3	YES	Neuropilin 2
OAZIN	BC013420	8q22.3	YES	Ornithine decarboxylase antizyme inhibitor
P2RY6	NM_176798	11q13.4	NO	Pyrimidinergic receptor P2Y
PAF1	NM_019088	19q13.1	NO	Paf1, RNA polymerase II associated factor, homolog
PER1	NM_002616	17p13.1	YES	Period 1

Gene Name	Assession no.	Chromosome	CpG Island	Gene Function
PES1	BC032489	**22q12.1**	**YES**	Pescadillo homolog 1
PLEKHK1	NM_145307	**10q21.2**	**YES**	Rhotekin 2
PLK	BC002369	**16p12.1**	**YES**	Polo-like kinase 1
PLXDC1	NM_020405	**17q21.1**	**YES**	Tumor endothelial marker 3 precursor
POLA	NM_016937	**Xp21.3**	**YES**	Polymerase DNA directed, alpha
POU2F1	BC052274	**1q22-q23**	**YES**	POU domain, class 2, transcription factor 1
POU3F3	NM_006236	**2q12.1**	**YES**	POU domain, class 3, transcription factor 3
PRKCE	NM_005400	**2p21**	**YES**	Protein kinase C, epsilon
PTX1	BC064522	**12p11.22**	**YES**	PTX1 protein
RAMP	BC033297	**1**	**YES**	L2DTL protein (RA-regulated nuclear
RHD	NM_016124	**1p36.11**	**Yes**	Rhesus blood group, D antigen
RNF121	AK023139	**11q13.4**	**NO**	Ring finger protein 121
RNPC2	L10911	**20q11.22**	**YES**	RNA-binding region (RNP1, RRM) containing 2
RPL3	BC004323	**12q13.1**	**YES**	Ribosomal protein L3
SEC23B	NM_032986	**20p11.23**	**YES**	Sec23 homolog B
SFRS3	NM_003017	**6p21.31**	**NO**	Splicing factor, arginine/serine rich 3
SHC1	NM_003029	**1q21**	**YES**	Src homology 2 domain containing transforming protein 1
SLC39A5	BC027884	**12q13.3**	**NO**	Solute Carrier family 39 (metal ion transporter)
SMAD9	BC067766	**13q12-q14**	**NO**	MADH9 protein
SNRPC	X12517	**6p21.31**	**YES**	Small nuclear ribonucleoprotein polypeptide C
TAOK2	AF061943	**16p11.2**	**YES**	Prostate derived STE20-like kinase PSK
TBC1D7	BC050465	**6p24.1**	**YES**	TBC1 domain family, member 7
TFAP2B	NM_003221	**6p21-p12**	**YES**	Transcriptional factor AP-2 beta
TMEM29	NM_014138	**Xp11.22**	**YES**	Transmembrane protein 29
TNFRSF6	NM_000043	**10q23.31**	**NO**	Tumor necrosis factor receptor superfamily, member 6
TPX2	AF287265	**20q11.2**	**YES**	Hepatocellular carcinoma-associated antigen 519
TTF2	BC030058	**1p22**	**YES**	Transcription termination factor, RNA polymerase II
WNT1	NM_005430	**12q13.12**	**NO**	Wingless type MMTU integration site family, member 1
ZBTB4	NM_020899	**17p13.1**	**YES**	Zinc finger and BT3 domain containing protein 4
ZINC1	D76435	**3q24**	**YES**	Zic family member 1
ZINC5	NM_0331321	**13q32.3**	**YES**	Zinc family member 5
ZMPSTE24	NM_005857	**1p34.2**	**YES**	zinc metalloproteinase
ZNF160	NM_198893	**19q13.41**	**YES**	Zinc finger protein 160
ZNF263	BC008805	**16p13.3**	**YES**	Zinc finger protein 263
ZNF307	NM_019110	**6p22.1**	**YES**	Zinc finger protein 307
ZNF432	NM_014650	**19q13.41**	**YES**	Zinc finger protein 432
ZNF614	NM_025040	**19q13.41**	**YES**	Zinc finger protein 614
ZYX	NM_003461	**7q32**	**NO**	Zyxin

VITA

Farahnaz Rahmatpanah was born, in Sanandaj, Kurdistan, Iran. After attending public school in Sanandaj, she received the following degrees: B.S. in Chemistry from Razi University, Iran (1987); M.S. in Biochemistry, University of Missouri, Columbia (1997). She accepted a position in the Department of Pathology and Anatomical Sciences, a Sr. Research Specialist (2000 –2008). In 1989 she married Moz Rahmatpanah and moved to the United States in 1992. She has two children, Parsa and Arwin.